THE UNIVERSITY OF MICHIGAN

INDUSTRY PROGRAM OF THE COLLEGE OF ENGINEERING

SWITCHING CRITERIA FOR CERTAIN CONTACTOR SERVOS WITH ARBITRARY INPUTS

(Carl Anderson)

Carl A. Anderson

A dissertation submitted in partial fullfilment
of the requirement for the degree of
Doctor of Philosophy in the
University of Michigan
1958

August, 1958

IP-308

Doctoral Committee:

Professor Robert M. Howe, Chairman
Associate Professor Thomas C. Adamson, Jr.
Assistant Professor Elmer G. Gilbert
Associate Professor Louis F. Kazda
Professor Lawrence L. Rauch

TABLE OF CONTENTS

LIST OF FIGURES

LIST OF FIGURES (CONT'D)

LIST OF FIGURES (CONT'D)

LIST OF FIGURES (CONT'D)

NOMENCLATURE

a	Damping parameter of second order servo.
B	Diagonal matrix.
D	Differential operator
e	Base of natural logarithms.
f	Input displacement.
$\mathcal{A}$	Number of computer seconds per unit of τ.
K	Vector with components $0, K_2, K_3, \ldots K_n$
K_i	Positive real constant; $i = 2, 3, \ldots n$
L_j^+, L_j^-	Positive j-switch locus, negative j-switch locus.
L_j	$\sum_{i=0}^{j} L_i^{\pm}$.
L^+, L^-	Phase plane positive locus function, phase plane negative locus function.
M_1, M_2, M_3	Points in phase plane.
p	Variable of characteristic equation.
P_i	Ith principal coordinate of input phase point.
r	Ratio of sweep time rate to problem time rate.
sat	Amplifier saturation level.
u_1, u_2	ϵ, ϵ'
W_i	Ith principal coordinate of error phase space.
X_1, X_2, X_3	$\theta, \theta', \theta''$
Z	Vector with components $Z_1, Z_2, \ldots Z_n$.
Z_i	Ith principal coordinate of output phase space.
ϵ	Error displacement; $\epsilon = f - \theta$.
θ	Output displacement.
τ	Time variable
Δf	Approximation to $\Delta_2 f - \Delta_3 f$.

NOMENCLATURE (CONT'D)

$\Delta_1 f$	$f(\tau) - f(\tau_o)$.
$\Delta_2 f$	$f(\tau_s) - f(\tau_{os})$.
$\Delta_3 f$	$f(\tau) - f(\tau_{os})$.
$\Delta\tau$	Travel time to go until interception.
$\Delta\tau_J$	Travel time over last J output arcs of interception trajectory.
$\Delta\tau_\ell, \Delta\tau_s$	Larger $\Delta\tau$, smaller $\Delta\tau$; $\Delta\tau_\ell > \Delta\tau_s$.
$\Delta_1\tau$	$\Delta\tau_\ell - \Delta\tau_s$.
$(\ )_o$	Initial value of ( ).
$(\ )_{os}$	Value of ( ) at initiation of sweep.
$(\ )_p$	Value of ( ) at a particular point in the phase plane.
$(\ )_s$	( ) value corresponding to swept time.
$(\ )_v$	Vertex coordinate of a parabolic locus.
$(\ )_1$	Value of ( ) at last switch point before interception.
$(\ )'$	$d(\ )/d\tau$.

I. INTRODUCTION

An increasingly important aspect of present day technology is the use of devices or systems to control automatically the operation of other devices or systems. Some of these automatic controllers are designed to perform their regulatory functions according to preset programs and operate independently of the actions of the controlled systems. Such controllers are often called open-loop automatic control systems. Other automatic controllers are designed to make their operations depend upon comparing information about the desired actions of the controlled systems with information of the actual actions of the systems being controlled. These latter controllers are called closed-loop automatic control systems or servomechanisms. This study is concerned with the action of a particular type of closed-loop automatic control system.

Servomechanisms may be classified as linear or non-linear. If the operation of a servo is satisfactorily described as a linear process, it is a linear servo; otherwise, it is not. Description of linear servo action is often in the form of linear differential equations. A servo may be non-linear due to inherent non-linearities, to non-linearities intentionally inserted to improve the response of the servo, or both. The particular type of system considered herein, the contactor servo, is inherently non-linear.

The contactor-servo, variously called on-off servo, relay servo, and bang-bang servo, is non-linear because the command signal to the servomotor is a discontinuous function of a dependent variable

or variables.

The command signal of a contactor servo can be of only two or three finite values. In the two-valued case, the servomotor is directed to exert full forcing in one direction or in the opposite direction. The three-valued case includes a zero forcing signal in addition. Zero forcing signals are also used to include in an analysis the effects of the dead zone and of the finite contact spacing of a physical relay. In the literature on contactor servos, it always has been assumed that the action of the servo can be described by a linear differential equation during the time a particular command signal is on. The same differential equation would describe the servo action whenever that particular value of command signal came on again. Such systems are sometimes called piece-wise linear systems. This study considers such a piece-wise linear contactor servo of the two-valued type.

Considerable material has been written in the last quarter century to describe the analysis of contactor servos. Hazen[1], in 1934, discussed the response of second order on-off servos to step and ramp inputs of position with the switching of command signal between values dependent upon the sign of the error, the difference between desired and actual positions of the system output. MacColl[2] analyzed similar cases in 1945, using phase plane analysis which has been used in other non-linear mechanics problems by Minorsky[3], Andronow and Chaikin[4], and others. In 1949, Kahn[5] developed a method for determining the responses of such servos which used a series of Laplace transforms. He also presented a method for determining stability from

a velocity-time plot. In the same year, Weiss[6] published a paper in which he concludes "an anticipatory signal to be the most promising for control of torque application in a high performance relay servomechanism."

The determination of an appropriate anticipatory signal has been analyzed in several papers since that time and is the subject of this study. McDonald[7] in 1950, used phase plane analysis to solve the problem for step and ramp inputs to a second order system with inertia only. He determined a boundary or switching curve which divided the error, error-rate plane into two regions of opposite forcing. The location of the point in this plane representing the state of the system prescribes the forcing value. Hopkin[8] evolved a similar boundary for use when a saturating servo operates in its saturated mode of operation. Then, in 1951, McDonald[9] suggested the dual mode servo consisting of a contactor mode using the switching curve approach to prescribe forcing for large error or error-rate values and a linear mode to operate for small error and error-rate values. This arrangement would reduce transient error faster than a linear servo and provide a smoother steady state response than a contactor servo. The problem of determining criteria for switching the forcing of second order contactor servos with step inputs was treated in a general fashion by Bushaw[10] in 1953 in a paper on discontinuously-forced differential equations. La Salle[11] added to Bushaw's work in 1953. Kazda[12] discussed errors in second order systems in 1953.

Switching criteria for contactor servos of order higher than two were first treated in 1953. Rose[13] extended Bushaw's analysis to

higher order servos whose differential equations have real characteristic roots. He considered the case of a zero input signal, and he showed that minimum transient time would be obtained by using n-1 changes of forcing for his n^{th} order servo. Also Bogner and Kazda[14] reported on an analysis carried out in a phase space with coordinates of error and derivatives of error. Switch boundaries for step inputs were generalized from the phase plane curve of the second order system to surfaces and hypersurfaces in phase space for higher order systems. Dependence of switching criteria on input signals was also shown. Still in 1953, Kang and Fett[15] developed a distance function to metrize this phase space. Time rate of change of distance from the origin of the error space was used to determine switch criteria.

In late 1953, Bass[16] brought out an extensive report analyzing the effects of relay characteristics on contactor servo operation. He presented a feedback technique to be used to eliminate detrimental oscillation and chattering of a relay. A long critical bibliography was included.

Higher order systems were investigated further by Silva[17] who, in 1954, described a switching method based on energy considerations in which the response to a step input would consist of a forced acceleration, a forced deceleration, and a zero forcing phase. Arbitrary inputs were to be handled by paralleling the contactor system with an auxiliary system designated the forward feed system. Hagin[18] in 1956, also used such a forward-feed system to supplement a contactor system acting on step-input switching criteria represented by surfaces or hypersurfaces in an error phase space. By an approach similar to

that Bushaw used on second order systems, Tajima[19] has recently developed switching criteria for higher order contactor systems including some whose differential equations have complex characteristic roots.

All of the aforementioned analyses limited permissible input signals to step and ramp types for switching criteria determination. With the input signals thus prescribed as functions of time, anticipatory switching schemes were devised on the basis of knowing the future input signal. Faced with an arbitrarily varying input signal, such switching mechanisms would operate as if extrapolating the input signal into future time at its instantaneous value or at its instantaneous value plus its instantaneous time rate of change multiplied by the increment of future time. For slowly varying inputs, prediction of this nature may allow satisfactory servo operation.

Statement of the Problem

The problem considered in this study is the development of a method of determining switching criteria for optimizing the responses of certain contactor servos to prescribed arbitrary input signals. The optimizing switching criteria are used to reduce simultaneously transient error and appropriate error derivatives to zero in minimum time when the input signal is a known arbitrary function of time of class C^{n-1} for an n^{th} order servo. Use of such a switching method in conjunction with a scheme using more information than simply instantaneous input value and time rate of change to predict the future input signal should improve transient response over that of previous methods. It is also felt that development of such switching criteria may provide a useful insight into the

nature of the problem of how best to switch the forcing signal of a contactor servomechanism. The report proceeds as follows:

In Chapter II, the phase space method of analysis is outlined. Phase plane analyses of second order systems are used to introduce and illustrate concepts which are extended to cover higher order systems. McDonald's dual mode concept is also presented.

Chapter III deals with the determination of switching criteria for certain contactor servos with prescribed input signals. The phase space analysis is used. The problem of predicting a future input signal is briefly discussed also.

Chapter IV describes an analog computer study which was made to check the theory of Chapter III. Second order systems were studied.

Chapter V gives the conclusions.

II. PHASE SPACE ANALYSIS

A phase space may be defined as "an ideal, multidimensional space in which the coordinates represent the variables required to specify the state of a substance or of a system[20]." The use of a phase space is common in works in Classical Mechanics[21] in describing the state of a system of n particles, each with three degrees of freedom, as a point in a 6n dimensional space with coordinates representing generalized displacements and momenta of each particle. The state of a system of only one particle with one degree of freedom is describable as a point in a phase plane. As the state of the system changes, the phase point describes a curve or trajectory in the phase space. The collection of possible trajectories, which the phase point for a particular system may trace, is termed a phase portrait of the system. Analysis of such phase portraits may provide valuable insight into the workings of systems under study. The phase plane portrait has proved useful in the study of second-order single degree of freedom devices, particularly non-linear devices for which the more common methods of treating linear differential equations have not sufficed.

Coordinates other than displacement and velocity have been found useful for describing system action in some cases. In phase plane analyses of second-order contactor servos, coordinates of error and error rate, the time rate of change of error, have been common although not universal. This phase plane will be used in the analysis which follows.

Second Order Contactor Servo with Inertia Only

The differential equations for a second order contactor servo with inertia only may be written in terms of the system output as

$$\frac{d^2\theta}{d\tau^2} = \ddot{\theta}'' = \pm 1 \quad , \tag{2.1}$$

in which θ = the output displacement,

τ = the time variable,

and ± 1 = the two normalized values of forcing with the choice of sign dependent on a prescribed switching criterion. Although written as a single equation, the expression represents the two equations of motion describing the servo action, one for positive forcing and one for negative forcing. This representation will be used throughout the paper.

The error is defined as

$$\epsilon = f - \theta \tag{2.2}$$

in which f is the desired output position or input signal. The equations of motion may then be expressed as

$$\epsilon'' = f'' \mp 1 \tag{2.3}$$

in which the top row of the sign on the forcing term still refers to the case of positive forcing. These equations point up the expected fact that error variation will, in general, depend on the input signal. This dependence will be removed by limiting the input signals to constant position and constant velocity. The equations of motion to be treated then are

$$\epsilon'' = \mp 1 \quad . \tag{2.4}$$

These equations are easily solved to give the time relationship

$$\tau - \tau_o = \mp(\epsilon' - \epsilon'_o), \tag{2.5}$$

and the equations of the phase plane trajectories

$$\epsilon - \epsilon_o = \frac{\mp[(\epsilon')^2 - (\epsilon'_o)^2]}{2} \tag{2.6}$$

Zero subscripts are used to designate initial values of variables.

Conventional uniqueness theorems for linear differential equations[22] can be used to show that only one trajectory for each forcing sign passes through each point in the ϵ, ϵ' phase plane. In general, similar uniqueness cannot be shown for solutions of Equations (2.3) due to the f'' term.

Figure 2.1 shows the ϵ, ϵ' phase plane with representative trajectories. Arrowheads show the direction of phase point motion on the curves, and consideration of Equations (2.4) shows that the dashed curves are for positive forcing, the solid curves for negative forcing. Time is implicit on the curves, but as can be seen from Equations (2.5) distance traveled in the ϵ' direction by the phase point is directly proportional to the time for such travel. This is true only for the particular problem being studied, of course. Time may also be computed for this particular phase plane by integrating the area between the ϵ axis and the $1/\epsilon'$ curve corresponding to the trajectory being traveled. That is,

$$\int \frac{1}{d\epsilon/d\tau}\, d\epsilon = \int d\tau \tag{2.7}$$

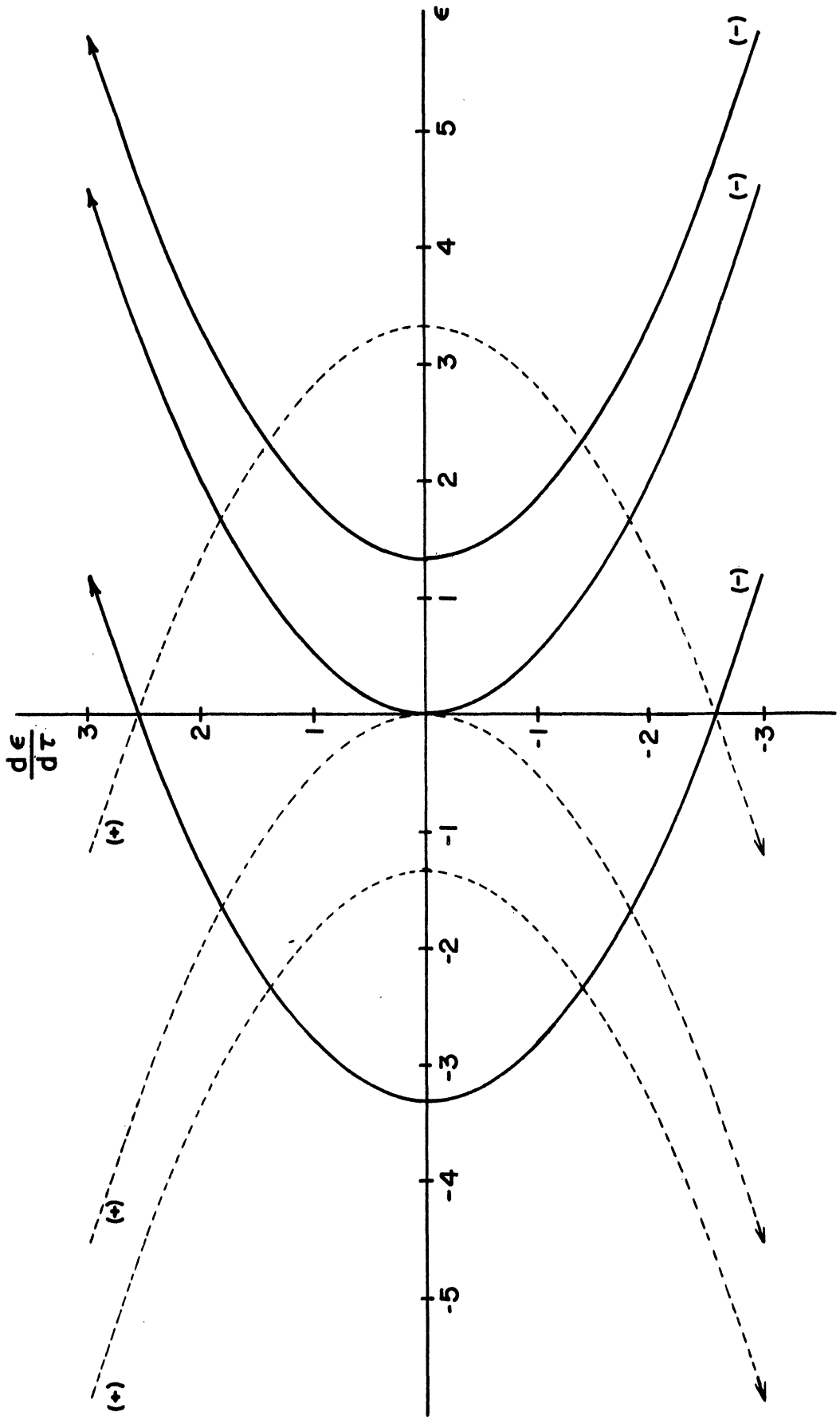

Figure 2.1 Error, Error-Rate Phase Plane Trajectories, Second Order Contactor Servo with Inertia Only.

It is desired that the phase point representing the state of the system be located at the origin of ϵ,ϵ' coordinates, this indicating attainment of the desired output response. For a phase point initially displaced from the origin, there exists the problem of how best to cause that phase point to move to the origin by choosing the appropriate forcing.

McDonald's[7] solution for optimum forcing is illustrated in Figure 2.2. The phase plane is divided into two regions by a curve formed by a positive arc terminating at the origin and a negative arc terminating at the origin. To arrive at the origin, the phase point must approach along one or the other of the two arcs. In the half-plane to the right of the curve so formed, shown dashed on the figure, positive forcing is applied causing the phase point to move toward the dividing curve. Upon arrival at the curve, the forcing is switched and the point moves on into the origin. The dividing curve is often called a switching curve, and its equation can be shown to be

$$\epsilon + \frac{|\epsilon'|\epsilon'}{2} = 0 \tag{2.8}$$

Had negative forcing been applied and held with the phase point to the right of the switching curve, observation of Figure 2.1 shows that the point could never arrive at the origin and would eventually diverge from the origin. Consideration of distance traveled in the ϵ' direction in the light of Equations (2.5) shows that any program of switching the forcing with the phase point in this right half plane other than that of applying positive forcing until arrival at the switching curve will

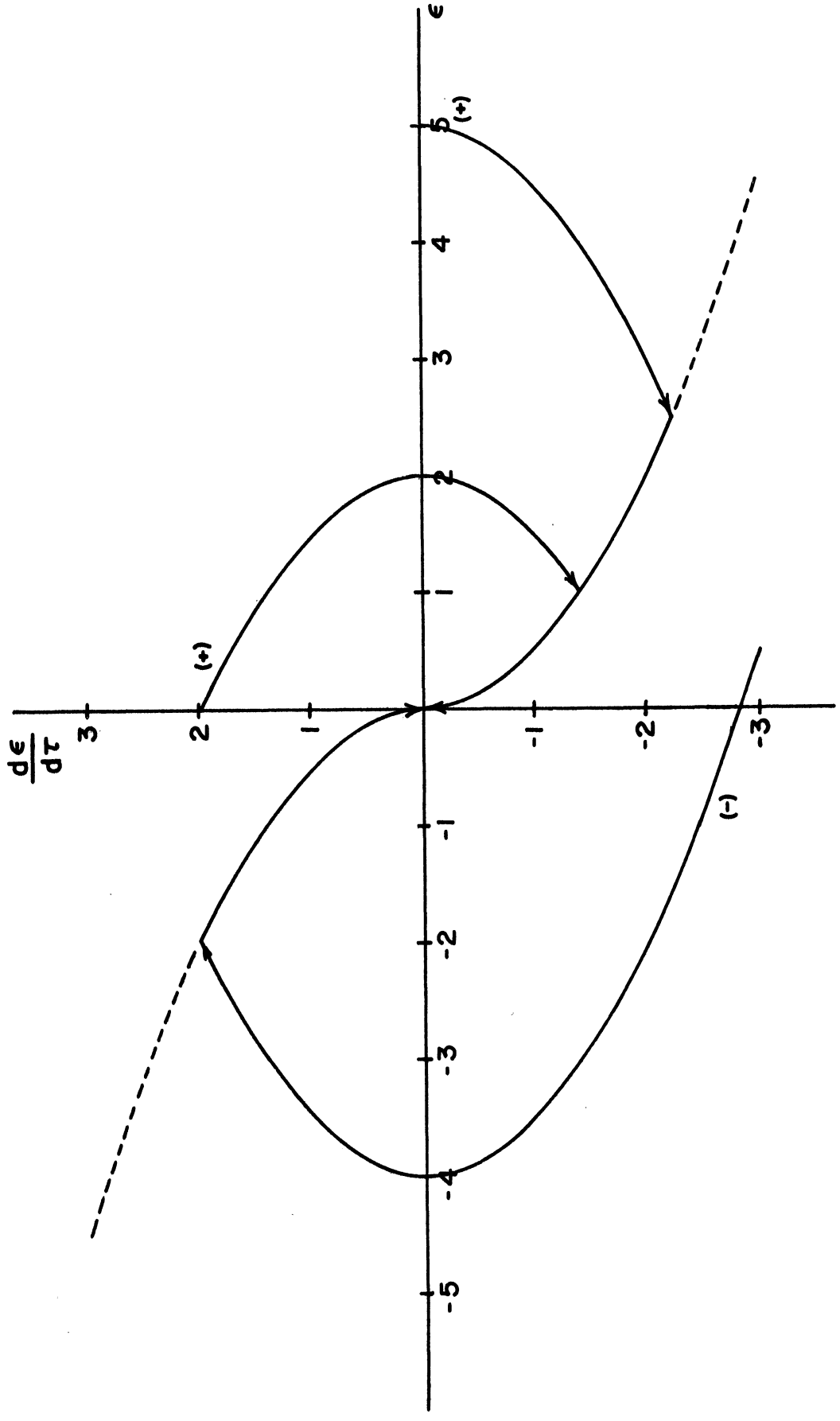

Figure 2.2 Switching Curve, Second Order Contactor Servo with Inertia Only.

cause the travel time to be longer. Similar considerations show the area to the left of the switching curve to be a region calling for negative forcing. Sample trajectories using the switching curve are shown in Figure 2.2.

It is worthwhile to point out that, for a constant input, reduction of initial error by a forcing program as outlined, makes use of the maximum available forcing during the transient period with no resulting overshoot of the steady state condition. Forcing would, of course, have to be removed as the phase point arrives at the origin of the ϵ,ϵ' phase plane. Thus the transient would be reduced in minimum time and, for this reason, such a response is often considered the optimum step response.

Second Order Contactor Servo with Inertia and Viscous Damping

The differential equations for a second order contactor servo with inertia and viscous damping may be written as

$$\frac{d^2\theta}{d\tau^2} + a\frac{d\theta}{d\tau} = \pm 1 \tag{2.9}$$

in which a is the damping parameter, and other symbols are as previously defined. In terms of ϵ and f the equations are

$$\epsilon'' + a\epsilon' = f'' + af' \mp 1 \tag{2.10}$$

By allowing only constant inputs, the equations are simplified to

$$\epsilon'' + a\epsilon' = \mp 1 \tag{2.11}$$

Solving Equations(2.11) for the equations of the phase plane trajectories gives

$$\epsilon - \epsilon_o = \frac{(\epsilon_o' - \epsilon')}{a} \pm \frac{1}{a^2} \ln\left(\frac{a\epsilon' \pm 1}{a\epsilon_o' \pm 1}\right) \tag{2.12}$$

Sample trajectories in the ϵ, ϵ' phase plane are shown in Figure 2.3 for an a value of one. The switching curve is indicated by the dashed curve. As can be seen from investigation of Equations(2.11), the half-plane to the right of the switching curve is shown as a region of positive forcing. The horizontal dashed lines represent the velocity saturation of the system. Once the phase point enters the region between the two dashed lines, it will remain in this region for all future step inputs.

The equation of the switch curve can be shown to be

$$a\epsilon + \epsilon' = \frac{\epsilon'}{a|\epsilon'|} \ln(a|\epsilon'| + 1) \tag{2.13}$$

Principal Coordinates

The phase portrait of Figure 2.3 was developed by determining system phase point motion in the ϵ and ϵ' directions. The same portrait could have been developed by determining phase point motion along any other two directions in the phase plane. In particular, in two directions which pass through the origin of ϵ, ϵ' coordinates, the phase plane principal directions of the system, the description of the motion is somewhat simplified and in a form more useful to the developments of Chapter III. Phase point motion for the second order contactor

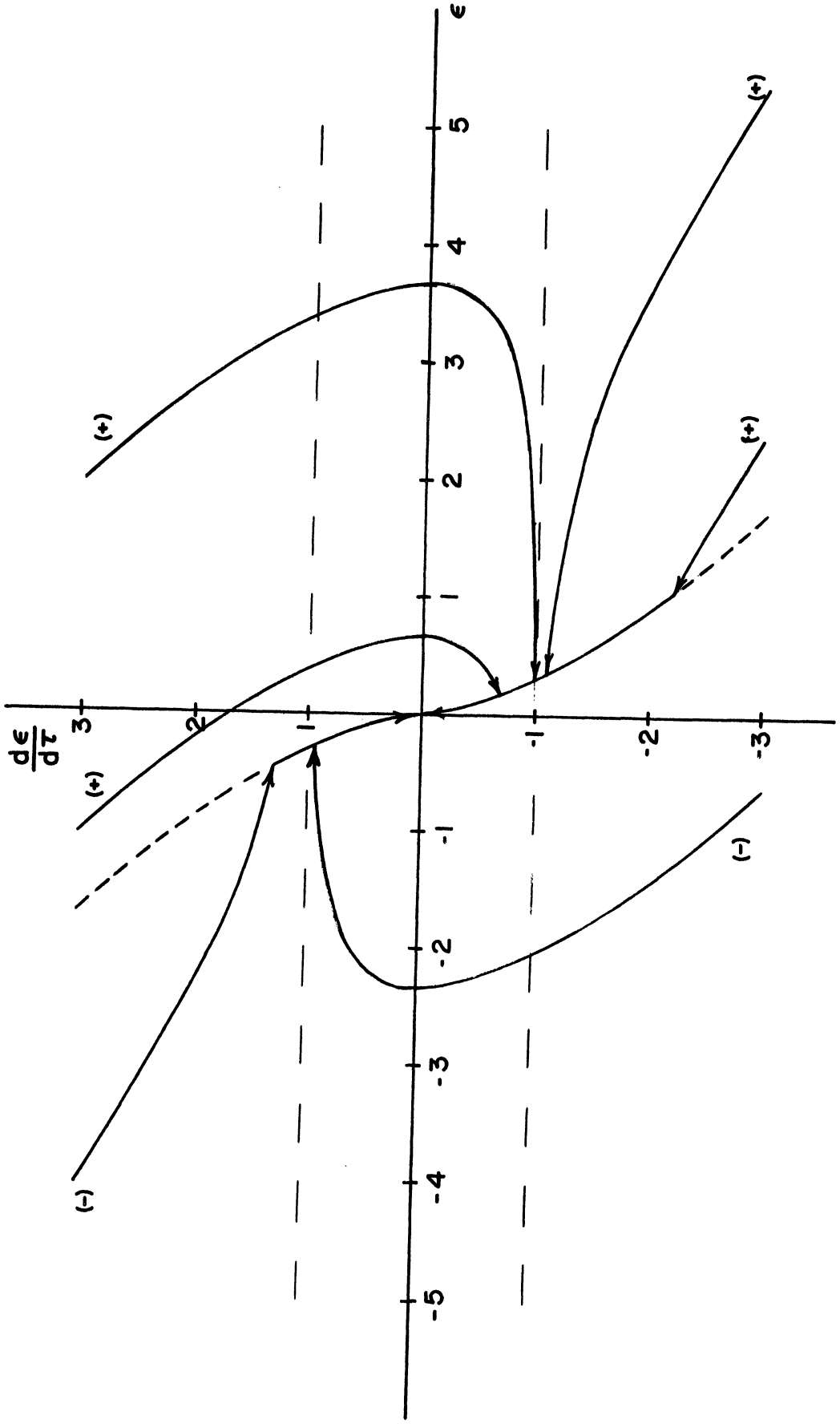

Figure 2.3 Error, Error-Rate Phase Plane Portrait, Second Order Contactor Servo with Inertia and Viscous Damping.

servo with inertia and viscous damping will be described using principal directions.

For a detailed description of the principal direction concept, the reader is referred to Reference 23 of the Bibliography. Here the concept will be used to transform the equations of motion in terms of ϵ and ϵ' to equations of motion in terms of coordinates along the principal directions. The new set of equations will then be solved to determine the phase portrait.

Let

$$u_1 = \epsilon \quad , \tag{2.14}$$

and

$$u_2 = \epsilon' \tag{2.15}$$

Equations (2.11) may then be replaced by the first order equations

$$u_1' = u_2 \tag{2.16}$$

$$u_2' = -a u_2 \mp 1 \tag{2.17}$$

Equations (2.16) and (2.17) are written in vector-matrix form as

$$\begin{pmatrix} u_1 \\ u_2 \end{pmatrix}' = \begin{Vmatrix} 0 & 1 \\ 0 & -a \end{Vmatrix} \begin{pmatrix} u_1 \\ u_2 \end{pmatrix} \mp \begin{pmatrix} 0 \\ 1 \end{pmatrix} \tag{2.18}$$

Equations (2.18) may be expressed in terms of principal coordinates W_1 and W_2 measured along the phase space principal directions

of the system. The necessary transformations are

$$\begin{pmatrix} u_1 \\ u_2 \end{pmatrix} = \begin{Vmatrix} 1/a & -1/a^2 \\ 0 & 1/a \end{Vmatrix} \begin{pmatrix} w_1 \\ w_2 \end{pmatrix} , \tag{2.19}$$

and

$$\begin{pmatrix} w_1 \\ w_2 \end{pmatrix} = \begin{Vmatrix} a & 1 \\ 0 & a \end{Vmatrix} \begin{pmatrix} u_1 \\ u_2 \end{pmatrix} \tag{2.20}$$

The transformed equations are

$$\begin{pmatrix} w_1 \\ w_2 \end{pmatrix}' = \begin{Vmatrix} 0 & 0 \\ 0 & -a \end{Vmatrix} \begin{pmatrix} w_1 \\ w_2 \end{pmatrix} \mp \begin{pmatrix} 1 \\ a \end{pmatrix} \tag{2.21}$$

Thus

$$w_1 = a\epsilon + \epsilon' , \tag{2.22}$$

and

$$w_2 = a\epsilon' . \tag{2.23}$$

The w_1 and w_2 directions may be drawn on the ϵ, ϵ' phase plane as shown in Figure 2.4 for $a=1$. These are the phase plane principal directions of the system.

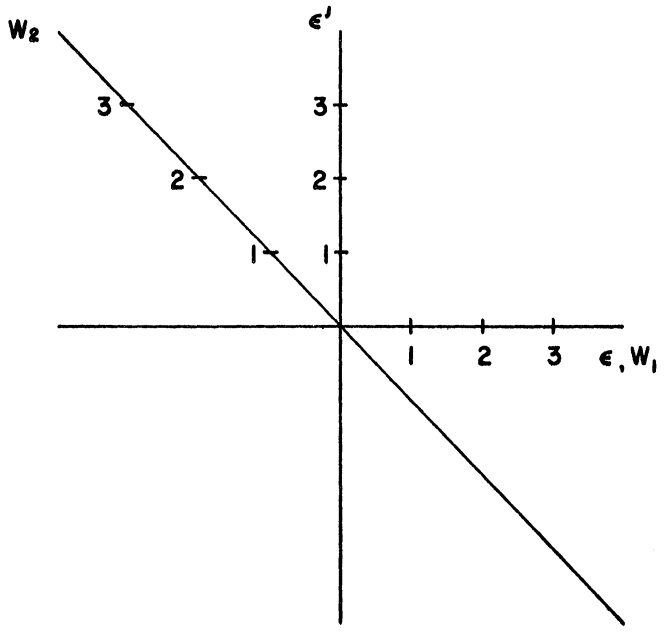

Figure 2.4 Phase Plane Principal Directions for $a=1$

In terms of W_1 and W_2 the equations of motion are

$$W_1' = \mp 1 \tag{2.24}$$

$$W_2' = -aW_2 \mp a \tag{2.25}$$

Solving Equations (2.24) gives

$$\tau - \tau_0 = \mp(W_1 - W_{10}) \tag{2.26}$$

Thus, change in phase point displacement in the W_1 direction is directly proportional to the time needed to make the change. This displacement time relationship will be used in Chapter III. Such a relationship did not hold for either the ϵ or ϵ' direction for this servo.

Solving Equations(2.25) gives

$$W_2 \pm 1 = (W_{2o} \pm 1)\, e^{-a(\tau - \tau_o)} \tag{2.27}$$

Eliminating τ between Equations (2.26) and (2.27) gives

$$W_2 \pm 1 = (W_{2o} \pm 1)\exp\left[\pm a(W_1 - W_{1o})\right], \tag{2.28}$$

the equations of the phase plane trajectories in terms of W_1 and W_2 measured along the principal directions. Equations(2.28) transform into Equations(2.12) by substituting for W_1 and W_2 from Equations (2.22) and (2.23).

As may be seen from Equations(2.21), the elements on the diagonal of the diagonal matrix are the roots of the characteristic equation

$$p(p+a) = 0 \tag{2.29}$$

formed from the differential Equations(2.11). In the vector-matrix Equations(2.18) they are the characteristic roots of the square matrix which are found by solving

$$\begin{vmatrix} 0-p & 1 \\ 0 & -a-p \end{vmatrix} = p(p+a) = 0 \tag{2.30}$$

for p . Thus, in the differential equations of phase point motion expressed in terms of motions in the principal directions, the displacement terms have these characteristic roots as coefficients. For the system with no forcing, phase point velocity along a principal direction is equal to its displacement from the origin along the same

principal direction times the appropriate characteristic root. This simple velocity-displacement relation holds along the principal directions only.

The developments of Chapter III are worked in terms of coordinates measured along the phase space principal directions of a system. It is convenient to think of these principal coordinates as the coordinates of a new phase space rather than as coordinates along certain directions of an original phase space. For the contactor servo with inertia and viscous damping, a W_1, W_2 phase plane portrait is shown in Figure 2.5 for $\alpha=1$. The switching curve is a dashed line, and the half plane to the right of the curve is a region of positive forcing. The horizontal dashed lines again represent the velocity saturation level of the system. In this plane these lines are always at $W_2 = \pm 1$ independent of the value of α. It may also be noted that in this plane the families of trajectories for positive forcing show mirror symmetry about the $W_2 = -1$ line. A similar symmetry is shown for the negatively forced trajectories and the $W_2 = +1$ line. As mentioned above, the change of phase point displacement in the W_1 direction is directly proportional to the time for such movement.

The equation of the switch curve in the W_1, W_2 plane is

$$1 + |W_2| = \exp(\alpha W_1 W_2 / |W_2|), \tag{2.31}$$

or

$$W_1 = \frac{W_2}{\alpha |W_2|} \ln (|W_2| + 1) \tag{2.32}$$

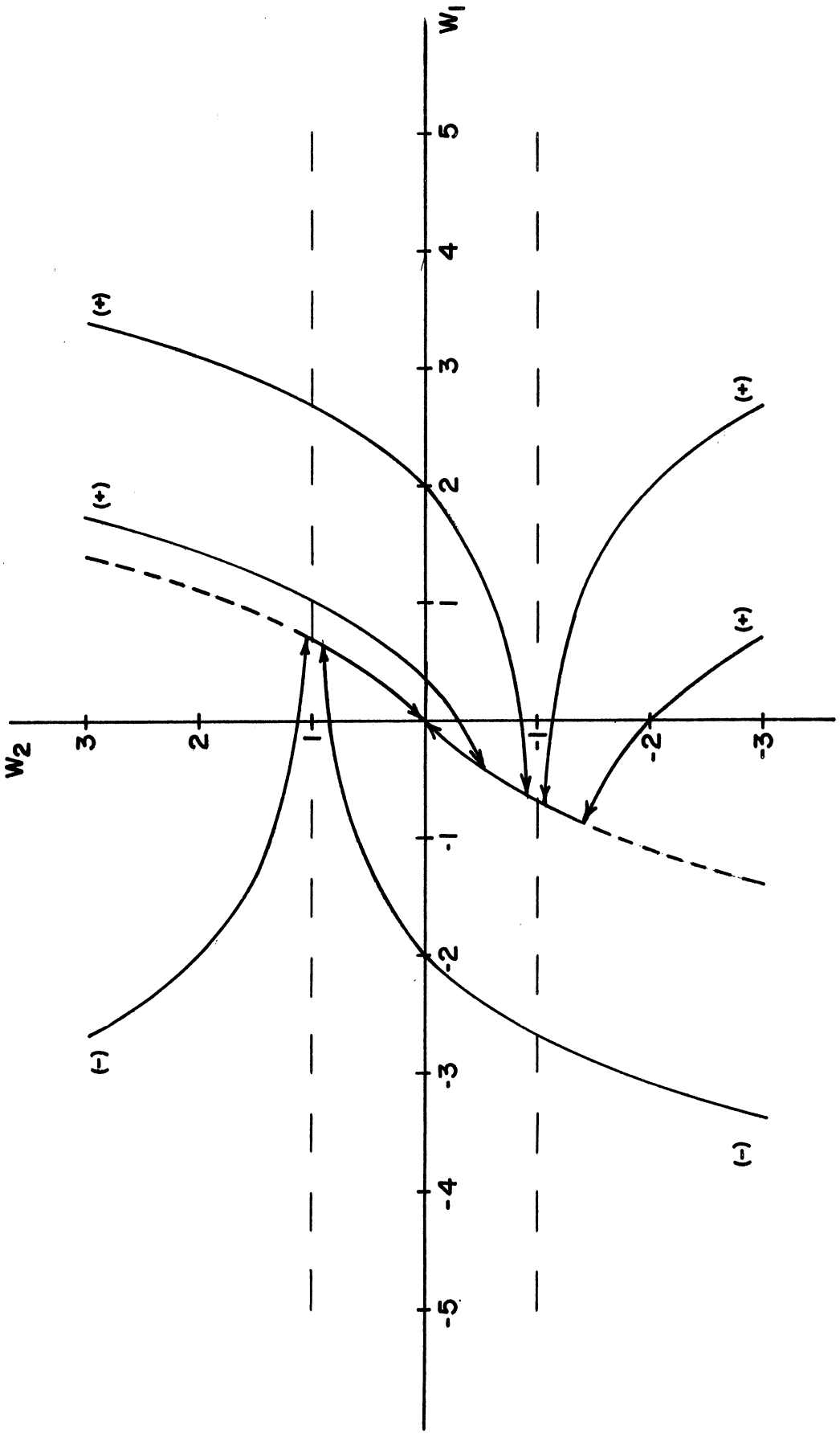

Figure 2.5 Principal Coordinate Phase Plane Portrait, Second Order Contactor Servo with Inertia and Viscous Damping.

Higher Order Contactor Servos

As mentioned in Chapter I, several investigators have considered the problem of determining switching criteria for contactor servos of order greater than two. The approach used by Bogner and Kazda[14] and Hagin[18] will be outlined here. Again, only constant input signals are allowed which eliminates the input signal dependence of the switching criteria.

For the higher order cases the error, error-rate portrait does not suffice to describe system action. In the second order case only one trajectory for each sign of the forcing goes through each point of the ϵ, ϵ' plane. However, in a third order system, for example, an infinity of trajectories for each sign of the forcing goes through each point in the ϵ, ϵ' plane; each trajectory corresponding to a different value of error acceleration or second time derivative of error. So a third dimension is added to the phase space which then has coordinates of ϵ , ϵ' and ϵ''. In this space only one trajectory goes through each point of the space for each sign of the forcing of a third order servo. An n dimensional space is used for an n^{th} order servo with coordinates of error and the first n-1 time derivatives of error. The analysis is often facilitated by working in a phase space whose coordinates correspond to displacements along the system principal directions in the error phase space.

As mentioned in Chapter I, Rose[13] analyzed servos whose differential equations have real characteristic roots. He showed that, to cause the phase point to move to the origin from an initial displacement away from the origin, n-1 switches of forcing are needed for

his n^{th} order contactor servos. The one switch for a second order servo is evident in Figures 2.2, 2.3 and 2.5.

The phase plane switching curves of second order systems generalize to switching surfaces and hypersurfaces for the higher order cases. A helpful method of visualizing such a surface for a third order system is illustrated in Figure 2.6. Bogner[14] and Hagin[18] have described this method. The space shown has dimensions W_1, W_2 and W_3 corresponding to the system principal coordinates in the error phase space. One trajectory for each sign of forcing goes through the origin. Therefore, the phase point must approach the origin along one or the other of these "zero trajectories." Naturally, only the portion of a zero trajectory on which the phase point moves toward the origin is of interest. Consider the zero trajectory into the origin from the bottom of the figure which is shown as a positively forced type. Trajectories for negative forcing are shown terminating on the positive zero trajectory. Such negative trajectories drawn to every point on the positive zero trajectory will describe the surface in the space on which the phase point must move in order to arrive at the positive zero trajectory. This surface and a similar surface described by positive trajectories drawn to every point on the negative zero trajectory divide the phase space into two regions of opposite forcing.

A sample trajectory is shown which pictures positive forcing until the phase point reaches the switching surface. Then negative forcing is imposed and the phase point moves along the switching surface until it hits the zero trajectory. The zero trajectory acts as a switching curve in the two dimensional surface, so the forcing is returned to its positive value, and the phase point moves to the origin.

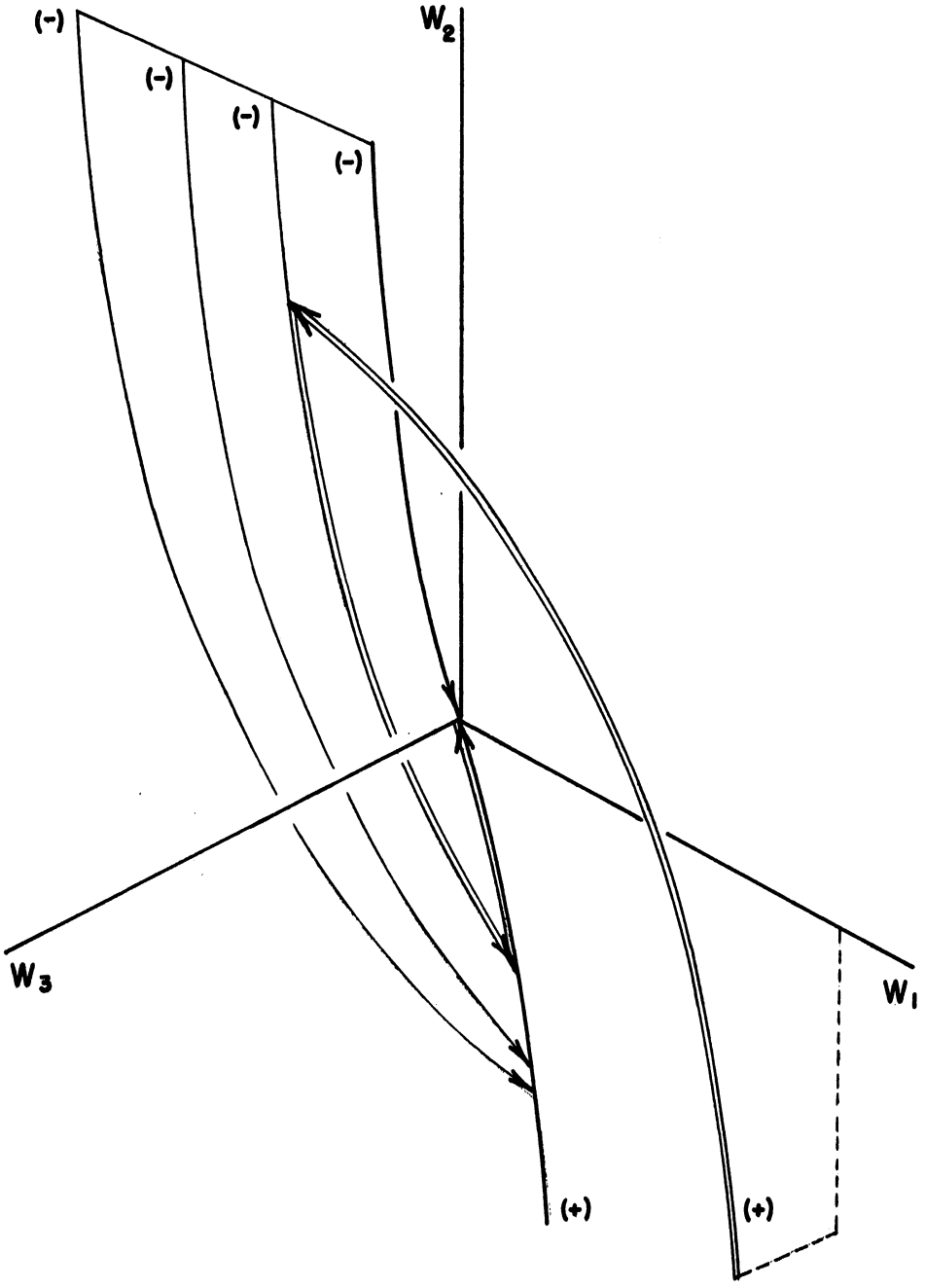

Figure 2.6 Switching Boundaries, Third Order Contactor Servo.

This idea of tracing trajectories backwards in time may be extended to higher order systems to get a concept of switching boundaries in many-dimensional phase spaces.

The Dual Mode Concept

In the previous examples of switching criteria determination it was assumed that, as the system phase point arrived at a switching boundary, the forcing was instantaneously switched. Thus the phase point moved directly into the origin of the space along a zero trajectory. In actuality, switching cannot be done instantaneously, and so the phase point will overshoot the switching boundary before forcing is reversed. Examination of Figure 2.2 shows that, in this case, the phase point will never arrive at the origin but will instead approach a limit cycle formed of a positive and a negative arc encircling the origin. The steady state response of the servo will then be rather jerky. For some servo uses, a certain amount of error may be acceptable. Then, a region of no forcing might be defined about the phase space origin large enough to include the limit cycle. Forcing would be turned off upon entry of the phase point into this region.

However, for less steady state error combined with a smoother steady state response, MacDonald[9] introduced his concept of a dual mode servo. The idea is illustrated in Figure 2.7 using the phase plane for the second order contactor servo with inertia only. As long as the system phase point is displaced a considerable distance from the origin, the servo would operate as a contactor servo utilizing full forcing. When the phase point enters a small region about the

origin the controller is switched to a linear mode of operation, and the servo then has the smoother response of a linear servo near its steady state condition. The idea is easily extended to the higher order cases.

Hopkin[8] and Howe and Rauch[24] have described servos which act with full forcing except for a narrow region of unsaturated operation along the switching curve. This unsaturated region thus encloses the origin also, and the resulting servo action is similar to that of a dual mode servo.

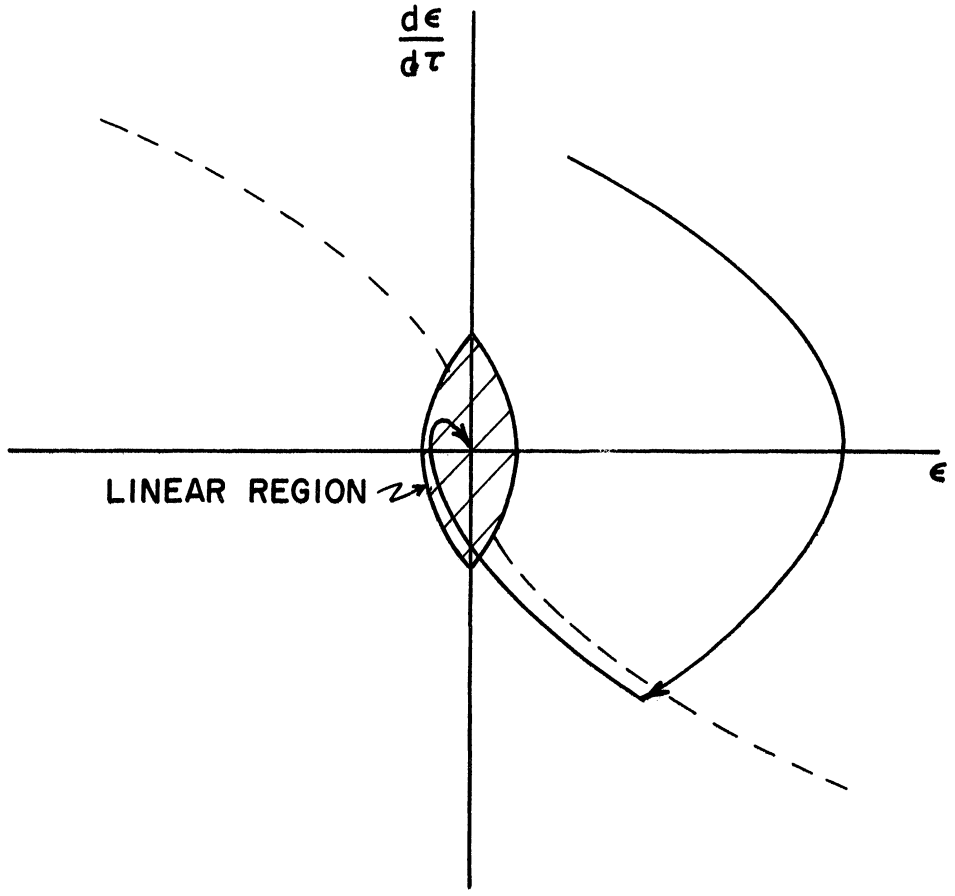

Figure 2.7 Phase Plane Portrait, Dual Mode Servo

III. SWEPT LOCUS SWITCHING

Switching Criteria for Known Inputs

In the previous chapter, analyses were shown which illustrated the phase space switching boundary approach for the determination of an appropriate anticipatory signal to control the application of forcing in a contactor servo. Describing the control signal as anticipatory indicates that knowledge of the future behavior of the input signal is used to control the forcing. This knowledge may be available or assumed. For constant position and constant velocity, as considered in Chapter II, the knowledge is available. If a contactor servo is forced with an input signal whose future values can be reasonably approximated by a constant position or constant velocity extrapolation from instantaneous values, switching criteria based on such inputs may give satisfactory servo operation. The extrapolation into the future, or prediction, would have to give a reasonably accurate approximation of the input at least during the time needed for reducing transient error and error derivatives to acceptable values.

For arbitrary input signals switching criteria based on constant position or velocity inputs may not suffice. It was mentioned in Chapter I that Silva[17] and Hagin[18] developed servos in which contactor-type controllers were paralleled with continuous-type controllers to provide composite forcing for the arbitrary input case. The contactor controllers worked on step input switching criteria and the continuous controllers, or forward feed systems, were to compensate for non-constant behavior of the input signals during the transient period. Such composite servos are no longer mere contactor servos, and they lose the

feature of the bang-bang principle stated by Bushaw, that of smashing the transient error to zero in minimum time for a limited forcing capability. In this study input signals more general than steps or ramps are considered on the basis of determining more general switching criteria for the contactor servo itself.

The point of view taken here is that the problem may be split into two parts, prediction of the future values of arbitrary inputs and determination of switching criteria for inputs known as functions of time. The second part is the principal concern of this study and will be discussed in the main body of this chapter. The prediction problem will be discussed briefly in the last section of the chapter.

The phase space switching boundary analyses previously shown were developed in phase spaces of error and error derivatives. Due to the restriction of the types of input signals, system phase point trajectories in such spaces did not depend on input signals. This simplified the analyses. For more general input signals the simplification is lost. However, observation of Equations (2.1) and (2.10) shows that, in a phase space with coordinates of system output position and its derivatives, the system phase point trajectories will always be independent of the input signals. An input signal, which may be considered as representing the desired condition of the output, can be shown as a phase point in this space also. It will move on a trajectory determined by the variation of the input signal and its derivatives as functions of time.

These ideas are illustrated in Figure 3.1 using the position-velocity phase plane of a second order contactor servo. A point

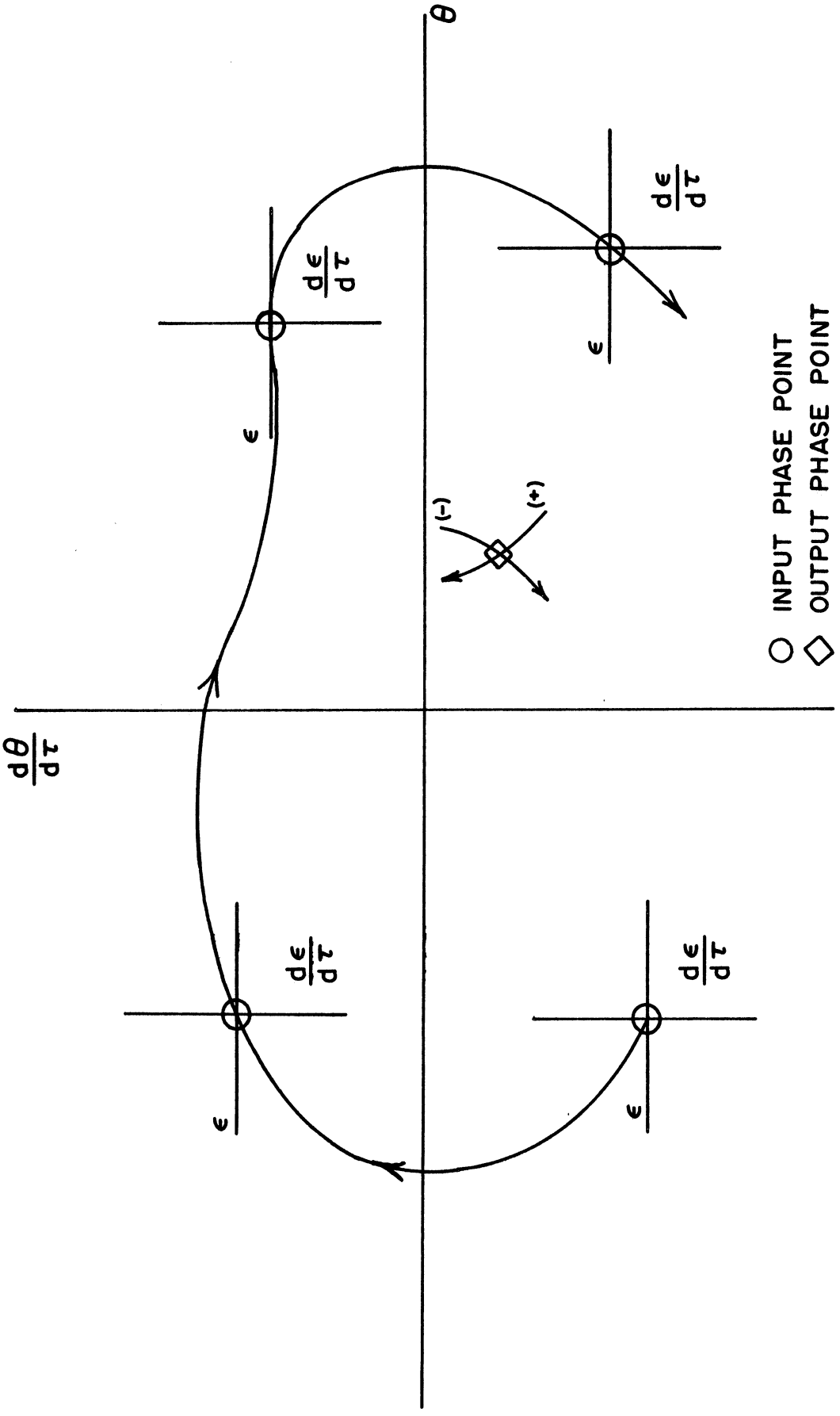

Figure 3.1 Displacement, Velocity Phase Plane.

representing the condition of the system output, the output phase point, is shown in the fourth quadrant of the phase plane. Two arcs pass through this point to indicate that the output phase point moves about the phase plane only on members of the two families of arcs corresponding to positive and negative forcing. Another point, the input phase point, is shown in several positions on a trajectory which describes the variation of the input signal. If the output phase point, constrained to move on arcs of positive and negative forcing, can be caused to intercept the input phase point, the desired condition of simultaneous zero error and error rate will be obtained. Interception, of course, means that the output and input phase points are at the same point in the plane at the same time.

Error, error-rate axes are drawn through each of the input phase points. System phase point movement in the error, error-rate phase plane is merely the relative motion of the output phase point with respect to the translating axes. This relative motion is, then, the difference between the output phase point movement with respect to the position, velocity axes and the input phase point movement with respect to the same axes. This merely restates the fact that error variation, in general, depends on the input signal. Removal of this dependence for the cases studied in Chapter II is easily seen.

The ideas described above in a phase plane can be carried over into phase spaces of more dimensions for higher order servos. Also, in some cases, it will be found convenient to work in phase spaces whose coordinates are the principal coordinates of the original spaces of output position and its derivatives.

For the output phase point to intercept the input phase point at some particular point in the phase space, it must first be able to move to the particular point, and second, time the movement to arrive at the particular point at the same time as the input phase point. The switching technique developed in this study is based on performing the second operation for output phase points capable of the first. The method will be introduced by analyzing the second order contactor servo with inertia only.

Second Order Contactor Servo with Inertia Only

The differential equations for a second order contactor servo, Equations (2.1), are repeated here.

$$\theta'' = \pm 1 \tag{3.1}$$

The equations of the θ, θ' phase plane trajectories can be obtained from Equations (3.1) just as Equations (2.6) were obtained from Equations (2.4). The trajectory equations are

$$\theta - \theta = \frac{\pm\left[(\theta')^2 - (\theta_o')^2\right]}{2} \tag{3.2}$$

Sample trajectories are shown in Figure 3.2 with directions of output phase point motion indicated by arrowheads. The phase plane is filled by the two families of these parabolas. Each member of a family has the same shape and orientation as any other member of the same family differing from any other member only by a translation in the θ direction. Conventional uniqueness theorems for linear differential equations[22] show there is but one trajectory of each type through any point of the phase plane.

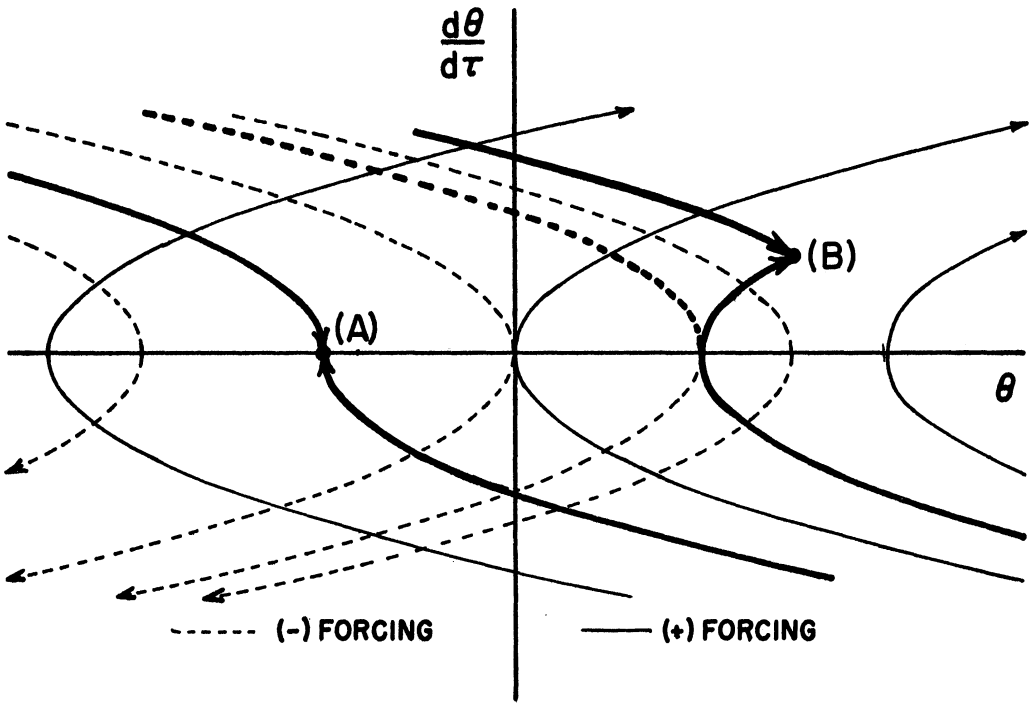

Figure 3.2 Displacement, Velocity Phase Plane Trajectories, Second Order Contactor Servo with Inertia Only.

Another feature to be observed in Figure 3.2 is that the output phase point can be moved to any point in the plane with no more than one switch of forcing.

Consider the point on the θ axis marked (A). For the output phase point to move to this point, it must arrive on one of the two trajectories through the point. Only the parts of these trajectories for which phase point travel is toward the point, will be used here. These zero trajectories are shown in heavy marking. The output phase point can be moved from any point on the zero trajectories to point (A) without changing the sign of the forcing term. The curve formed of the zero trajectories and point (A) divides the phase plane into two regions. Inspection of the figure shows that for any point to the right of the curve, there is a unique path from the point to point (A) if only one change of forcing is allowed. The path, of course, consists of an arc of negative forcing from the point to the positive zero trajectory and thence along the positive zero trajectory to point (A). Similarly, a unique positive-negative path exists for any point to the left of the curve. As both families of trajectories are unchanged by translation in the θ direction point (A) may be any point on the θ axis.

Consider next a point (B) above the θ axis. Zero trajectories are again heavy lines, and the curve formed of the zero trajectories and point (B) divides the plane into two regions. A unique one-switch path to (B) from any point to the right of this curve again exists. This fact holds also for the region to the left of the curve and below the heavy dashed line. For any point to the left of the curve and on or above the heavy dashed line, it is easily seen that two

one-switch paths to point (B) exist. Moving point (B) to any other position in the upper half-plane will not change the qualitative picture. A similar result can be obtained in the lower half plane by symmetry.

So, the output phase point can be moved to any point in the phase plane from any other location in the plane using no more than one switch of forcing. Timing the movement is to be investigated next.

Convenient relationships between time and phase plane travel can be obtained as were Equations (2.5). These relationships are

$$\tau - \tau_0 = \pm(\theta' - \theta_0') \tag{3.3}$$

The top row of a $\pm$ sign corresponds to positive forcing, the bottom row, to negative forcing.

To use Equations (3.3), a new concept is introduced. This is the concept of the locus of points in the phase plane from which the output phase point can be moved to some particular point in the plane by a one-switch process in a specified time. An expression for the locus will now be derived. The locus will be made up of two parts, a positive locus for paths with initial positive forcing, and a negative locus for paths with initial negative forcing.

Let θ and θ' be the instantaneous coordinates of the output phase point; and θ_P and θ_P' , the coordinates of the particular point to be reached. Let the specified travel time be $\Delta\tau \geqq 0$. For the one-switch path, the forcing is changed when the output phase point is at the switch point, (θ_1, θ_1')

From Equations (3.2) the equation describing the initial arc from (θ, θ') to (θ_1, θ_1') are

$$\theta_1 - \theta = \frac{\pm\left[(\theta_1')^2 - (\theta')^2\right]}{2} \tag{3.4}$$

The forcing is changed at $(\theta_1 \quad \theta_1')$, and the zero trajectory is described by

$$\theta_p - \theta_1 = \frac{\mp\left[(\theta_p')^2 - (\theta_1')^2\right]}{2} \tag{3.5}$$

Adding Equations (3.4) to Equations (3.5) by adding corresponding sides gives

$$\theta_p - \theta = \frac{\pm\left[2(\theta_1')^2 - (\theta')^2 - (\theta_p')^2\right]}{2} \tag{3.6}$$

From Equations (3.3) a time relationship is obtained:

$$\Delta\tau = \pm(\theta_1' - \theta') \mp (\theta_p' - \theta') \tag{3.7}$$

Rearranging,

$$\theta_1' = \frac{\pm\Delta\tau + \theta' + \theta_p'}{2} \tag{3.8}$$

Substituting Equations (3.8) into Equations (3.6) to eliminate θ_1' gives, after minor rearrangement and collection of terms,

$$\theta - \theta_p = \pm\left[\frac{(\theta')^2}{4} + \frac{(\theta_p')^2}{4} - \frac{(\Delta\tau)^2}{4} - \frac{\theta'\theta_p'}{2} \mp \frac{\theta'\Delta\tau}{2} \mp \frac{\theta_p'\Delta\tau}{2}\right] \tag{3.9}$$

Completing the square in the bracket gives

$$\theta - \theta_p = \pm\left[\frac{(\theta')^2}{4} + \frac{(\theta_p')^2}{4} + \frac{(\Delta\tau)^2}{4} - \frac{\theta'\theta_p'}{2} \mp \frac{\theta'\Delta\tau}{2} \pm \frac{\theta'\Delta\tau}{2}\right] + \mp\frac{(\Delta\tau)^2}{2} - \theta_p'\Delta\tau \tag{3.10}$$

Equations(3.10) may be written as

$$\theta - \left[\theta_p - \theta'_p \Delta\tau \mp \frac{(\Delta\tau)^2}{2}\right] = \frac{\pm[\theta' - (\theta'_p \pm \Delta\tau)]^2}{4} \qquad (3.11)$$

Equations(3.11) state that points on the positive locus with coordinates θ and θ' satisfy the relationship

$$\theta - \left[\theta_p - \theta'_p \Delta\tau - \frac{(\Delta\tau)^2}{2}\right] = \frac{[\theta' - (\theta'_p + \Delta\tau)]^2}{4} \qquad (3.12)$$

Equation (3.12) is the equation of a parabola in the θ, θ' plane of form $\theta = (\theta')^2/4$, a parabola opening in the positive θ direction. Its vertex is removed from the θ, θ' origin by a θ distance of $\theta_p - \theta'_p \Delta\tau - (\Delta\tau)^2/2$ and a θ' distance of $\theta'_p + \Delta\tau$ Obviously the positive locus corresponding to a finite $\Delta\tau$ cannot include the whole parabola, but it is some limited portion of the parabola. The negative locus for the same $\Delta\tau$ is some limited portion of the parabola of form $\theta = -(\theta')^2/4$ whose equation is

$$\theta - \left[\theta_p - \theta'_p \Delta\tau + \frac{(\Delta\tau)^2}{2}\right] = \frac{-[\theta' - (\theta'_p - \Delta\tau)]^2}{4} \qquad (3.13)$$

By substituting the vertex coordinates of each parabola into the equation of the other, it can be shown that the vertex of each parabola is on the other parabola.

Let θ_v and θ'_v be the vertex coordinates of a parabola. From Equations(3.11)

$$\theta_v = \theta_p - \theta'_p \Delta\tau \mp \frac{(\Delta\tau)^2}{2} \quad , \qquad (3.14)$$

and

$$\theta_v' = \theta_p' \pm \Delta\tau \tag{3.15}$$

Eliminating $\Delta\tau$ between Equations (3.14) and (3.15) gives

$$\theta_v - \theta_p = \frac{\pm\left[(\theta_p')^2 - (\theta_v')^2\right]}{2} \tag{3.16}$$

Comparison of Equations (3.16) and Equations (3.5) shows that the vertices are on the output phase point arcs including the zero trajectories which lead to the particular point

The phase plane picture of the locus is clarified by referring to Figure 3.3. In part (A) of the figure the boundaries of the two leaf-shaped regions are loci corresponding to the particular point shown as a small circle on the θ axis. The smaller region is for a smaller $\Delta\tau$ Positive loci are the lower parabolic arcs; negative loci, the upper. In part (B) of the figure, similar loci are shown which correspond to the particular point at the right edge of the figure.

Figure 3.3 will be used to compare loci for switch programs of more than one switch with the locus for a one-switch program for the same specified travel time. First, however, the use of the locus concept to time output phase point movement to cause interception of the input phase point will be discussed.

The input signal is taken as a known function of time, so that the future phase plane path of the input phase point is known. The input is limited to signals giving continuous phase plane paths. The travel time for the input phase point to reach any point on its future path

from its instantaneous location is known. For each succeeding point on the future input path a one-switch locus can be constructed which corresponds to output phase point movement to the particular point in a $\Delta\tau$ equal to the actual input travel time to the point. As these succeeding loci are constructed, eventually a first one will be found which contains the output phase point if interception is possible. This locus corresponds to the future location of the input phase point at which interception is first possible by a one-switch program, In fact, it corresponds to the point for minimum time interception for a program of any number of switches, because higher switch loci for each succeeding point are shown below to be within the region bounded by the one-switch locus. Due to the continuity condition imposed above on the input signal, the output phase point cannot get into such a region without first passing through a one-switch locus. Zero-switch loci correspond to the end points of the one-switch locus.

To see that higher-switch loci for reaching a particular point in a certain $\Delta\tau$ are within the region bounded by the one-switch loci for the same $\Delta\tau$, consider Figure 3.3. For particular points on the θ axis, part (A) of the figure is used. The larger locus is taken as corresponding to some fixed $\Delta\tau = (\Delta\tau)_l$. The smaller locus represents the case for a $\Delta\tau = (\Delta\tau)_s$ which is less than $(\Delta\tau)_l$ Let $\Delta_1\tau$ be the difference between the two,

$$\Delta_1\tau = (\Delta\tau)_l - (\Delta\tau)_s \tag{3.17}$$

Starting from any point on the smaller positive locus (lower arc) a point on the larger positive locus may be generated by following

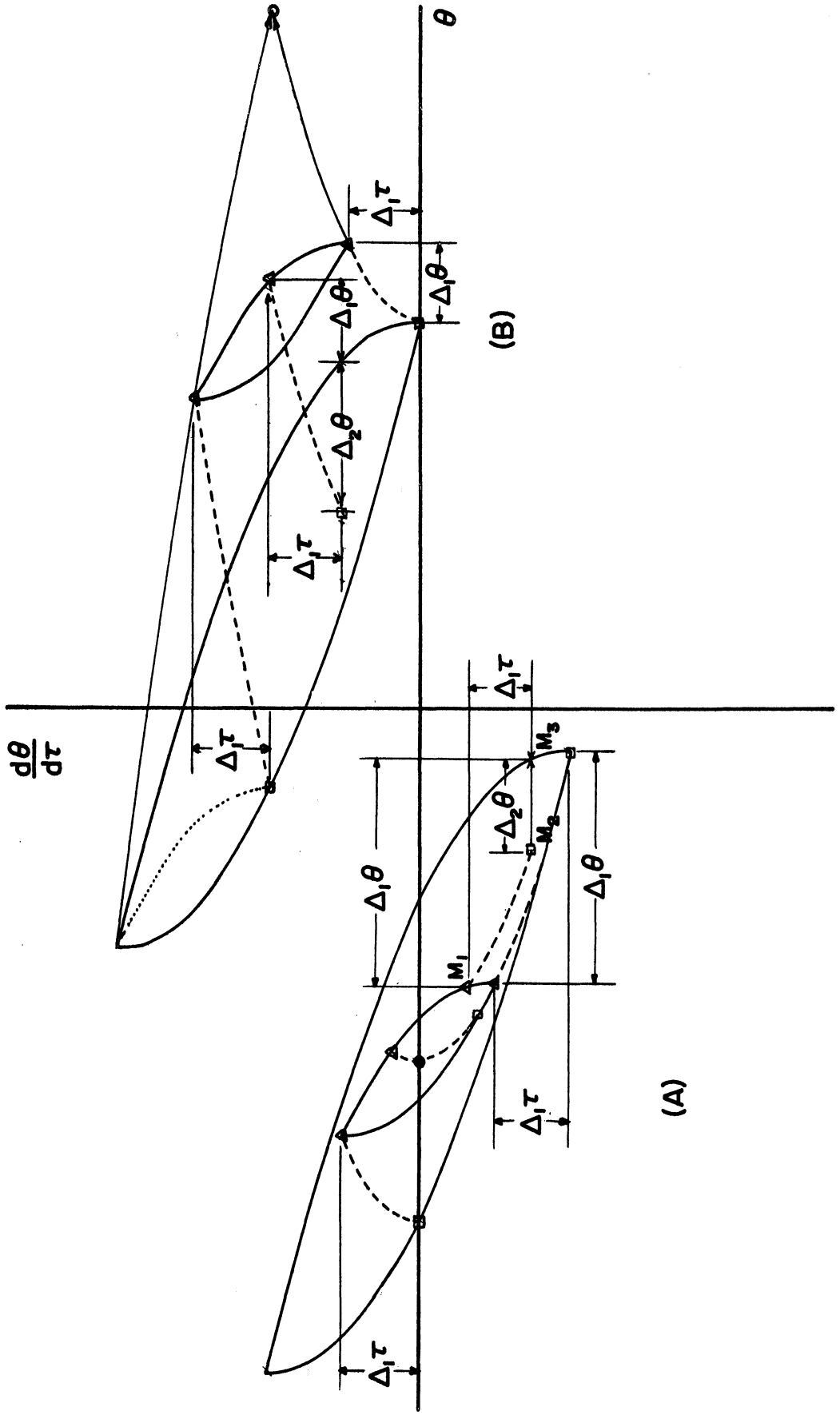

Figure 3.3 One-Switch Loci, Second Order Contactor Servo with Inertia Only.

a positive trajectory backward in time for a time of $\Delta_1\tau$. This is illustrated in the figure by the dashed lines from the triangles at the ends of the smaller locus to the two squares on the larger locus. Using Equation (3.3), the time length is shown as a distance in the θ' direction. From the continuity of the smaller locus and the uniqueness and space-filling properties of the family of positive trajectories, it can be seen that the part of the larger positive locus between the two squares is generated from the points on the smaller positive locus.

A different arc between the same two squares may be generated by moving back in time $\Delta_1\tau$ along positive trajectories starting at every point of the smaller negative locus. Each point of this arc will be above the point with the same θ coordinate on the part of the larger positive locus between the two squares. Also, as will be shown in the next paragraph, each point of this arc will be to the left of the point with the same θ' coordinate on the larger negative locus. Thus, this second arc between the two squares, will be completely within the region bounded by the larger locus.

Consider any point, M_1 on the smaller negative locus, which generates a point M_2 on this second arc. Because the negative loci are translated curves of the same form and orientation as noted above, a point, M_3 , on the larger negative locus is generated by such translation from M_1 on the smaller locus. M_2 and M_3 have the same θ' coordinate as shown by Equation (3.13). M_2 is to the left of M_3 due to the properties of the respective parabolic trajectories which generate them from M_1 .

The arc of all points M_2 is merely the locus of points for the case of output phase point movement to the particular point in time

$(\Delta\tau)_\ell$ by means of a certain positive-negative-positive, two-switch program. This is the two-switch program whose first switch is on the chosen, smaller locus. It is entirely within the region bounded by the one-switch locus. The two-switch locus of negative-positive-negative order is similarly within the region. The result holds for any $(\Delta\tau)_4$ less than $(\Delta\tau)_\ell$ and for any $(\Delta\tau)_\ell$. Thus, for particular points on the θ axis, two-switch loci are always within the region bounded by the one-switch locus for the same $\Delta\tau$.

The same results can be shown for points above the θ axis by using Figure 3.3 (B). The symmetry of the trajectories about the θ axis extends them to points below the θ axis.

Figure 3.3 (B) will be used for consideration of the three-switch case. Take any point on the smaller negative locus. For convenience of display, the top end point of the locus will be used. Consider this point as the particular point to be arrived at by a one-switch program of negative-positive order in time $\Delta_1\tau$ and find the corresponding negative locus. It is easily seen that the dotted line represents the desired locus. As the chosen point on the smaller negative locus is selected lower and lower, the dotted line moves correspondingly lower and lower. Its upper end rides the larger negative locus, and its lower end rides the two-switch locus of positive-negative-positive order previously described. This result and similar considerations for the other three-switch locus show that three-switch loci are entirely within the region bounded by the one-switch locus for the same $\Delta\tau$.

Successive application of these analyses to points on higher-switch loci will give the result that all loci for higher-switch

programs are within the region bounded by the one-switch locus for the same $\Delta\tau$.

Thus, the interception problem reduces to determining the first one-switch locus containing the output phase point because the output phase point location on this locus fixes the unique path for minimum time interception. To do this, let future input values and travel times be swept through Equations (3.11) until one of the equations is satisfied with actual output phase point coordinates inserted for θ and θ' . For this swept locus scheme, Equations (3.11) will be given in terms of input values. Let f and f' be the instantaneous θ and θ' coordinates respectively of the input phase point. The instantaneous time is represented by τ , and an increment of time measured into the future from τ is designated $\Delta\tau_s$. This increment of time is to be varied, or swept, through values from zero to as large a positive value as needed. It is called the sweep time increment. The actual future time equaling τ plus $\Delta\tau_s$ is labeled τ_s . The future values of f and f' corresponding to future time τ_s are f_s and f'_s respectively. The new equations are

$$\theta - \left[f_s - f'_s \Delta\tau_s \mp \frac{(\Delta\tau_s)^2}{2} \right] = \frac{\pm \left[\theta' - (f'_s \pm \Delta\tau_s) \right]^2}{4} \qquad (3.18)$$

If switching could be done instantaneously when the output phase point reaches the switch point on its interception path, it might be worthwhile for a switching mechanism to store information describing switch point location. However, as the output phase point will override the switch point due to switching time lags, it actually will be faced with a one-switch intercept condition once more. Therefore, a switching

computer which rapidly and repetitively determines initial forcing by a swept locus scheme would be sufficient for all switch determination. As long as the repetitions are fast enough, a good approximation to the intercept trajectory should be achieved and the expense of a switch-point memory device eliminated.

In an actual servo such a method could be used to determine all contactor switching with a continuous forcing mode added to the servo to be used when the output phase point enters a limited region around the error phase space origin. Such an arrangement falls under McDonald's dual mode idea presented in Chapter II.

It is worth noting that the switch method described above is consistent with the fact that for the type servo being considered, there are always only two possible choices, positive or negative forcing.

To illustrate the swept locus switching idea and relate it to the switch-curve approach of Chapter II, some commonly analyzed input signals are illustrated in Figures 3.4 through 3.7.

For a constant input signal of $f = f_s = 1$ and $f' = f'_s = 0$ loci are shown for three values of $\Delta\tau_s$ in Figure 3.4 (B). The parabolic arcs bounding the innermost leaf-shaped region are the loci for $\Delta\tau_s = 1$. The positive locus is on the negative θ side of the dashed line. Arcs bounding the intermediate leaf-shaped region are the loci for $\Delta\tau_s = 2$, and the outermost arc for $\Delta\tau_s = 3$. The figure shows that, as the loci sweep out the phase plane, the positive locus will sweep over the area to the left of the dashed line, and the negative locus, the area to the right. The dashed line described by the contiguous points of the swept loci divides the phase plane into regions of

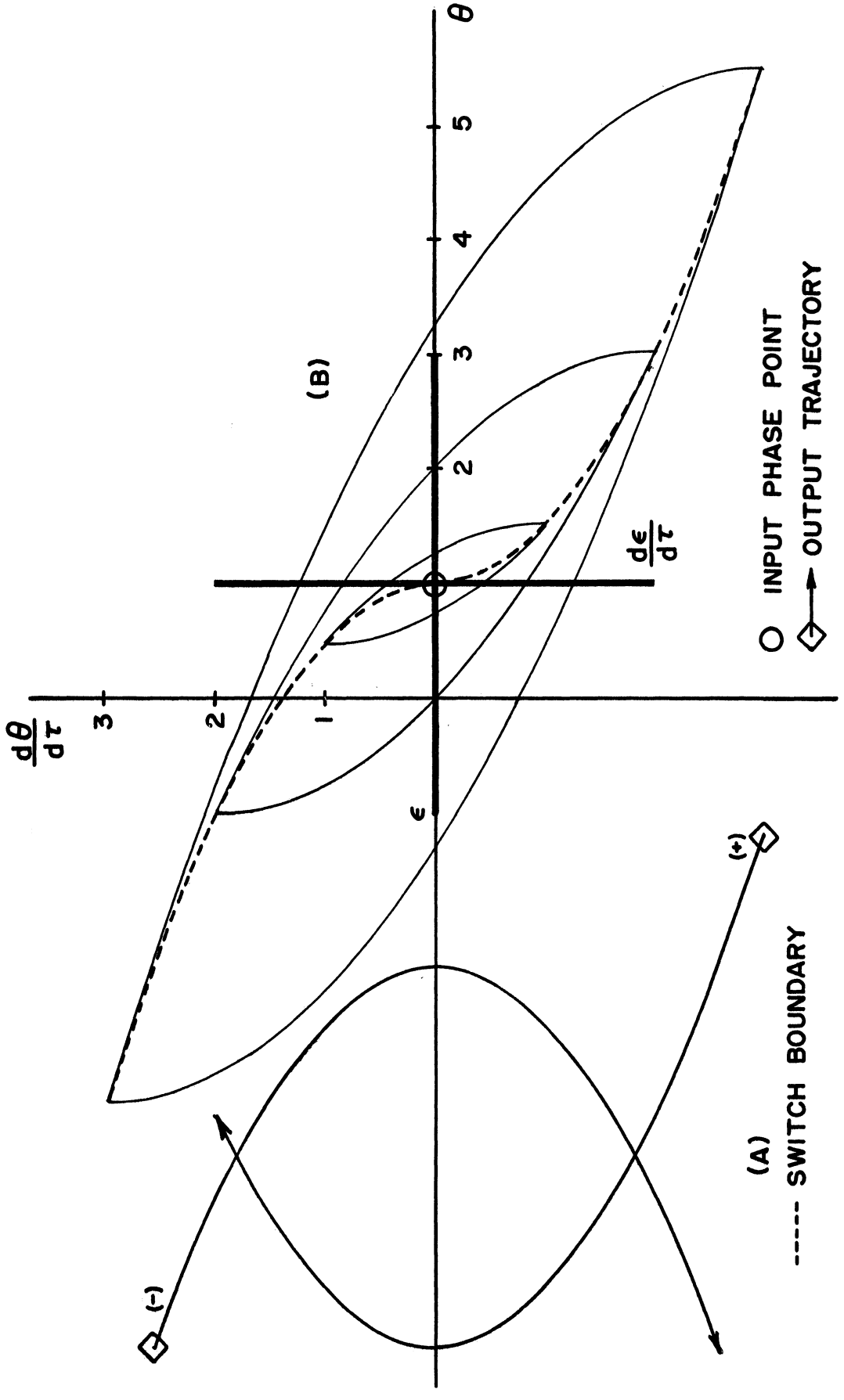

Figure 3.4 Constant Input, Contactor Servo with Inertia Only.

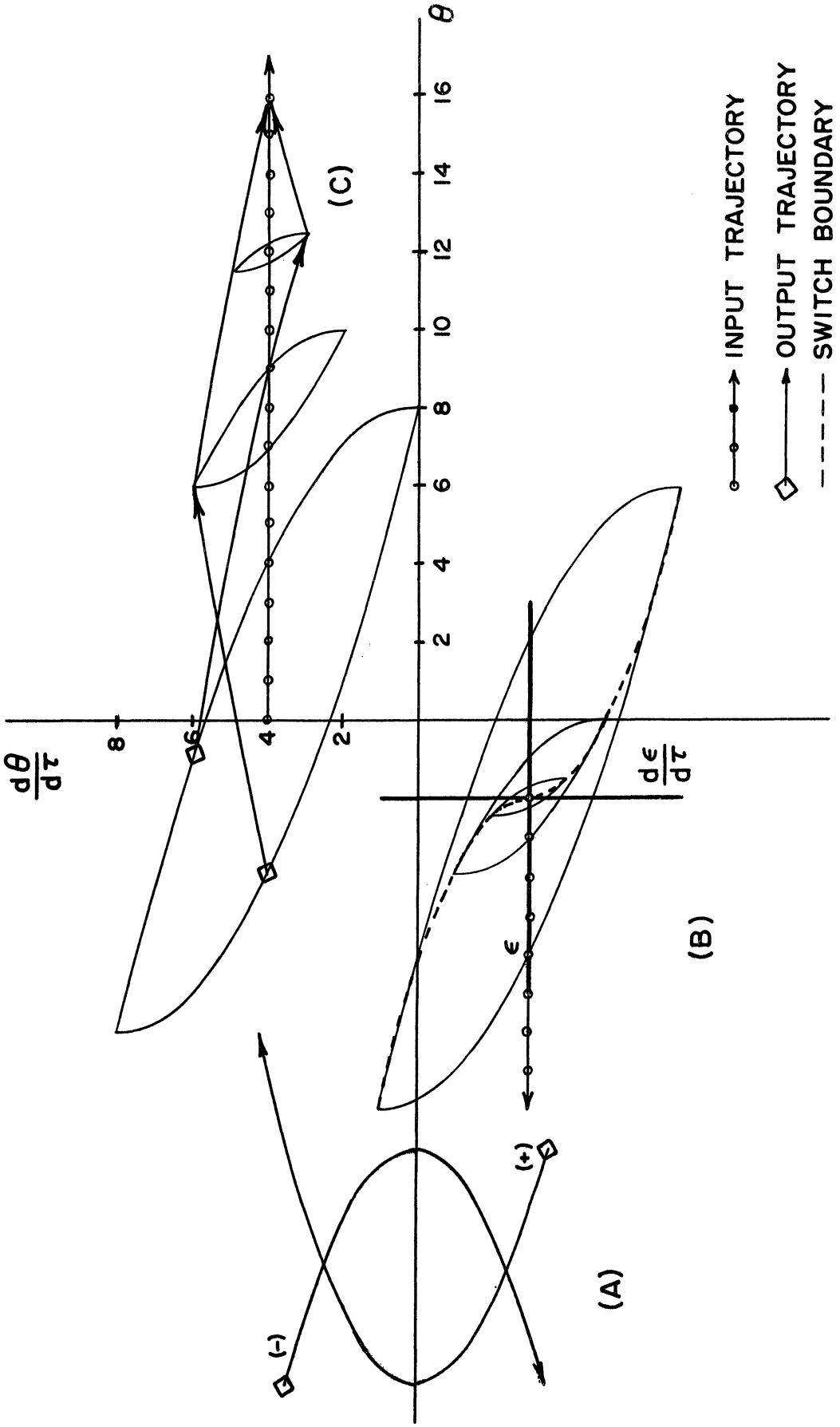

Figure 3.5 Constant Velocity Inputs, Contactor Servo with Inertia Only.

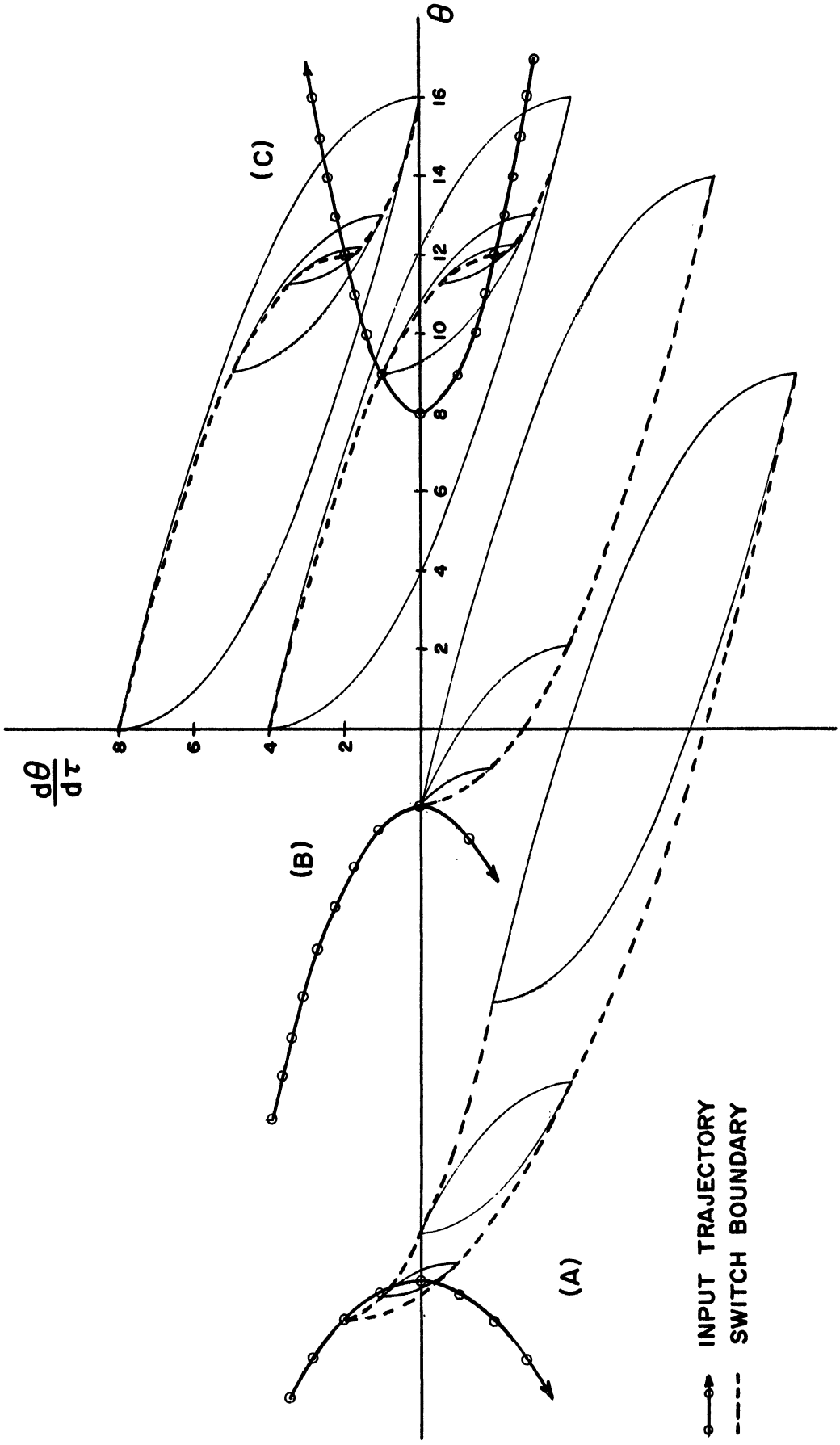

Figure 3.6 Constant Acceleration Inputs, Contactor Servo with Inertia Only.

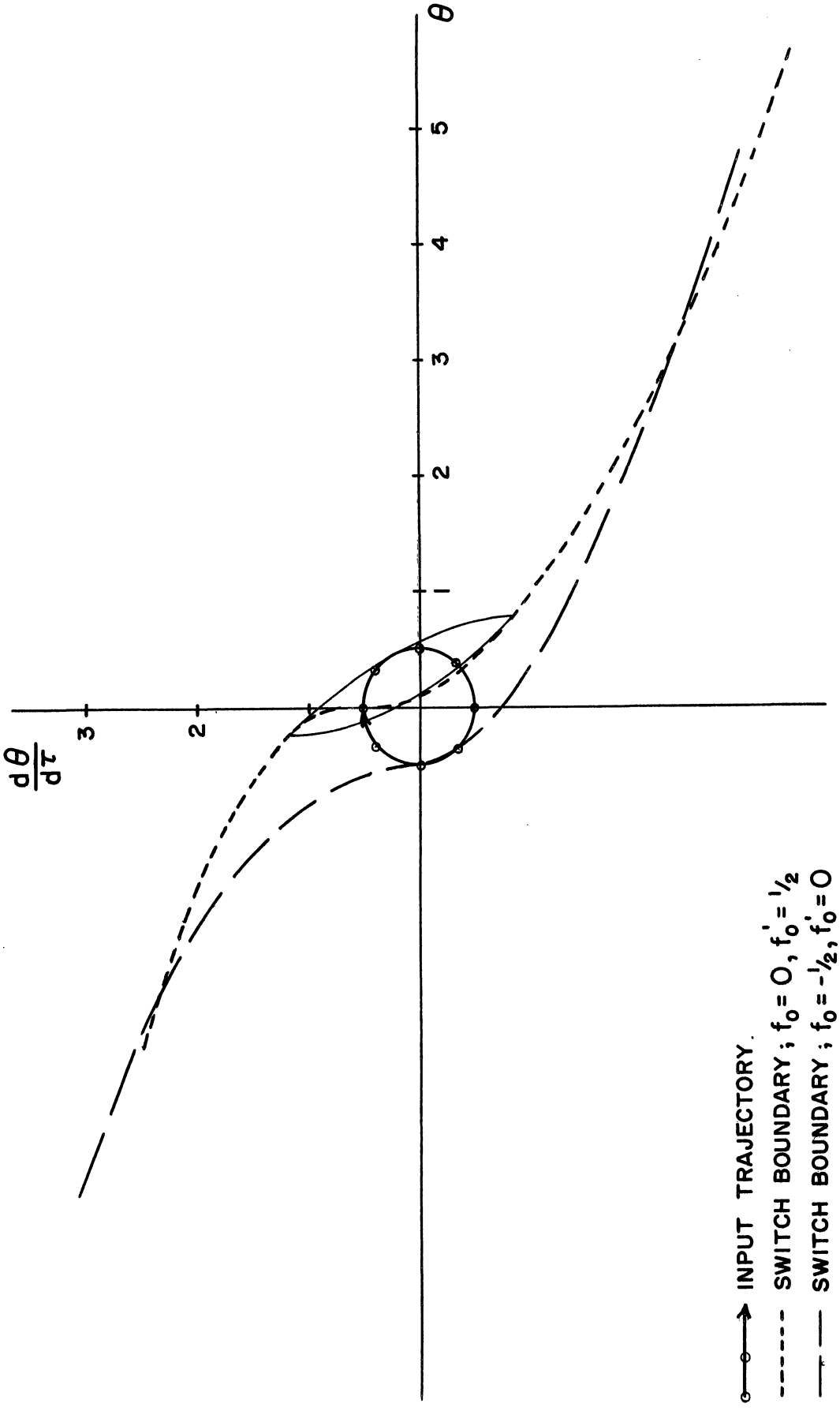

Figure 3.7 Input of Form (Sine τ)/2, Contactor Servo with Inertia Only.

positive and negative forcing. Therefore, it is a switch boundary. Error, error-rate axes are indicated, and comparison with Figure 2.2 shows the switch boundaries are the same. Note that the two contiguous points are the zero-switch loci.

Figure 3.5 illustrates the case of constant velocity input signals. In Figure 3.5 (B) is an instantaneous switch boundary through the initial location of the input phase point. Again the same error phase plane switching boundary as shown in Figure 2.2 is obtained. Output phase points on the innermost loci could intercept the input phase point in $\Delta\tilde{\tau}=1$ with perfect switching. Those on the outermost loci would have a travel time of $\Delta\tilde{\tau}=4$. In Figure 3.5 (C) sample perfect switch intercept trajectories are shown for two points on loci corresponding to an initial $\Delta\tilde{\tau}_s=4$. The intermediate loci show the contiguous points or zero-switch loci, on the zero trajectories.

Switch boundaries described by swept loci are shown in Figure 3.6 for three parabolic inputs. In the case of a constant acceleration input signal with acceleration greater than that of the servo, the accessibility region of the phase plane is limited. Figure 3.6 (A) shows a limited accessibility region between the dashed lines drawn from the instantaneous position of the input phase point. The equal acceleration case is shown in Figure 3.6 (B). Here the instantaneous accessibility region is limited to the area between the dashed line and a line parallel to the θ axis through the instantaneous input phase point. Input acceleration is less than servo acceleration for Figure 3.6 (C). The accessibility region covers the whole phase plane, but the switch boundaries differ above and below the input phase point. Equations for the switch boundaries are easily derived for constant acceleration inputs to this simple servo.

Sample switch boundaries are shown for a sinusoidal input in Figure 3.7. The swept loci would still have the same shape and orientation in space, but the switch boundaries vary in shape and orientation.

For arbitrary known input signals to this servo, this variance of the switch boundaries could seemingly cause difficulty in designing a computer which would determine the sign of forcing from switch boundary information. It is believed that it would be easier to design a computer operating on the swept locus basis. The logic of one such scheme will be described in Chapter IV, which covers an analog computer study of the theory developed in this chapter. The approach used above will now be applied to another servo.

Second Order Contactor Servo with Inertia and Viscous Damping

Equations (2.9), the differential equations for a second order contactor servo with inertia and viscous damping, are repeated here.

$$\theta'' + a\theta' = \pm 1 \tag{3.19}$$

It is convenient to treat this servo in its principal coordinate phase plane. Let the principal coordinates be Z_1 and Z_2 where

$$Z_1 = a\theta + \theta' \tag{3.20}$$

and

$$Z_2 = a\theta' \tag{3.21}$$

These equations may be derived in the same way from Equations (3.19) as were Equations (2.22) and (2.23) from Equations (2.11). The equations

of the Z_1, Z_2 phase plane trajectories are

$$Z_2 \mp 1 = (Z_{2o} \mp 1) \exp\left[\mp a(Z_1 - Z_{1o})\right] \quad , \tag{3.22}$$

and the time-distance relationships are

$$\tau - \tau_o = \pm(Z_1 - Z_{1o}) \tag{3.23}$$

Sample phase plane trajectories are shown in Figure 3.8. It is evident that translation in the Z_1 direction does not affect trajectory shape as Equations(3.22) indicate. The horizontal dashed lines indicate the velocity limiting values, $\pm 1/a$, expected from inspection of Equations(3.19).

The three points (A), (B), and (C) represent the types of particular points to which it may be desired to move the output phase point. Zero trajectories to the points are again in heavy lines. It is easily seen that point (A), a point on the Z_1 axis, is accessible from any point in the phase plane by a unique path with no more than one switch of forcing. This also applies to point (B), a point off the Z_1 axis but within the velocity-limit boundaries, except that in the region between the heavy dashed line and the negative zero trajectory and above the positive zero trajectory two one-switch paths are available for each point. All points within the velocity-limit boundaries are accessible from the whole plane by one-switch paths. Point (C) is accessible only from the region above the zero trajectories. Two one-switch paths are available for every point within this region. Point (C) is not accessible from any other part of the phase plane by more than one switch either.

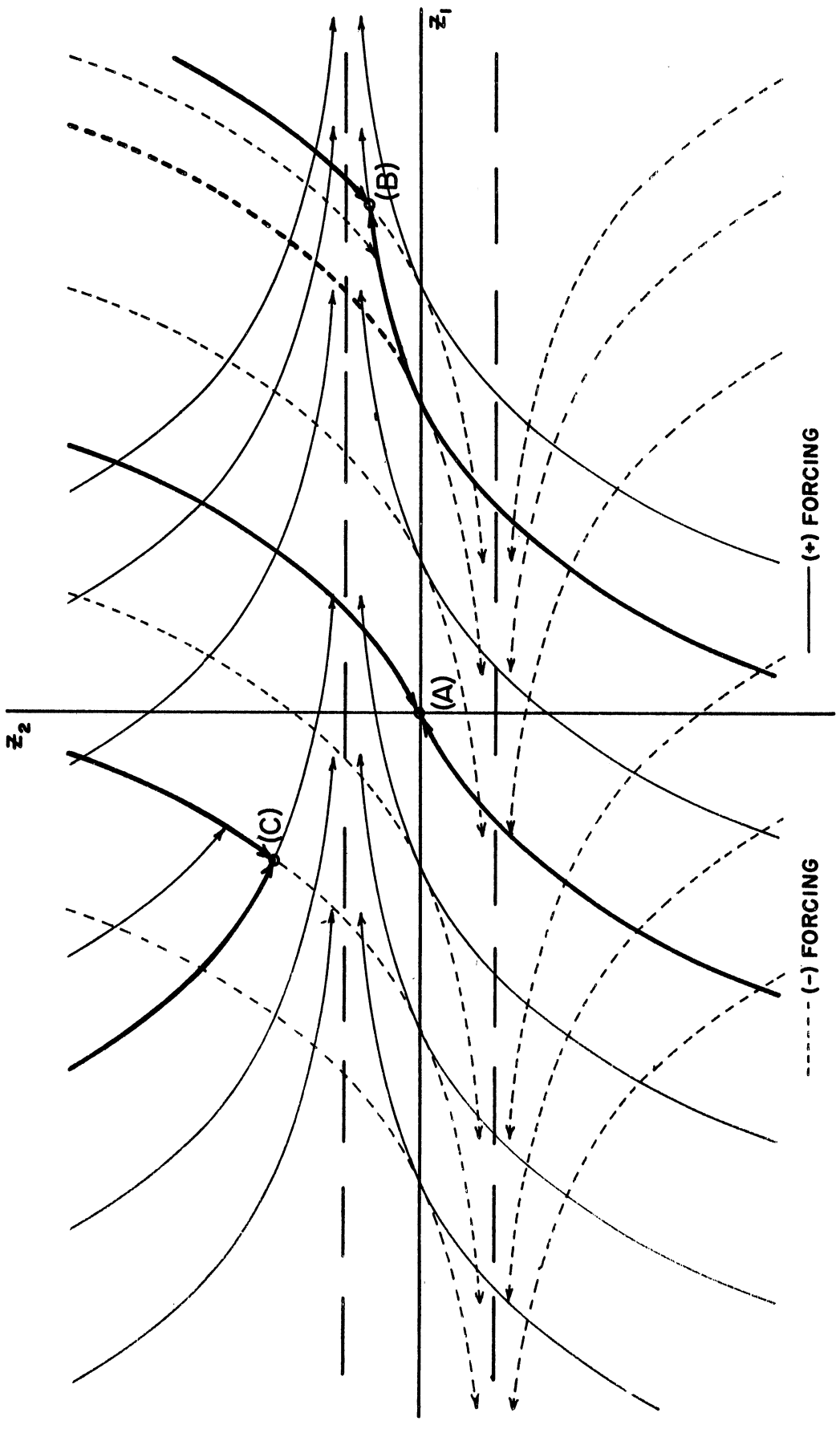

Figure 3.6 Principal Coordinate Phase Plane Trajectories, Second Order Contactor Servo with Inertia and Viscous Damping.

The expressions for the curves containing the positive and negative loci will be derived directly in terms of input values for this case. Some new symbology is needed to develop these expressions in the Z_1, Z_2 phase plane. Let Z_1 and Z_2 be the instantaneous coordinates of the output phase point and Z_{11} and Z_{21} be the coordinates of the intermediate switch point. Let P_1 and P_2 be the instantaneous coordinates of the input phase point where

$$P_1 = af + f' \quad , \tag{3.24}$$

and

$$P_2 = af' \quad . \tag{3.25}$$

Then, P_{15} and P_{25} locate the input phase point at time equal to τ plus $\Delta\tau_S$.

For the output phase point to be on the positive or negative locus of (P_{1S}, P_{2S}) , equations describing the arc to the zero trajectory and the zero trajectory itself are respectively

$$Z_{21} \mp 1 = (Z_2 \mp 1)\exp\left[\mp a(Z_{11} - Z)\right] \quad , \tag{3.26}$$

and

$$P_{2S} \pm 1 = (Z_{21} \mp 1) \quad \left[\pm a(P_{1S} - Z_{11})\right] \tag{3.27}$$

The time equations are

$$Z_{11} = \frac{\pm\Delta\tau_S + Z_1 + P_{1S}}{2} \tag{3.28}$$

The switch point coordinates Z_{11} and Z_{21} are to be eliminated from Equations (3.26), (3.27), and (3.28) leaving expressions describing the interception loci of (P_{1S}, P_{2S})

Substituting for Z_{11} from Equations (3.28) in Equations (3.27) and (3.26) and for Z_{21} in Equations (3.26) from Equations (3.27) gives

$$(P_{2s} \pm 1)\exp\left[\mp\frac{a}{2}(\mp\Delta\tau_s - Z_1 + P_{1s})\right] \mp 2 = \qquad (3.29)$$

$$= (Z_2 \mp 1)\exp\left[\mp\frac{a}{2}(\pm\Delta\tau_s - Z_1 + P_{1s})\right]$$

Solving for $(Z_2 \mp 1)$ gives

$$(Z_2 \mp 1) = (P_{2s} \pm 1)\exp(a\Delta\tau_s) \mp 2\exp\left[\pm\frac{a}{2}(\pm\Delta\tau_s - Z_1 + P_{1s})\right] \qquad (3.30)$$

which may be written as

$$Z_2 - \left[\pm 1 + (P_{2s} \pm 1)\exp(a\Delta\tau_s)\right] = \mp 2\exp\left\{\mp\frac{a}{2}\left[Z_1 - (P_{1s} \pm \Delta\tau_s)\right]\right\}. \qquad (3.31)$$

Equations (3.31) reveal that the positive locus is on an exponential curve of form $Z_2 = -2\left[\exp(-aZ_1/2) - 1\right]$ The equation in this form describes a curve through the origin of coordinates. Equation (3.31) shows that the shape and orientation of this curve is fixed, but that its location in the phase plane is determined by a translation of the origin which depends on $\Delta\tau_s$ and corresponding input values. Similarly, the negative locus is on a translating exponential curve of form $Z_2 = 2\left[\exp(aZ_1/2) - 1\right]$, the general form being that of a curve through the origin of coordinates.

As was done for the first servo treated, it can be shown that the point on each of the curves corresponding to the translated origin of its general form is on the other curve. These translated origins are also on the zero trajectories into the point (P_{1s}, P_{2s}) .

Loci for the three types of particular points of Figure 3.8 are shown as the boundaries of the leaf-shaped regions in Figure 3.9. Again the larger loci are for greater travel times than the smaller. For this servo, just as for the previous one, it can be shown that loci for higher-switch paths are included within the regions bounded by the one-switch locus for the particular point for the same travel time. This, then, results in the same minimum intercept time as before for input signals with continuous phase paths. Of course, for the servo to follow the input signal, it must be such that the input phase point stays between the limiting velocity boundaries.

Consideration of part (A) of Figure 3.9 is sufficient to show that higher switch loci are within the region bounded by the one-switch locus. The remarks are easily applied to parts (B) and (C) of the figure. The upper arc of each locus is the positive locus, and its translating origin is at its upper end point. Lower arcs are negative loci with translating origins at the lower end-points.

Moving backwards in time along positive trajectories from points on the smaller positive locus, the corresponding part of the larger positive locus is found just as before. It is that part between the small squares on the dashed lines from the ends of the smaller locus. An intermediate point on the smaller positive locus and its corresponding point on the larger positive locus are also shown.

Moving backwards in time the same way from points on the smaller negative locus gives an arc within the region bounded by the larger locus. One point of this arc is shown. It corresponds to a point on the smaller negative locus with the same Z_2 coordinate as the

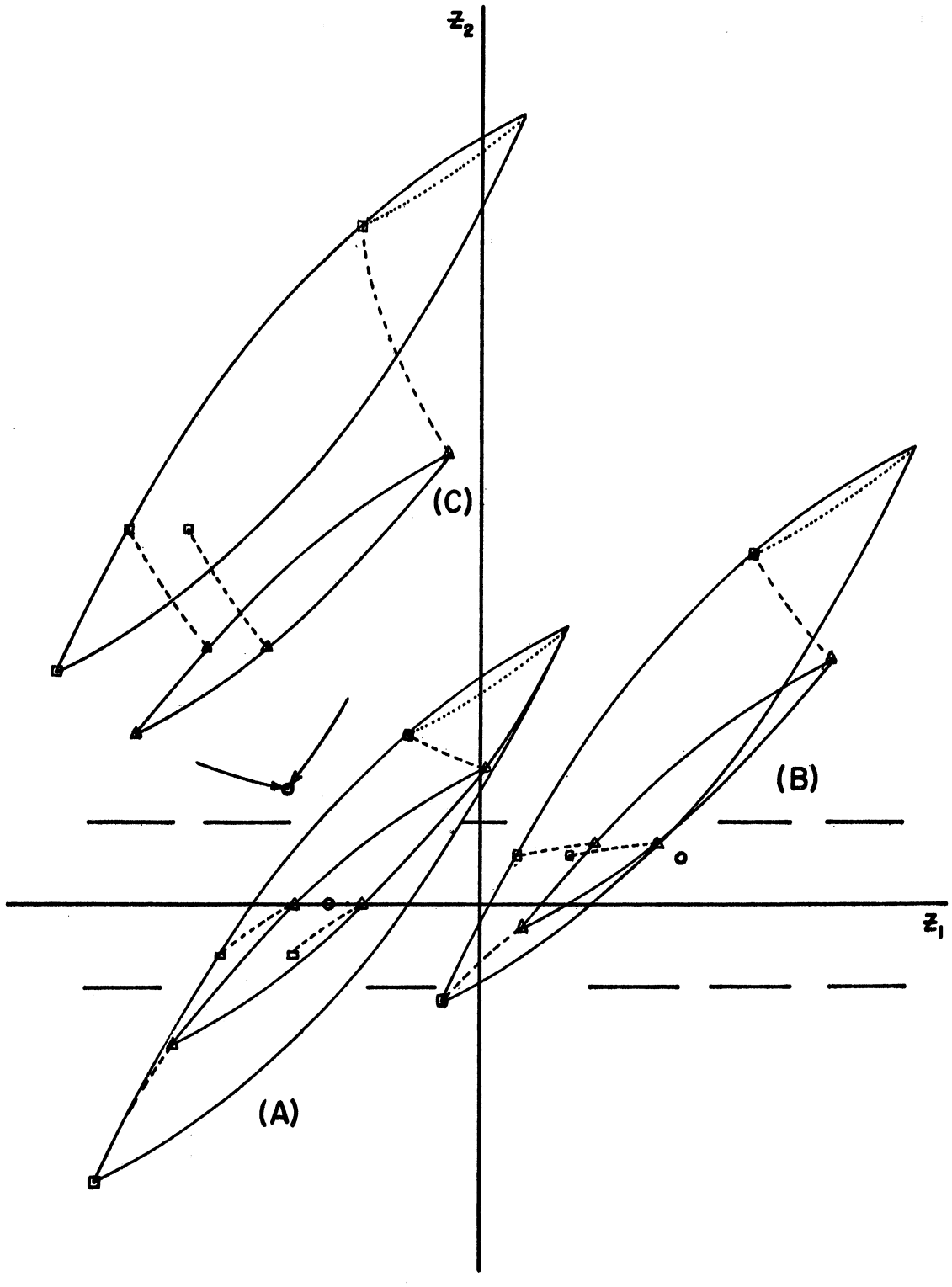

Figure 3.9 One-Switch Loci, Second Order Contactor Servo with Inertia and Viscous Damping.

intermediate point mentioned above. The translatability in the $\bar{z}_1$ direction of positive trajectories shows this point, the small square, is to the right of the larger positive locus.

Proof that the point is above the larger negative locus is needed. The two negative loci are merely translated curves of the same form and the translation between corresponding points on the two is shown by the translation of the lower end-points. Properties of the positive trajectories show that the small square is above the point on the larger negative locus corresponding to translating its base point on the smaller negative locus. The arc is then completely above the larger negative locus. So, the arc which is the desired two-switch positive locus is entirely within the region. The arguments used for the previous servo are then applicable to show that all two-switch positive loci for arriving at a particular point in a specified time are within the region bounded by the corresponding one-switch locus.

The previous arguments also carry over for the three-switch case which then allows extension to the higher switch cases.

Common input signals are treated in Figures 3.10 through 3.12.

Figure 3.10 is for a constant input signal. a is taken as one. Typical output arcs are shown in part (A) of the figure. The positive and negative swept loci are shown in part (B). Positive loci are to the left of the dashed switch boundary. From inside out loci are shown for $\Delta\tau_s = 1/2$, 1 , and $3/2$.

Figure 3.11 pictures the same servo with constant velocity inputs. In part (A) the zero-switch loci sweep out an instantaneous switching boundary. The velocity term in the differential equation of

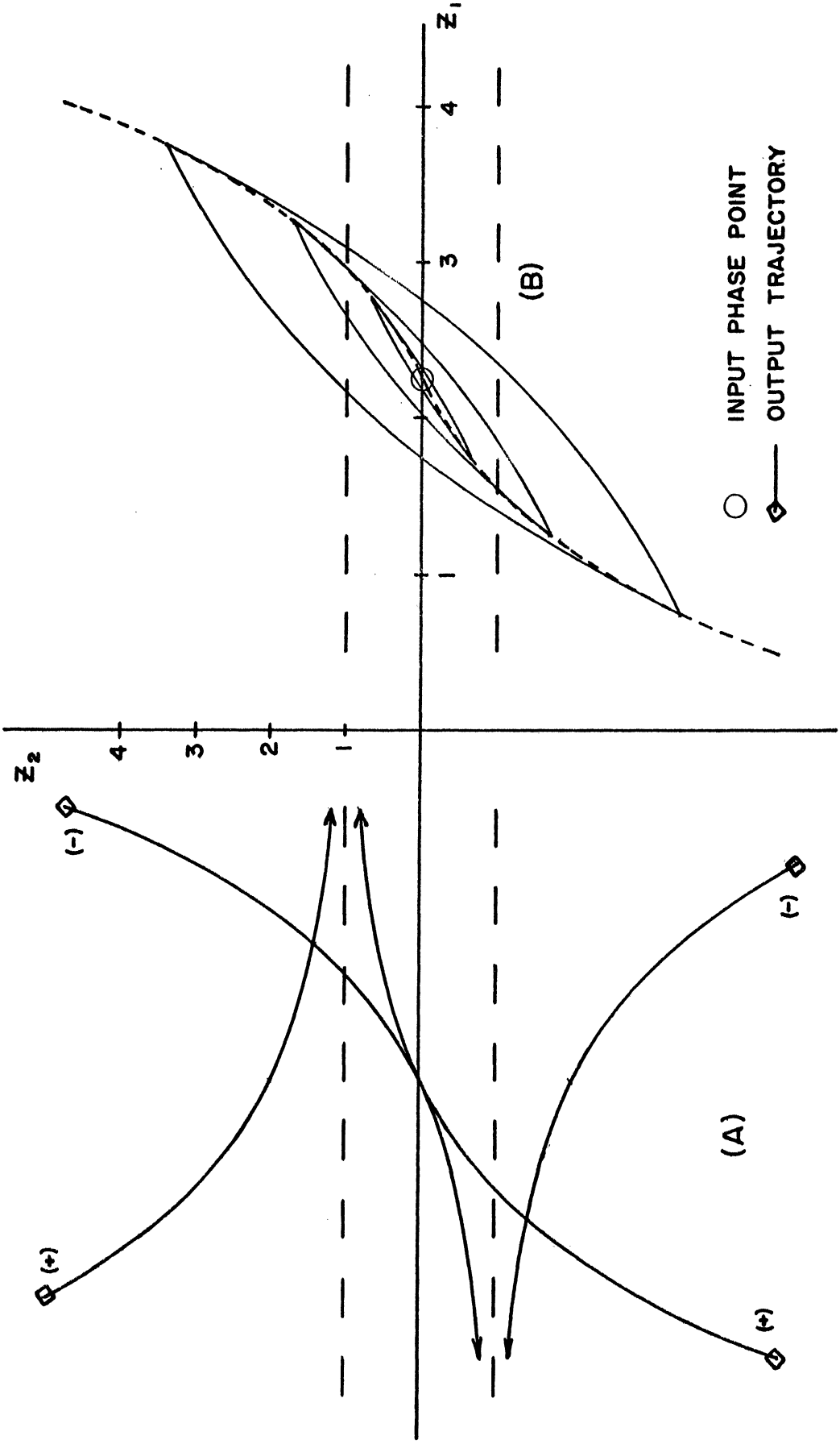

Figure 3.10 Constant Input, Contactor Servo with Inertia and Viscous Damping.

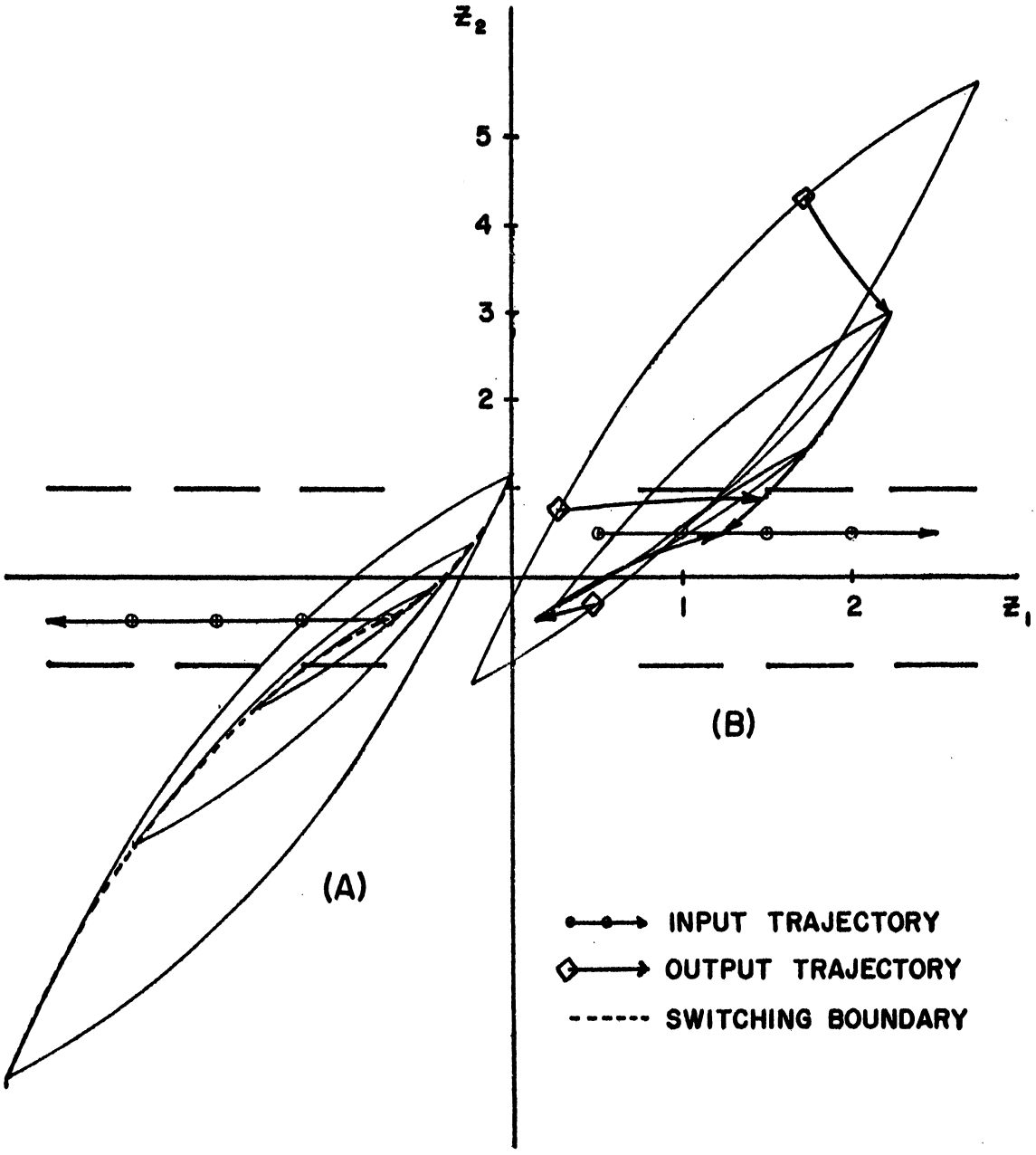

Figure 3.11 Constant Velocity Inputs, Contactor Servo with Inertia and Viscous Damping,

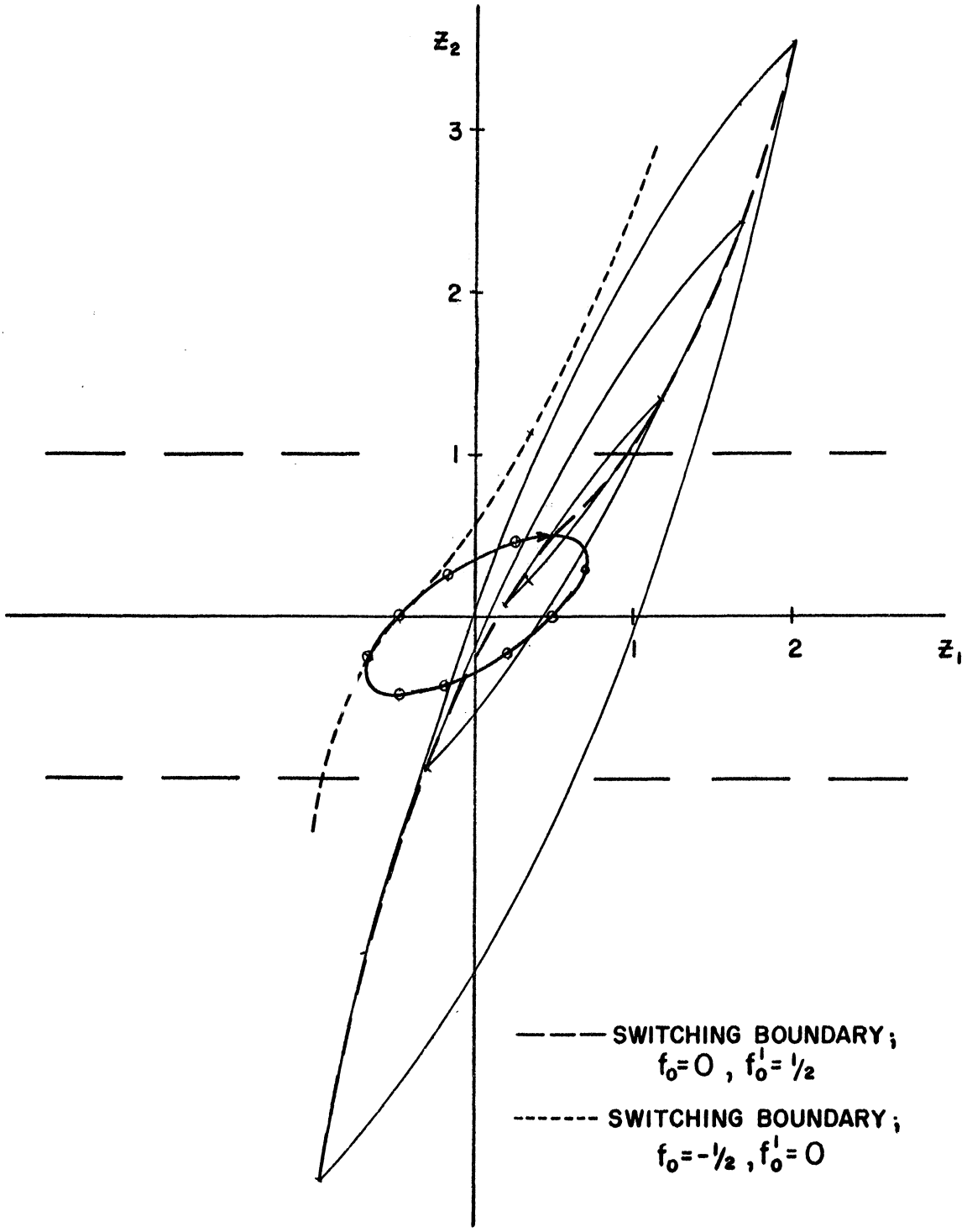

Figure 3.12 Input of Form (Sine τ)/2, Contactor Servo with Inertia and Viscous Damping.

this servo causes the switch boundary to be unsymmetrical through the instantaneous input phase point. In part (B) of the figure, three sample intercept trajectories are shown for an initial $\Delta\tau_s = 3/2$. Intermediate loci are shown for $\Delta\tau_s = 1$ and $\Delta\tau_s = 1/2$.

Figure 3.12 shows two instantaneous switching boundaries for a sinusoidal input signal. The variation is evident.

A switching scheme for this servo utilizing the swept locus approach is included in the computer study in Chapter IV.

A Third Order Contactor Servo

The third order contactor servo to be analyzed is of the type whose action may be described by the differential equations:

$$\theta''' + (K_2+K_3)\theta'' + K_2K_3\theta' = \pm 1 \quad , \tag{3.32}$$

or

$$D(D + K_2)(D + K_3)\theta = \pm 1 \quad , \tag{3.33}$$

where D stands for the differential operator $d/d\tau$, the K's are distinct real positive constants, and $K_2 > K_3$.

Equations (3.32) may be replaced by the first order equations

$$X_1' = X_2 \quad , \tag{3.34}$$

$$X_2' = X_3 \quad , \tag{3.35}$$

and

$$X_3' = -(K_2 + K_3)X_3 - K_2K_3X_2 \pm 1 \quad , \tag{3.36}$$

by letting

$$X_1 = \theta \quad , \tag{3.37}$$

$$X_2 = \theta' \quad , \tag{3.38}$$

and

$$X_3 = \theta'' \quad . \tag{3.39}$$

The equations of motion given in Equations (3.34), (3.35), and (3.36) may be written in vector-matrix form as

$$\begin{pmatrix} X_1 \\ X_2 \\ X_3 \end{pmatrix}' = \begin{Vmatrix} 0 & 1 & 0 \\ 0 & 0 & 1 \\ 0 & -K_2K_3 & -(K_2+K_3) \end{Vmatrix} \begin{pmatrix} X_1 \\ X_2 \\ X_3 \end{pmatrix} \pm \begin{pmatrix} 0 \\ 0 \\ 1 \end{pmatrix} \tag{3.40}$$

Equations (3.40) may be expressed in terms of principal coordinates Z_1, Z_2, and Z_3 measured along the phase space principal directions of the system. The necessary transformations are

$$\begin{pmatrix} X_1 \\ X_2 \\ X_3 \end{pmatrix} = \begin{Vmatrix} \frac{1}{K_2K_3} & \frac{1}{K_2^2(K_2-K_3)} & \frac{-1}{K_3^2(K_2-K_3)} \\ 0 & \frac{-1}{K_2(K_2-K_3)} & \frac{1}{K_3(K_2-K_3)} \\ 0 & \frac{1}{K_2-K_3} & \frac{-1}{K_2-K_3} \end{Vmatrix} \begin{pmatrix} Z_1 \\ Z_2 \\ Z_3 \end{pmatrix} \quad , \tag{3.41}$$

and

$$\begin{pmatrix} Z_1 \\ Z_2 \\ Z_3 \end{pmatrix} = \begin{Vmatrix} K_2K_3 & K_2+K_3 & 1 \\ 0 & K_2K_3 & K_2 \\ 0 & K_2K_3 & K_2 \end{Vmatrix} \begin{pmatrix} X_1 \\ X_2 \\ X_3 \end{pmatrix} \tag{3.42}$$

The transformed equations are

$$\begin{pmatrix} Z_1 \\ Z_2 \\ Z_3 \end{pmatrix}' = \begin{Vmatrix} 0 & 0 & 0 \\ 0 & -K_2 & 0 \\ 0 & 0 & -K_3 \end{Vmatrix} \begin{pmatrix} Z_1 \\ Z_2 \\ Z_3 \end{pmatrix} \pm \begin{pmatrix} 1 \\ K_2 \\ K_3 \end{pmatrix} \tag{3.43}$$

The equations of motion in the principal directions are

$$Z_1' = \pm 1 \quad , \tag{3.44}$$

$$Z_2' + K_2 Z_2 = \pm K_2 \quad , \tag{3.45}$$

and

$$Z_3' + K_3 Z_3 = \pm K_3 \quad . \tag{3.46}$$

In terms of the output variable θ the principal coordinates are

$$Z_1 = K_2 K_3 \theta + (K_2 + K_3)\theta' + \theta'' \quad , \tag{3.47}$$

$$Z_2 = K_2 K_3 \theta' + K_2 \theta'' \quad , \tag{3.48}$$

and

$$Z_3 = K_2 K_3 \theta' + K_3 \theta'' \quad . \tag{3.49}$$

From solving Equations (3.44),

$$\tau - \tau_0 = \pm (Z_1 - Z_{10}) \quad . \tag{3.50}$$

Solving Equations (3.45) results in

$$Z_2 \mp 1 = (Z_{20} \mp 1) \exp(-K_2 \tau - \tau_0) \quad , \tag{3.51}$$

which, upon substitution from Equations (3.50), can be written

$$Z_2 \mp 1 = (Z_{20} \mp 1) \exp\left[\mp K_2 (Z_1 - Z_{10})\right] \tag{3.52}$$

In similar fashion

$$Z_3 \mp 1 = (Z_{30} \mp 1) \exp\left[\mp K_3 (Z_1 - Z_{10})\right] \tag{3.53}$$

can be obtained by solving Equations (3.46).

Equations (3.52) and (3.53) represent the projections in the Z_1, Z_2 and Z_1, Z_3 planes respectively of the phase space trajectories of the servo's output phase point. The actual trajectories are, of course, the intersections of their projecting cylinders. Sample trajectories are shown in Figure 3.13 for $K_2 = 2$ and $K_3 = 1$. Positive arcs approach the intersection of the $Z_2 = 1$ and $Z_3 = 1$ planes with increasing time. From Equations (3.48) and (3.49), this asymptote can be shown to represent a condition of velocity limitation of $\theta' = 1/K_2K_3$. This velocity limitation is evident from Equation (3.32). Naturally, negative arcs show a similar asymptotic behavior. The asymptotes are shown as heavy dashed lines in parts (A), (B), and (D) of the figure and as dots in part (C). Part (C) shows as a crosshatched region with heavy boundaries the region in the plane to which output phase point motion is confined once the region is entered. In the phase space this determines a cylindrical region about the Z_1 axis within which the input phase point must stay if the servo is to follow the input signal. In a $\theta, \theta', \theta''$ phase space the cylindrical region appears as a combined velocity-acceleration limitation due to the relay output voltage being fixed and finite.

For determination of the interception loci the instantaneous coordinates of the output phase point are Z_1, Z_2, and Z_3. Instantaneous coordinates of the input phase point are P_1, P_2, and P_3 where

$$P_1 = K_2K_3f + (K_2 + K_3)f' + f'' , \tag{3.54}$$

$$P_2 = K_2K_3f' + K_2f'' , \tag{3.55}$$

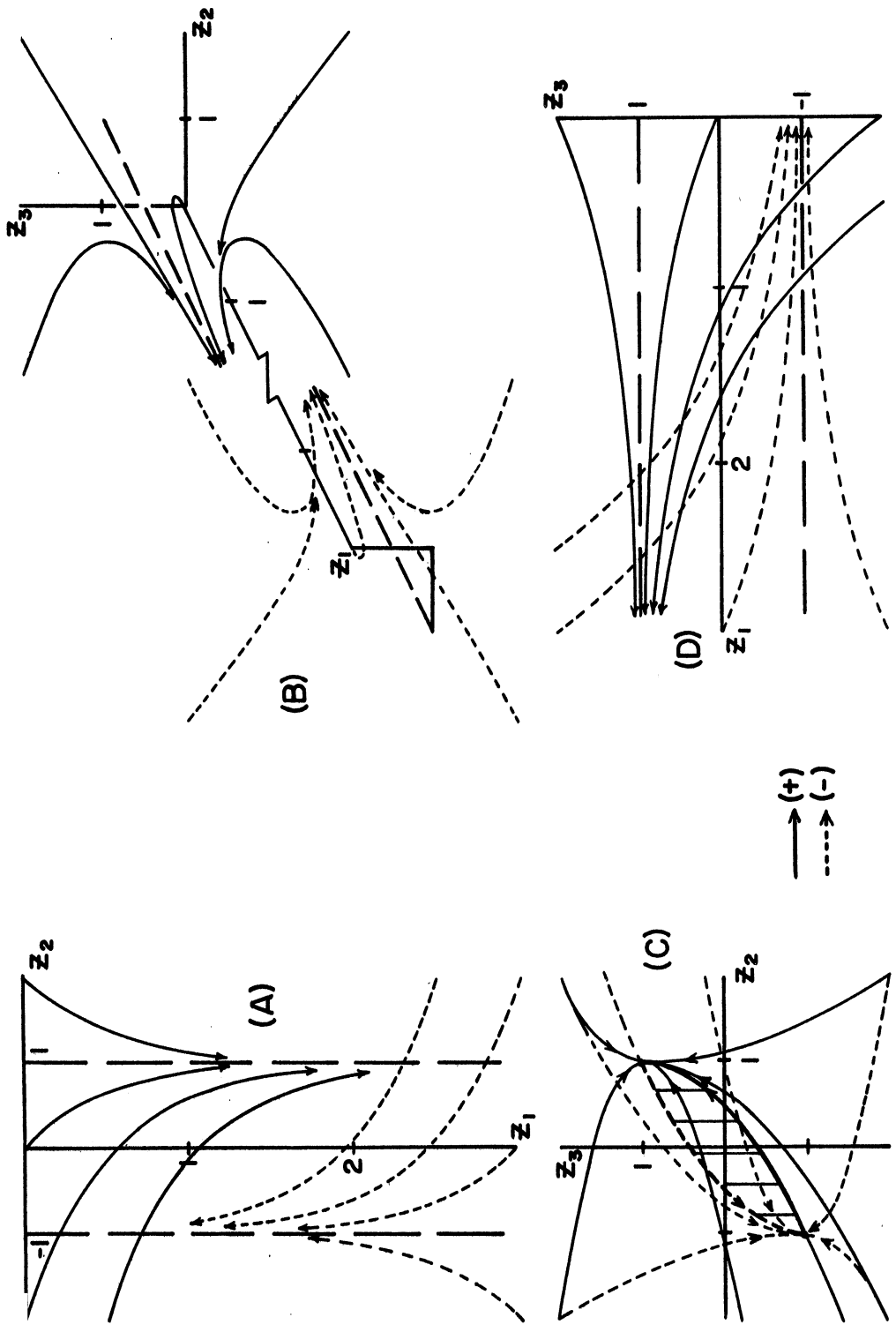

Figure 3.13 Phase Space Trajectories, Third Order Contactor Servo.

and

$$P_3 = K_2 K_3 f' + K_3 f'' \tag{3.56}$$

So, P_{1s}, P_{2s}, and P_{3s} locate the input phase point at a time equal to τ plus $\Delta\tau_s$. For the third order servo, two intermediate switch points are used. The first switch point to be arrived at is given the coordinates Z_{12}, Z_{22}, and Z_{32}; the second, Z_{11}, Z_{21}, and Z_{31}.

Writing the equations of the two projections for each of the three arcs of each intercept trajectory gives

$$Z_{22} \mp 1 = (Z_2 \mp 1) \exp\left[\mp K_2 (Z_{12} - Z_1)\right] , \tag{3.57}$$

$$Z_{32} \mp 1 = (Z_3 \mp 1) \exp\left[\mp K_3 (Z_{12} - Z_1)\right] , \tag{3.58}$$

$$Z_{21} \pm 1 = (Z_{22} \pm 1) \exp\left[\pm K_2 (Z_{11} - Z_{12})\right] , \tag{3.59}$$

$$Z_{31} \pm 1 = (Z_{32} \pm 1) \exp\left[\pm K_3 (Z_{11} - Z_{12})\right] , \tag{3.60}$$

$$P_{2s} \mp 1 = (Z_{21} \mp 1) \exp\left[\mp K_2 (P_{1s} - Z_{11})\right] , \tag{3.61}$$

$$P_{3s} \mp 1 = (Z_{31} \mp 1) \exp\left[\mp K_3 (P_{1s} - Z_{11})\right] \tag{3.62}$$

Using Equations(3.50), the time equations are

$$\Delta\tau_s = \pm (Z_{12} - Z_1) \mp (Z_{11} - Z_{12}) \pm (P_{1s} - Z_{11}), \tag{3.63}$$

which, upon rearrangement, gives

$$Z_{12} - Z_{11} = \frac{\pm \Delta\Upsilon_s + Z_1 - P_{1s}}{2} \tag{3.64}$$

Eliminating Z_{22} between Equations (3.57) and (3.59) gives

$$\begin{aligned} Z_{21} \pm 1 = (Z_2 \mp 1)\exp\left[\mp K_2(2Z_{12} - Z_{11} - Z_1)\right] \\ \pm 2\exp\left[\pm K_2(Z_{11} - Z_{12})\right] \end{aligned} \tag{3.65}$$

Then, eliminating Z_{21} between Equations (3.65) and (3.61) gives

$$\begin{aligned} P_{2s} \mp 1 = (Z_2 \mp 1)\exp\left[\mp K_2(2Z_{12} - 2Z_{11} - Z_1 + P_{1s})\right] \\ \pm 2\exp\left[\mp K_2(Z_{12} - 2Z_{11} + P_{1s})\right] \mp 2\exp\left[\mp K_2(P_{1s} - Z_{11})\right] \end{aligned} \tag{3.66}$$

Equations(3.66) can be rearranged as

$$\begin{aligned} (Z_2 \mp 1)\exp(\pm K_2 Z_1) - (P_{2s} \mp 1)\exp\left[\pm K_2(2Z_{12} - 2Z_{11} + P_{1s})\right] = \\ = \pm 2\exp(\pm K_2 Z_{12})\left\{\exp\left[\pm K_2(Z_{12} - Z_{11})\right] - 1\right\} \end{aligned} \tag{3.67}$$

Substituting for $(Z_{12} - Z_{11})$ from Equations (3.64) and solving for $\exp(\pm K_2 Z_{12})$ gives

$$(\pm K_2 Z_{12}) = \frac{\exp(\pm K_2 Z_1)\left[Z_2 \mp 1 - (P_{2s} \mp 1)\exp(K_2 \Delta\Upsilon_s)\right]}{\pm 2\left\{\exp\left[\pm \frac{K_2}{2}(Z_1 - P_{1s} \pm \Delta\Upsilon_s)\right] - 1\right\}} \tag{3.68}$$

In like fashion, Equations (3.58), (3.59), (3.62), and (3.64) can be combined to give

$$(\pm K_3 Z_{12}) = \frac{\exp(\pm K_3 Z_1)\left[Z_3 \mp 1 - (P_{3s} \mp 1)\exp(K_3 \Delta\Upsilon_s)\right]}{\pm 2\left\{\exp\left[\pm \frac{K_3}{2}(Z_1 - P_{1s} \pm \Delta\Upsilon_s)\right] - 1\right\}} \tag{3.69}$$

Z_{12} is eliminated by raising both sides of Equations (3.68) to the K_3 power and both sides of Equations (3.69) to the K_2 power, and, with left sides then equal, equating the right sides to give after cancelling common factors

$$\left[\frac{Z_2 - \left[\pm 1 + (P_{2s} \mp 1)\exp(K_2\Delta\Upsilon_s)\right]}{\pm 2\left(\exp\left\{\pm\frac{K_2}{2}\left[Z_1 - (P_{1s} \mp \Delta\Upsilon_s)\right]\right\} - 1\right)}\right]^{K_3} =$$

$$= \left[\frac{Z_3 - \left[\pm 1 + (P_{3s} \mp 1)\exp(K_3\Delta\Upsilon_s)\right]}{\pm 2\left(\exp\left\{\pm\frac{K_3}{2}\left[Z_1 - (P_{1s} \mp \Delta\Upsilon_s)\right]\right\} - 1\right)}\right]^{K_2} \qquad (3.70)$$

Equations (3.70) show the positive locus to be on a translatable surface of form

$$Z_2^{K_3} = \frac{\left\{2\left[\exp\left(\frac{K_2 Z_1}{2}\right) - 1\right]\right\}^{K_3}}{\left\{2\left[\exp\left(\frac{K_3 Z_1}{2}\right) - 1\right]\right\}^{K_2}} Z^{K_2} \qquad (3.71)$$

The negative locus is on a similar translatable surface of form

$$Z_2^{K_3} = \frac{\left\{-2\left[\exp\left(\frac{-K_2 Z_1}{2}\right) - 1\right]\right\}^{K_3}}{\left\{-2\left[\exp\left(\frac{-K_3 Z_1}{2}\right) - 1\right]\right\}^{K_2}} Z_3^{K_2} \qquad (3.72)$$

As

$$\frac{\left\{-2\left[\exp\left(\frac{-K_2 Z_1}{2}\right)-1\right]\right\}^{K_3}}{\left\{-2\left[\exp\left(\frac{-K_3 Z_1}{2}\right)-1\right]\right\}^{K_2}} = \frac{\left\{2\left[\exp\left(\frac{K_2 Z_1}{2}\right)-1\right]\right\}^{K_3}\exp\left(\frac{-K_2 K_3 Z_1}{2}\right)}{\left\{2\left[\exp\left(\frac{K_3 Z_1}{2}\right)-1\right]\right\}^{K_2}\exp\left(\frac{-K_2 K_3 Z_1}{2}\right)} \quad , \tag{3.73}$$

the loci are on surfaces of the same form.

Figure 3.14 pictures the general form of the surface. It is composed of two sheets which are contiguous at their translating origin. The figure is drawn for $K_2=2$ and $K_3=1$. The sheets are symmetrical through the translating origin and are almost ruled surfaces. They actually are slightly bowl-shaped rather than cone-shaped.

It can be shown from Equations (3.70) that the contiguous point of the two sheets which include one of the loci is always on the surface which includes the other locus. Also, the contiguous points are on the zero trajectories of the future input phase point, (P_{1S} , P_{2S} , P_{3S}).

The positive locus is on the upper half of the sheet in the foreground in Figure 3.14, and the negative locus is on the lower half of the sheet in the background. The loci are bounded by the intersection of these surfaces. Sample loci are pictured in Figure 3.15 for $\Delta C_S = 1$ and $P_{1S} = P_{2S} = P_{3S} = 0$. The figure is of a clamshell-shaped closed surface. The shaded surface is convex toward the viewer and represents the negative locus for two-switch paths. The positive locus for two-switch paths is on the rear side, its shape being indicated by the

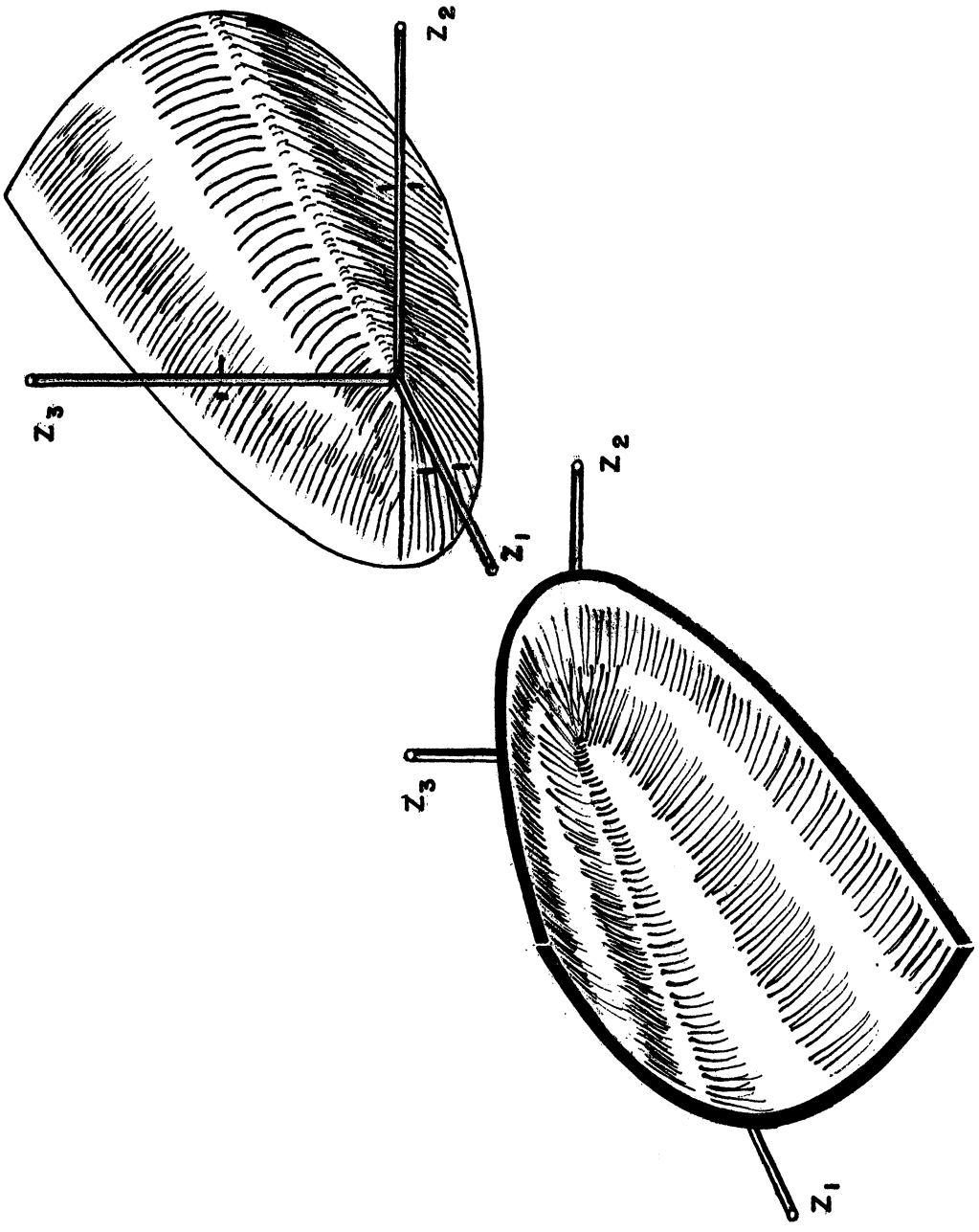

Figure 3.14 Surface Containing Loci, Third Order Contactor Servo.

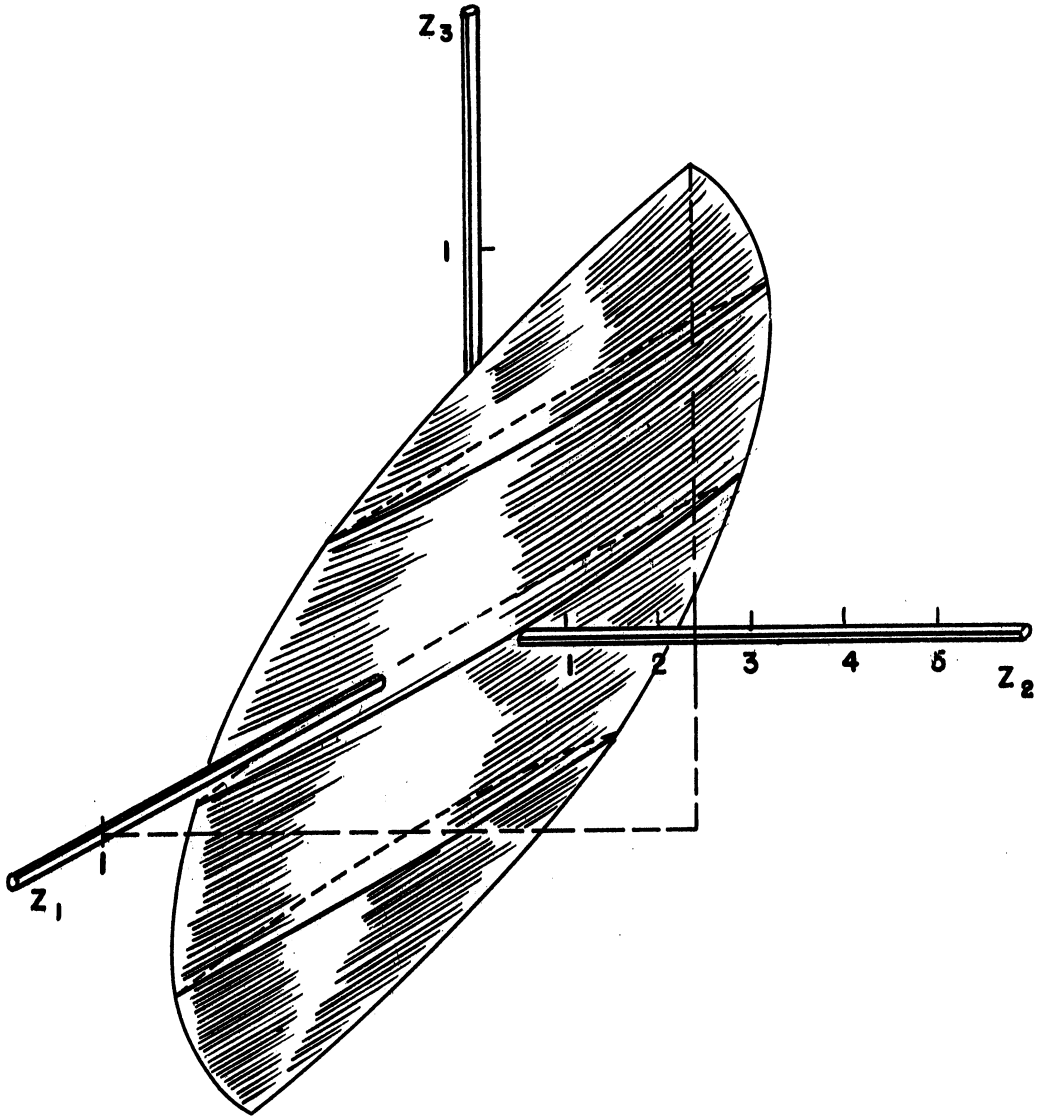

Figure 3.15 Loci, Third Order Contactor Servo.

dashed lines of traces of constant Z_1 planes. The top point is on the negatively forced zero trajectory and is the zero-switch negative locus; the bottom point, on the zero trajectory with positive forcing is the zero-switch positive locus. The positive and negative one-switch loci are represented respectively by the right and left edges of the clam-shell.

Comparison of the concept illustrated in Figure 3.15 with that illustrated in Figure 2.6 shows the zero-switch loci describing the zero trajectories for a step input. The one-switch loci would describe the switching surfaces in the phase space. Of course, this comparison does not hold for general inputs whose P_{1S}, P_{2S}, and P_{3S} vary with time.

Inclusion of loci for programs of more than two switches within the region bounded by a locus as described above for the same $\Delta\gamma_S$ is shown by considering an n^{th} order contactor servo in the next section of this chapter.

Higher Order Contactor Servos

In this section it will be shown that the swept locus switching concept is applicable to certain contactor servos of order greater than two or three. An n^{th} order system generalized from the previous two systems analyzed will be investigated.

The system differential equations are

$$D(D+K_2)(D+K_3)\cdots(D+K_n)\theta = \pm 1 \quad , \tag{3.74}$$

where the K's are real constants, and

$$K_n > K_{n-1} > \cdots > K_3 > K_2 > 0 \quad .$$

Equations (3.74) can be expressed as first order equation in terms of phase space principal coordinates $Z_1, Z_2, \ldots, Z_n$. Using notation similar to Rose[13] the equations are

$$Z' = B Z \pm K \tag{3.75}$$

where

$$Z = \begin{pmatrix} Z_1 \\ Z_2 \\ \cdot \\ \cdot \\ Z_n \end{pmatrix} , \tag{3.76}$$

$$B = \begin{Vmatrix} 0 & & & \\ & -K_2 & & \bigcirc \\ & & \cdot & \\ & \bigcirc & & \cdot K_n \end{Vmatrix} , \tag{3.77}$$

and

$$K = \begin{pmatrix} 1 \\ K_2 \\ \cdot \\ \cdot \\ K_n \end{pmatrix} \tag{3.78}$$

The equations of the system phase space trajectories are

$$Z = e^{B\tau} Z_0 \pm e^{B\tau} \left[\int_0^{\tau} e^{-Bs}\, ds \right] K \tag{3.79}$$

where

$$e^{B\tau} = \begin{Vmatrix} 1 & & & \\ & e^{-K_2\tau} & & \bigcirc \\ & & \cdot & \\ & \bigcirc & & \cdot e^{-K_n\tau} \end{Vmatrix} \tag{3.80}$$

Conventional existence and uniqueness theorems for linear differential equations[22] show there is a unique trajectory of each sign of forcing through each point of the phase space.

Let L_j^+ symbolize the set of points in the phase space which make up the positive j-switch locus for a particular point, Z_p, in the phase space. L_j^- stands for the set of points making up the corresponding negative j-switch locus. L_j^+ varies with the specified travel time, $\Delta\tau$, also; so

$$L_j^\pm = L_j^\pm(Z_p, \Delta\tau) \quad , \tag{3.81}$$

with

$$j = 0, 1, 2, \ldots . \tag{3.82}$$

Let $\Delta\tau_J$ stand for the travel time over the last J arcs of the output phase point's path. Thus, $\Delta\tau_I$ stands for zero-trajectory travel time. Capital letters and Roman Numerals will be used in the subscripts of these symbols for intermediate travel times. The $\Delta\tau_J$'s satisfy the relations

$$\Delta\tau > \Delta\tau_{N-I} > \Delta\tau_{N-II} > \ldots > \Delta\tau_{II} > \tau_I > 0 .$$

The points, $(Z^\pm)_o$, on $L_o^\pm$ satisfy the equations

$$(Z^\pm)_o = e^{-B\Delta\tau} Z_p \pm e^{-B\Delta\tau}\left[\int_o^{-\Delta\tau} e^{-Bs}\,ds\right]K \tag{3.83}$$

obtained by following the zero trajectories backwards in time.

The points $(Z^{\pm})_1$ on $L_1^{\pm}$ are obtained by going backwards in time from each point on the zero trajectories between Z_φ and $(Z^{\pm})_0$. From the zero trajectory, an arc of opposite forcing is followed. Any point on this part of the zero trajectories comes from

$$(Z^{\pm})_I = e^{-B\Delta\tau_I} Z_\varphi \pm e^{-B\Delta\tau_I}\left[\int_0^{-\Delta\tau_I} e^{-Bs}\,ds\right]K \qquad (3.84)$$

where $(Z^{\pm})_I$ indicates switch points closest in time to Z_φ.

So

$$(Z^{\pm})_1 = e^{-B(\Delta\tau-\Delta\tau_I)}(Z^{\mp})_I \pm e^{-B(\Delta\tau-\Delta\tau_I)}\left[\int_0^{-(\Delta\tau-\Delta\tau_I)} e^{-Bs}\,ds\right]K. \qquad (3.85)$$

This gives

$$(Z^{\pm})_1 = e^{-B\Delta\tau} Z_\varphi \pm e^{-B\Delta\tau}\left[e^{B\Delta\tau_I}\int_0^{-(\Delta\tau-\Delta\tau_I)} e^{-Bs}\,ds - \int_0^{-\Delta\tau_I} e^{-Bs}\,ds\right]K. \qquad (3.86)$$

Similarly, $(Z^{\pm})_{n-1}$, the points on $L_{n-1}^{\pm}$ are described by

$$(Z^{\pm})_{n-1} = e^{-B\Delta\tau} Z_\varphi \pm e^{-B\Delta\tau}\left[e^{B\Delta\tau_{N-I}}\int_0^{-(\Delta\tau-\Delta\tau_{N-I})} e^{-Bs}\,ds - e^{B\Delta\tau_{N-II}}\int_0^{-(\Delta\tau_{N-I}-\Delta\tau_{N-II})} e^{-Bs}\,ds + \ldots\right.$$

$$\left. \ldots - (-1)^{n-1} e^{B\tau_I}\int_0^{-(\Delta\tau_{II}-\Delta\tau_I)} e^{-Bs}\,ds + (-1)^{n-1}\int_0^{-\Delta\tau_I} e^{-Bs}\,ds\right]K. \qquad (3.87)$$

Equations(3.83) for points on $L_o^{\pm}$ can be rewritten as

$$\begin{pmatrix} Z_1 \\ Z_2^{\pm} \\ \cdot \\ \cdot \\ Z_n^{\pm} \end{pmatrix}_0 = \begin{pmatrix} Z_{1p} \\ Z_{2p}\, e^{K_2 \Delta\tau} \\ \cdot \\ \cdot \\ Z_{np} e^{K_n \Delta\tau} \end{pmatrix} \pm \begin{pmatrix} -\Delta\tau \\ 1 - e^{K_2 \Delta\tau} \\ \cdot \\ \cdot \\ 1 - e^{K_n \Delta\tau} \end{pmatrix} , \tag{3.88}$$

Equations(3.86) for points on $L_1^{\pm}$ as

$$\begin{pmatrix} Z_1^{\pm} \\ Z_2^{\pm} \\ \cdot \\ \cdot \\ Z_n^{\pm} \end{pmatrix}_1 = \begin{pmatrix} Z_{1p} \\ Z_{2p} e^{K_2 \Delta\tau} \\ \cdot \\ \cdot \\ Z_{np} e^{K_n \Delta\tau} \end{pmatrix} \pm \begin{pmatrix} -\Delta\tau + 2\,\Delta\tau_I \\ 1 + e^{K_2 \Delta\tau} - 2\, e^{K_2(\Delta\tau - \Delta\tau_I)} \\ \cdot \\ \cdot \\ 1 + e^{K_n \Delta\tau} - 2\, e^{K_n(\Delta\tau - \Delta\tau_I)} \end{pmatrix} , \tag{3.89}$$

and Equations (3.87) for points on $L_n^{\pm}$ as

$$\begin{pmatrix} Z_1^{\pm} \\ Z_2^{\pm} \\ \cdot \\ \cdot \\ Z^{\pm} \end{pmatrix}_{n-1} = \begin{pmatrix} Z_{1p} \\ Z_{2p}\, e^{K_2 \Delta\tau} \\ \cdot \\ \cdot \\ Z_{np} e^{K_n \Delta\tau} \end{pmatrix} +$$

$$\begin{pmatrix} -\Delta\tau + 2\,\Delta\tau_{N-I} - 2\,\Delta\tau_{N-II} + \ldots + (-1)^{n-1} \Delta\tau_I \\ 1 - (-1)^{n-1} e^{K_2 \Delta\tau} - 2\, e^{K_2(\Delta\tau - \Delta\tau_{N-I})} + \ldots + (-1)^{n-1} 2\, e^{K_2(\Delta\tau - \Delta\tau_I)} \\ \cdot \qquad\qquad \cdot \qquad\qquad \cdot \\ \cdot \qquad\qquad \cdot \qquad\qquad \cdot \\ 1 - (-1)^{n-1} e^{K_n \Delta\tau} - 2\, e^{K_n(\Delta\tau - \Delta\tau_{N-I})} + \ldots + (-1)^{n-1} 2 e^{K_n(\Delta\tau - \Delta\tau_I)} \end{pmatrix} . \tag{3.90}$$

Investigation of the above locus equations shows that dependence on Z_p effects only a translation in the phase space on these loci. As can be seen, the first term on the right side of each locus equation is the same for loci of n-1 and less switches for the same Z_p and $\Delta\Upsilon$, and it is independent of the locus parameters, the $\Delta\Upsilon_J$'s . The second terms on the right sides of the locus equation do not depend on Z_p Thus, for a certain Z_p and $\Delta\Upsilon$, all points of these loci are translated in the phase space by the amount of the first term; and the loci for a particular $\Delta\Upsilon$ are of the same geometric shape regardless of the location of Z_p in the phase space. These properties were noted in the previous second and third order systems.

The particular point, Z_p, will be taken as the origin of the phase space in order to obtain certain properties of the loci by using the results of Rose's work[13]. These properties will then hold for any Z_p due to the translation property.

Rose showed that for minimum travel time, there is a unique path of n-1 or less switches from each point in the phase space to the origin for an n^{th} order servo of the type being considered. He also showed that the regions in the phase space from which the origin is accessible by such switching programs are continuous and mutually exclusive of one another when discrimination is on the basis of initial sign of forcing and of number of switches.

Therefore, take any particular locus, say L_j^+ , and sweep $\Delta\Upsilon$ monotonically through all positive values. As this is done $L_j^+(0,\Delta\Upsilon)$ sweeps out the positive J -switch accessibility region only. This result stems from Roses's work and the descriptions of the loci

given above. Every other $L_j^{\pm}$ similarly sweeps out its own corresponding accessibility region only. This gives the result that the loci are mutually exclusive of one another when discrimination is based on the initial sign of forcing and of number of switches.

From the uniqueness and space-filling properties of the families of positive and negative continuous arcs used in the continuous process of constructing the $L_j^{\pm}$'s is obtained the result that each $L_j^{\pm}$ is continuous and devoid of holes. Each $L_j^{\pm}$ is then a portion of a hypersurface.

Inspection of the locus equation shows that, for $j < n$ and a fixed $\Delta\Upsilon$,

$$\lim_{\Delta\Upsilon_{N-I} \to \Delta\Upsilon} L_j^{\pm} = L_{j-1}^{\mp} \quad , \tag{3.91}$$

and

$$\lim_{\Delta\Upsilon_I \to 0} L_j^{\pm} = L_{j-1}^{\pm} \quad , \tag{3.92}$$

Let

$$L_j = \sum_{i=0}^{j} L_i^{\pm} \quad , \qquad n-1 > j > 0 \tag{3.93}$$

Equations (3.91) and (3.92), together with the locus properties previously noted, tell that, for $j < n$ and a fixed $\Delta\Upsilon$, L_j is a

closed n-dimensional hypersurface of the n-dimensional phase space. L_{n-1} is, then, a closed (n-1)-dimensional hypersurface of the n-dimensional phase space which completely encloses a portion of the n-dimensional space.*

---

* It is interesting to note that that L_{n-1} is devoid of holes can be seen as outlined below:

Take an $L_{n-1}(0, \Delta\tau)$ for a certain $\Delta\tau$, and let there be a hole in an L_j^+ or an L_j^- making up the L_{n-1}. From every point of the accessibility region containing the j-switch locus chosen there is a unique minimum-time path to the origin, and a family of initial arcs of the same forcing fill the region. It is easily seen that each of these initial arcs can intersect the j-switch locus no more than once. Therefore, the j-switch locus is oriented so that at least one of these arcs will go through any hole. Take one such arc and construct from it the unique minimum-time path to the origin. Then starting at the origin and moving along this path backwards in time, back along the initial arc if necessary, eventually a point can be found from which the travel time to the origin is greater than the $\Delta\tau$ of the chosen L_{n-1}. On the path between this point and the origin is a point from which the travel time to the origin is equal to the $\Delta\tau$ of the chosen

If this point is on one of the lower switch loci for the chosen $\Delta\tau$, following the unique minimum-time path backwards in time causes one to go outside L_{n-1} at the point; movement on an arc intersecting L_{n-1} is from outside to inside in the forward time direction. Direction of movement through a hole in L_{n-1} can be given the same inside-outside orientation. Continuing back in time the path never goes back inside L_{n-1}, so the point must be in the j-switch accessibility region for a minimum time path to the origin to be constructed from the initial arc through the hole. But the j-switch locus was constructed to contain all such points in this region. Therefore, the initial arc must intersect the chosen j-switch locus at the point rather than pass through a hole.

For the case considered, Z_p is the origin, and

$$\lim_{\Delta\Upsilon \to 0} L_{n-1} = Z_p \tag{3.94}$$

As $\Delta\Upsilon$ increases without limit L_{n-1} sweeps out the entire phase space.* As L_{n-1} passes over any point in the space the instantaneous $\Delta\Upsilon$ is that for the minimum time path from the point to the origin. Any path from the point to the origin of more than n-1 switches will have a greater travel time. Thus, it is easily seen that higher-switch loci are within the n-dimensional region enclosed by the L_{n-1} for the same $\Delta\Upsilon$.

That this locus property extends to the case of Z_p's other than the origin is easily shown. An $L_{n-1}(0,(\Delta\Upsilon)_2)$ is taken for a fixed $\Delta\Upsilon$, and an $L_{n-1}(0,(\Delta\Upsilon)_4)$ is taken for a lesser $\Delta\Upsilon$. The $L_{n-1}(Z_p,\Delta_1\Upsilon)$ for any point on the $L_{n-1}(0,(\Delta\Upsilon)_4)$ is completely within the region enclosed by the $L_{n-1}(0,(\Delta\Upsilon)_4)$, $\Delta_1\Upsilon$ being the difference between $(\Delta\Upsilon)_2$ and $(\Delta\Upsilon)_4$. The second terms on the right side of the loci equations are available for comparison. Doing the same thing for a Z_p off the origin gives the standard translation terms, and the second terms on the right side of the loci equations are the same as those for the case of Z_p at the origin. So, higher-switch loci are within the region enclosed by L_{n-1} for the same $\Delta\Upsilon$ for any Z_p.

Lastly, L_{n-1} is used in the swept locus switching scheme for a known input signal. For a continuous input phase path in the

---

* The uniqueness of minimum time paths from each point in the space to the origin shown by Rose results in the L_{n-1}'s being mutually exclusive when discriminated between on the basis of travel times. Consideration of two L_{n-1}'s of almost equal travel times will then show that the L_{n-1}'s are topologically equivalent to hyperspheres. In turn, an L_j^+ or L_j^- can be seen as topologically equivalent to a bounded portion of a hyperplane.

n-dimensional phase space the input signal must be a function of time of class C^{n-1}. The swept locus switching scheme will approximate minimum time interception for such input signals.

Input Prediction

In order to apply the switching technique developed above to a contactor servo faced with an input signal not known as a function of time, the future input information (previously assumed known) must be furnished by a predicting mechanism operating on the present and past input signal. The problem is compounded by the fact that the input signal may be corrupted by a noise component.[25] Considerable literature has been published on the subject of prediction theory[26,27] much of it traceable in concept to Wiener's work[25]. Generally, the published theories have been derived for fixed prediction times, whereas the switching method of this paper requires sweeping through a range of predicting times. It is not the intent here to attempt derivation of a new theory to facilitate design of a mechanism for such swept prediction. Rather, utilization of the existing work to approximate swept prediction will be discussed briefly.

The prediction problem is often considered in two parts, the first of which is the defining of optimum prediction for the application under consideration. The prediction error is defined as the difference between the desired or perfect prediction and the actual output from the predictor. Here, it must be noted, that the quantity being predicted may be some function of the input signal rather than the value of the input signal itself. Minimization of some function of the prediction error is usually taken as a definition of optimum prediction. The best known example of such a definition is that calling for minimization of

the mean square prediction error. The second part of the prediction problem consists of using all known information about the input signal to determine the description of a physically realizable optimum predictor for the input considered.

The actual mechanism doing the predicting may operate by combining the operations of extracting desired input information from a noisy input signal and of extrapolating the input information into the future. The two operations also may be done separately. This would be the case if one mechanism extrapolates the input into the future as a function of time of known form by using function parameters extracted from the noisy input signal by another mechanism. Block diagrams of predicting systems with swept prediction time using predictors of the two types mentioned are shown in Figures 3.16 and 3.17.

Figure 3.16 shows a system using predictors of the first type mentioned. Sweep time is not swept continuously, but is stepped through the sweep range. There is a predictor for each desired function of the input for each step of sweep time. Predicted values are transmitted to the locus computer through the ganged commutators. Needless to say, very small sweep-time steps would make such a system rather complex.

Figure 3.17 shows a system using predictors to extract present input values from a noisy signal and a series extrapolation for future input values. Other extrapolation functions could be used dependent on the input signal. An elementary series extrapolation method was used in the computer study described in Chapter IV.

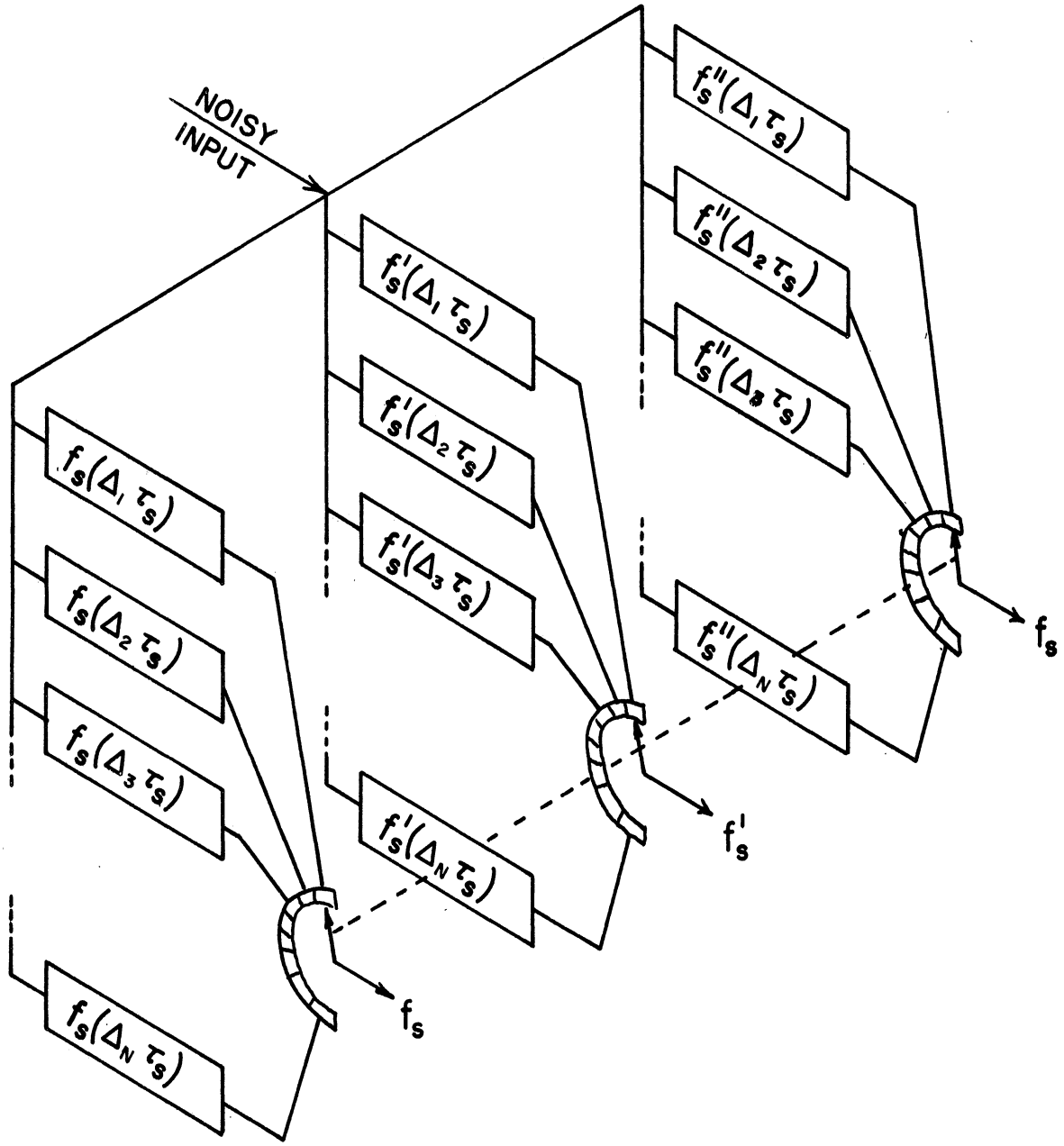

Figure 3.16 Prediction with Commutated Filters

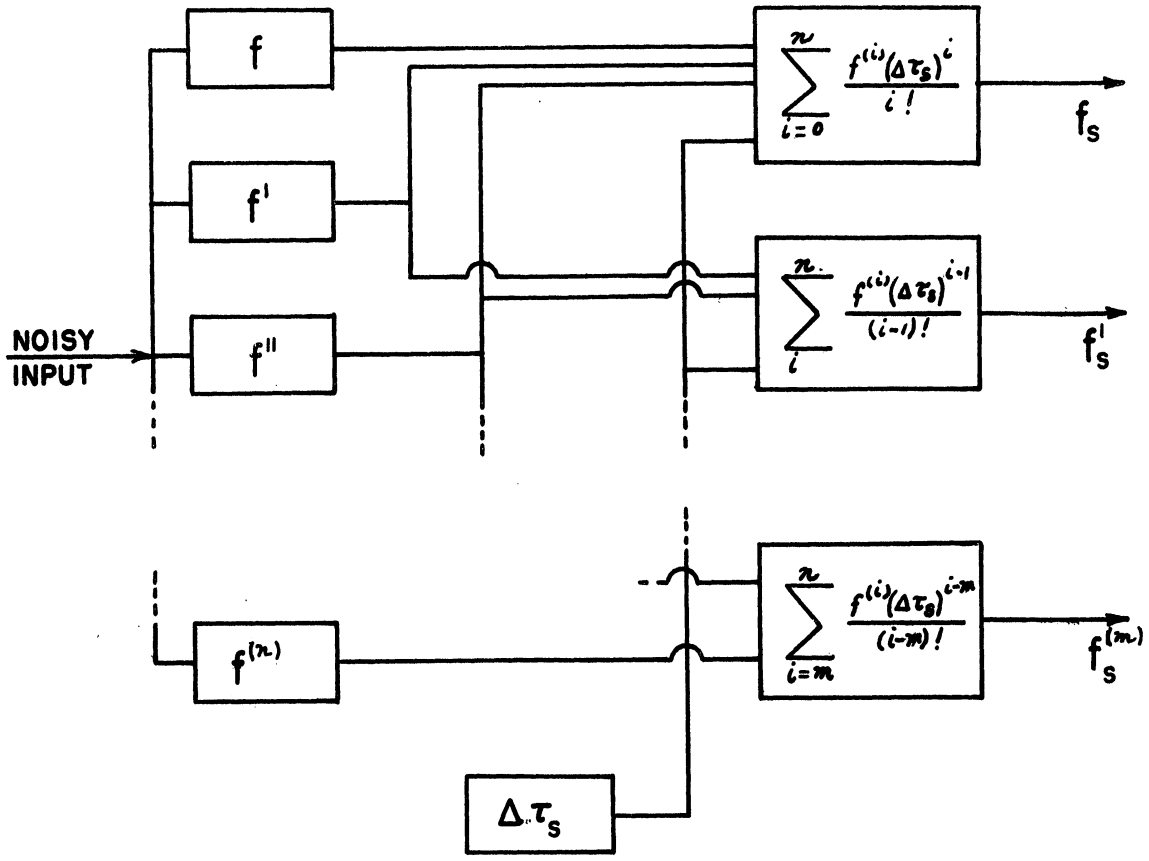

Figure 3.17 Prediction with Series Extrapolation.

Although in the systems diagrammed only input displacement and derivative values are predicted, it is conceivable that the predictors could be built to predict desired functions of these variables instead. Such a device would perform some of the functions of the locus computer, and it is possible that better locus approximations might be achieved. However, such a system concept for the combined predictor and locus computer would be expected to give different designs for input signals with different characteristics. This could be an economic disadvantage for the combined system when comparing it to a system consisting of a fixed locus computer and a separate input-dependent predictor.

To obtain the best design for an actual application, it is believed that the problem would have to be considered on an overall basis to include the first step of defining optimum prediction. It is, in fact, quite reasonable to state that in the designing of a predictor and locus computer system for a practical servo the non-ideal characteristics of the overall servo system would have to be considered. Bass's work[16] mentioned in Chapter I, would be very useful in these considerations.

IV. COMPUTER STUDY

This chapter describes an electronic analog computer study which was carried out to check the theory of Chapter III. The study was also expected to point out some problem areas inherent in a swept-locus switching scheme. The systems studied were the two second order contactor servos whose loci were determined in Chapter III. Switching mechanisms were operated on the basis of having a known future input signal and on the basis of performing a very simple prediction of the future input signal.

Locus Determination

The idea of the swept-locus switching scheme is to determine whether the output phase point is on the positive or on the negative locus corresponding to earliest interception of the input phase point using perfect switching. Then, having determined the locus, forcing of the same sign is applied to the system until a later sweep shows the output phase point to be on the locus of the opposite sign. For the output phase point to be on one of the loci its coordinates will satisfy one of Equations (3.11) for the contactor servo with inertia only. These equations are repeated here slightly rearranged to define functions L^+ and L^- :

$$L^{\pm} = \frac{\pm\left[\theta' - \left(f_s' \pm \Delta\tau_s\right)\right]^2}{4} - \theta + \left[f_s - f_s'\Delta\tau_s \mp \frac{(\Delta\tau_s)^2}{2}\right] \qquad (4.1)$$

L^+ is defined using the top row of signs; L^-, the bottom. If $L^+ = 0$ with the appropriate input and output values inserted, the output phase

point is on the curve which includes the positive locus. Such a curve is shown in Figure 4.1 (A) as a dashed line. However, the positive locus for the case shown is only that part of the curve which forms the left boundary of region V of the figure. In like fashion, $L^- = 0$ indicates the output phase point to be on the solid curve which includes the negative locus on the right boundary of region V.

To locate the output phase point as being on either the left or right boundary of region V the behavior of region V is considered. At the initial instant of a sweep, when $\Delta\gamma_s = 0$, region V is merely the instantaneous input phase point. As $\Delta\gamma_s$ is increased, region V expands and, in general, moves about the phase plane. Initially the output phase point is outside of region V. Eventually, if interception is possible, the output phase point will be inside region V for some period of time. Finding which boundary, right or left, that it crosses to go from outside to inside solves the problem. The possibilities of the output phase point merely touching the boundary of region V and not going in or moving inside through the intersection points of $L^+ = 0$ and $L^- = 0$ are not considered in the study for the following reasons: The first represents the case of interception at a point on the input phase path after which the servo cannot follow the input. Interception with the possibility of following the input for a period of time was considered preferable. The second possibility, entering region V through a particular point on a locus curve, would have zero probability for the perfect switch servo. For a practical system, the probability could be made arbitrarily small by increasing the sensitivity of the device for determining boundary crossings.

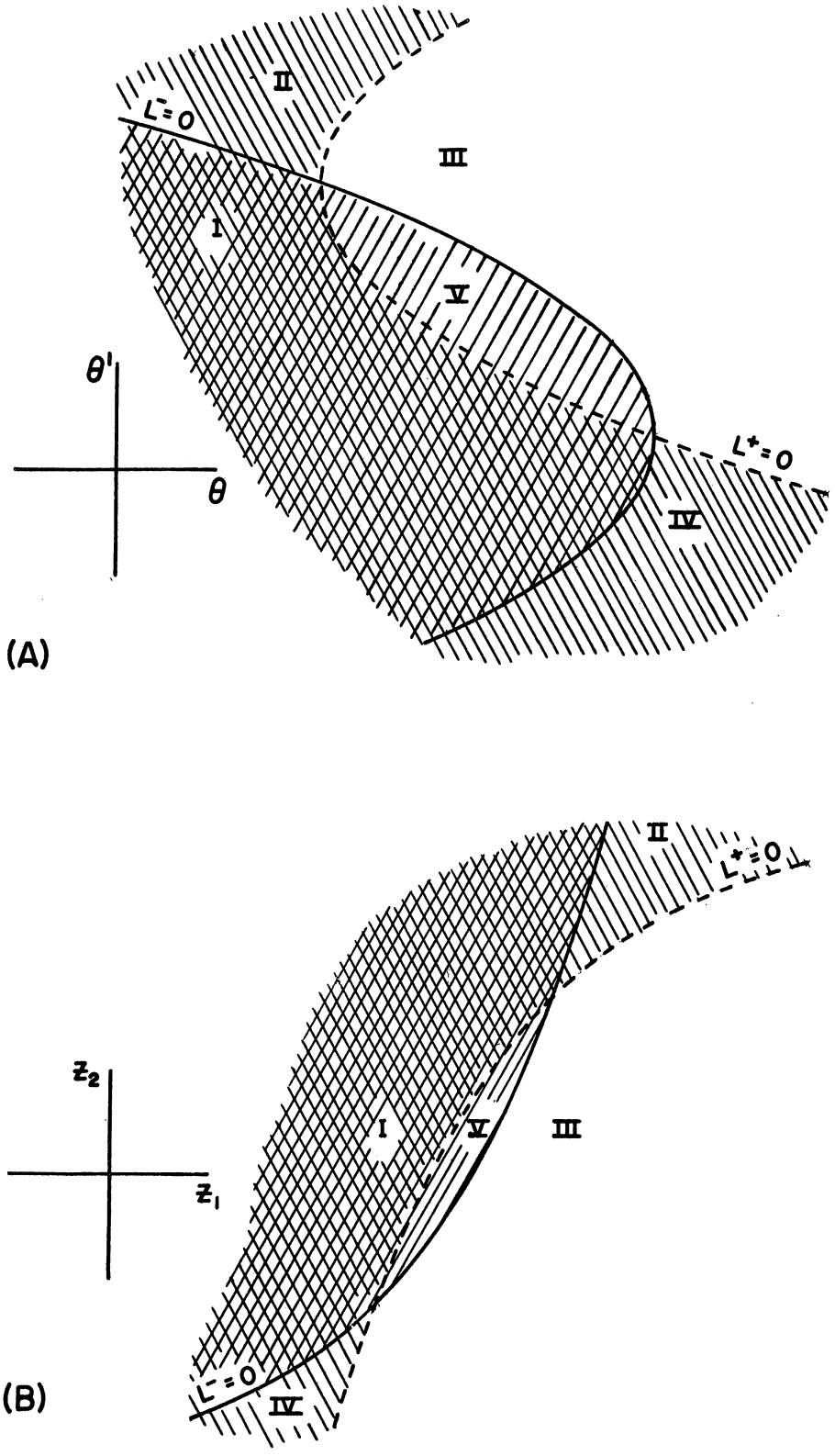

Figure 4.1 Curves of $L^{\pm} = 0$ for Contactor Servo with (A) Inertia Only and (B) Inertia and Viscous Damping.

The logic of the scheme used in the computer study for this boundary crossing determination is relatively simple. To get into region V, the output phase point comes from either region I or region III. In region I, both L^+ and L^- are greater than zero. In region III, they are both less than zero. In region V, L^- is greater than zero, but L^+ is less than zero. As the output phase point crosses the positive locus between regions I and V, L^+ changes from positive to negative, but L^- stays positive. So, let there be an indicator which exhibits a positive signal, while the output phase point is in region I where both L's are positive. When L^+ goes negative, but L^- stays positive, the positive signal is then read from the indicator. The sweep is then stopped and repeated. If the output phase point moved to region III via region II or IV rather than going into region V, the indicator should exhibit a negative signal when both L's are negative. If the output phase point then crossed the negative locus, the indicator would be read as the positive L^- , and negative L^+ condition of region V is obtained. The indicator would not be read under the condition of $L^+ > 0$ and $L^- < 0$ for the output phase point in region II or IV.

Summarizing:

$L^+ > 0$, $L^- > 0$, for positive indication;

$L^+ < 0$, $L^- < 0$, for negative indication;

read indicator as $L^+ < 0$, $L^- > 0$ condition is reached;

having read, stop the sweep and repeat.

For the contactor servo with inertia and viscous damping L^+

and L^{-} are defined using Equations (3.29). These give

$$L^{\pm} = Z_2 - \left[\pm 1 + (P_{2s} \pm 1)\exp(\alpha \Delta\tau_s)\right] \pm 2\exp\left\{\pm \frac{\alpha}{2}\left[Z_1 - (P_{1s} \pm \Delta\tau_s)\right]\right\} . \quad (4.2)$$

With the L's so defined, the locus determination pattern given at the end of the preceding paragraph holds for this servo also. This may be seen by using Equations (4.2) and Figure 4.1 (B).

Input Information

The L's are computed from the instantaneous output displacement and velocity values, the instantaneous value of sweep time increment, and the input signal displacement and velocity values corresponding to the swept time. In the computer study, output values were taken from the appropriate computer amplifiers, and sweep time increment was taken from repetitive integration of a constant voltage. However, input values for the known input case were obtained by a more roundabout method because of a limited availability of function generation equipment and a desire to avert the differentiation noise problem. The input velocity was set on function generators. Appropriate swept input velocity was then read directly, and the swept input displacement was obtained by integration.

The idea of the integration process used can be explained using Figure 4.2. Initial problem time is shown as τ_0, and instantaneous time as τ .

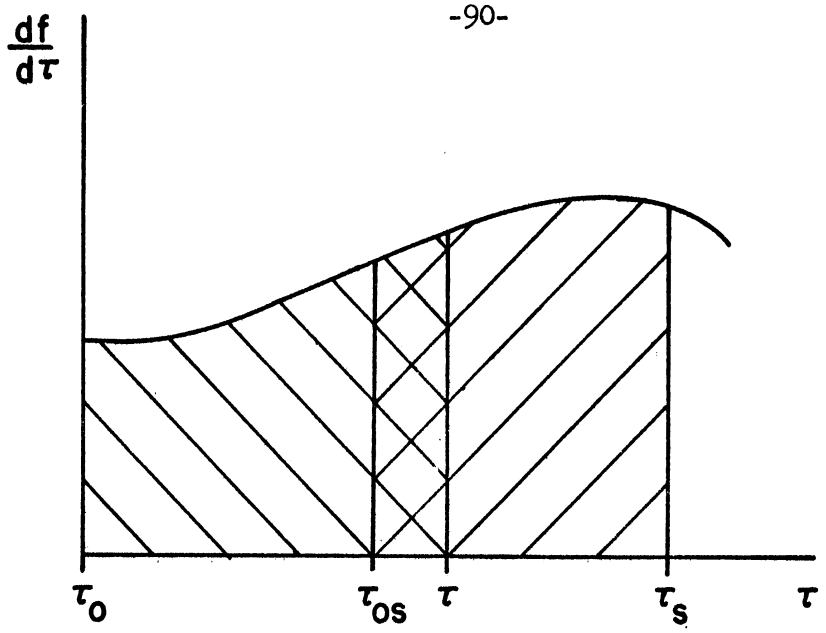

Figure 4.2 Determination of f_5.

The instantaneous value of the change of input position from the initial input position,

$$\Delta_1 f = f - f_o \quad , \tag{4.3}$$

is represented by the area with negatively-sloped cross-hatching between τ_o and τ. For the cases studied $f_o = 0$ was used, so the area actually represented f.

Time corresponding to the initiation of a sweep is shown as τ_{os}, and the instantaneous sweep time as τ_s. Instantaneous sweep time increment is, as before,

$$\Delta\tau_s = \tau_s - \tau \quad . \tag{4.4}$$

Let r be the ratio of sweep time rate to problem time rate, both rates being constant. Then,

$$r = \frac{\tau_s - \tau}{\tau - \tau_{os}} \quad , \tag{4.5}$$

and

$$\Delta\tau_s = \Upsilon(\tau - \tau_{os}) \tag{4.6}$$

For the sweep to scan a reasonable portion of the future input signal while the input phase point travels only a negligible amount,

$$\Upsilon >> 1 \tag{4.7}$$

Let the area on the figure between τ_{os} and τ_s shown with positively-sloped crosshatching be called $\Delta_2 f$. Let the overlap of the $\Delta_1 f$ and $\Delta_2 f$ areas, that doubly cross hatched area between τ_{os} and τ be called $\Delta_3 f$. Then, as can be seen from the figure,

$$f_s = f_o + \Delta_1 f + \Delta_2 f - \Delta_3 f \tag{4.8}$$

$\Delta_1 f$, $\Delta_2 f$, and $\Delta_3 f$ may be expressed as

$$\Delta_1 f = \int_{\tau_o}^{\tau} f'(\tau)\, d\tau \quad , \tag{4.9}$$

$$\Delta_2 f = \int_{\tau_{os}}^{\tau_s} f'(\tau)\, d\tau = (\Upsilon+1) \int_{\tau_{os}}^{\tau} f'\left[\tau_{os} + (\Upsilon+1)(\tau - \tau_{os})\right] d\tau \,, \tag{4.10}$$

and

$$\Delta_3 f = \int_{\tau_{os}}^{\tau} f'(\tau)\, d\tau \tag{4.11}$$

The $(\Upsilon+1)$ in the argument of the integrand of Equation (4.10) is due to the fact that the argument is swept through at a rate

equal to the sum of the rates of problem time and sweep time. The $(\Upsilon+1)$ factor multiplying the integral scales up the $\Delta_2 f$ value accordingly.

Equation (4.8) was approximated in the computer study by letting $\Upsilon+1=\Upsilon$ in the multiplicative factor of Equation (4.10) and $\tau=\tau_{os}$ in Equation (4.11). There, then, remains

$$f_s = f_o + \int_{\tau_o}^{\tau} f'(\tau)\, d\tau + \Upsilon \int_{\tau_{os}}^{\tau_s} f'\left[\tau_{os} + (\Upsilon+1)(\tau-\tau_{os})\right] d\tau \quad . \quad (4.12)$$

For constant position and constant velocity inputs, Equation (4.12) is exact.

Computer Circuits

It is believed that an explanation of some of the computer circuitry used is in order. The computer solutions were run in slow time. Three ratios of seconds of computer time to units of τ time were used. The servo with inertia only was simulated using a 20:1 ratio, a 10:1 ratio was used for the damped servo with prescribed inputs, and 5:1 for the damped servo with predicted inputs. The symbol $\not k$ indicates the ratio in the circuit diagrams.

Symbols used in the sample circuits of Figure 4.6 through Figure 4.13, are shown in Figure 4.3. The "Reeves" symbols refer to REAC Mod C101 computer and Mod S101 C050 servo components of the Reeves Instrument Corporation. "Goodyear" symbols are for GEDA L-3 and N-3 components made by the Goodyear Aircraft Corporation. "Philbrick" symbols are for GAP/R K-3 components made by George A. Philbrick

REEVES

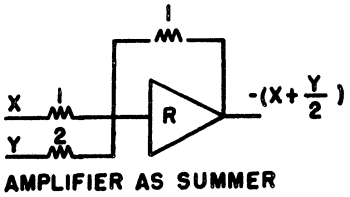

AMPLIFIER AS SUMMER

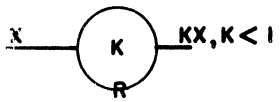

POTENTIOMETER

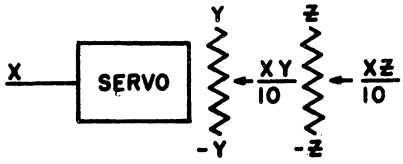

SERVO MULTIPLIER

GOODYEAR

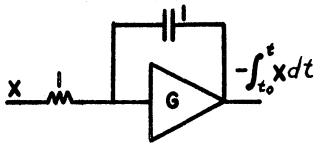

AMPLIFIER AS INTEGRATOR

LIMITER JACK

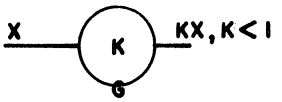

POTENTIOMETER

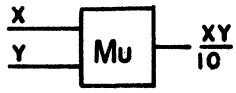

ELECTRONIC MULTIPLIER

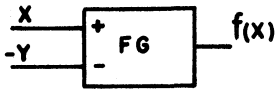

FUNCTION GENERATOR

PHILBRICK

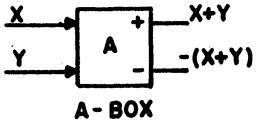

A-BOX

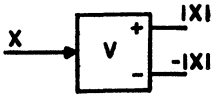

V-BOX

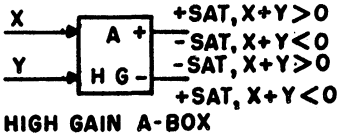

HIGH GAIN A-BOX

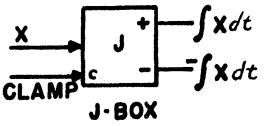

J-BOX

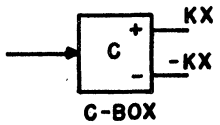

C-BOX

OTHER

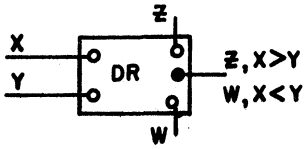

DIFFERENTIAL RELAY

Figure 4.3 Computer Circuit Symbols. Resistors in megohms and capacitors in microfarads unless marked otherwise. Reference voltage = ± 100. Unity voltage level = 10.

Researches, Incorporated. The differential relay was a locally fabricated item at the Air Force Institute of Technology.

The symbols refer to standard computer components except for the high gain A-box shown in the Philbrick section of the figure. The standard Philbrick A-box used consisted of a summer stage and an inverter stage. For the high gain A-box, a voltage divider was inserted in the feedback of the summer stage as pictured in Figure 4.4. The voltage divider raised the gain across the summer stage by a factor of approximately five hundred, so that a very small net voltage at the input of the summer would saturate the A-box.

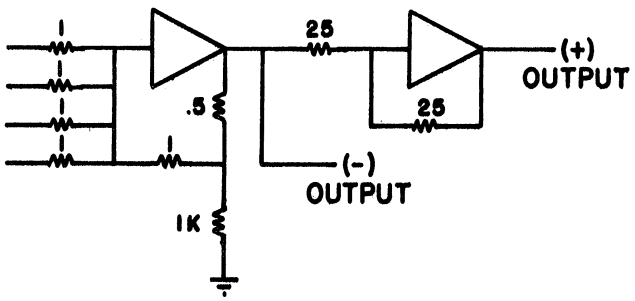

Figure 4.4 High Gain A-Box

The functional operation of the computer circuits used is shown in block form in Figure 4.5. During a locus sweep, the sweep box feeds the sweep time increment into the input block for use in determination of f_s' and f_s. It also feeds $\Delta\gamma_s$ to the third block where it is combined with f_s, f_s', θ, and θ' to continuously form L^+ and L^-. The L^+ and L^- values are monitored by the fourth block

in accordance with the locus determination pattern given above. When the locus decision is made, it is passed on as a command to the forcing block which, accordingly, either maintains its same forcing on the controlled system, or switches the forcing. The decision information is also passed back to the sweep block which then deactivates the decision block and resets the input block for a new sweep. At the end of the reset period, the sweep block reactivates the decision block and initiates a new sweep.

The sample circuits begin with Figure 4.6 which shows the simulations for the output data of the two servos studied. The circuits are straightforward second order systems with forcing signals applied at the left ends.

Figure 4.7 shows two sweep circuits used. Part (A) of the figure is the sweep circuit for known inputs. Replacing the dashed portion of part (A) by part (B) gives the sweep circuit used in the predicted input work. Considering part (A), it is seen that the (-) output, the output of the summer stage, of the high gain A-box is saturated negatively during a sweep. The (+) output is saturated positively and is fed into the clamping terminal of the upper J-box. The J-box output is then clamped at zero. The V-box has zero output until a decision pulse arrives later during the sweep. The high gain A-box and potentiometer combination acts as a bistable flip-flop as shown by Howe[28]. The operational amplifier without feedback of Howe's paper is replaced by the modified summer stage here. It was necessary to use the modification described above for the high gain amplifier in order to overcome the effects of positive feedback in the Philbrick amplifier. The (-) output of the high gain A-box feeds into the dashed

A-box which feeds a GEDA limiter circuit. The limiter is adjusted so that the following J-box sweeps $\Delta\gamma_S$ at the desired rate. The J-boxes used were set for the same integration rate as the REAC and GEDA integrators, but it was found that their rate, although constant, was not the same as that of the others. The limiter output was set accordingly. The (=) output lead to the clamping terminal of this J-box activates it during sweep. The (-) output also feeds the two A-box half-wave rectifier which furnishes the activate-deactivate signal for the decision block. This rectification action was also described by Howe[28].

When a decision is made, a positive or negative pulse is sent to the V-box, which then feeds a negative pulse to the high-gain A-box. The pulse overrides the potentiometer output, and the flip-flop reverses. The half-wave rectifier output then deactivates the decision block. The (=) output of the high-gain A-box clamps the dashed J-box, resetting the input block. The (-) output feeds the then activated upper J-box through the C-box. The J-box output builds up until it overrides the potentiometer output and the flip-flop reverses to its original state for a new sweep.

In the circuit of Figure 4.7 (B), $\Delta\gamma_S$ is not clamped to zero during the reset period but merely decreases, as the integrator has an input of opposite sign. The first limiter controls both sweep rate and reset rate for $\Delta\gamma_S$. The second limiter merely prevents $\Delta\gamma_S$ from going negative in case that might give a false decision.

Figure 4.8 is the circuit for determination of swept input values. It operates in accordance with Equation (4.12). The Δf

symbol refers to the last term of Equation (4.12). The J-box is clamped by the (-) output of the sweep circuit high-gain A-box.

Figure 4.9 is a straight forward circuit utilizing summers and electronic multipliers to form L^+ and L^- for the servo with inertia only and a known input.

Figure 4.10 illustrates L^+ and L^- computation for the servo with inertia and viscous damping and a known input. The exponential terms required were approximated by the first four terms of the exponential series;

$$(X) = 1 + X + \frac{X^2}{2} + \frac{X^3}{6} + \ldots . \qquad (4.3)$$

A value of 1/5 was used for the damping parameter, α.

Figure 4.11 is discussed in the section on the prediction problem.

The decision circuit is drawn in Figure 4.12. The two amplifiers on the left of the figure are connected as damped linear second order systems, and serve as low pass filters. Such filter analogs have been described by Nichols and Rauch[29]. The circuits used have damping ratios of .71, undamped natural frequencies of 60 radians/second, and gain constants of 1. The two differential relays are thus fed L^+ and L^- values free of much sixty cycle noise.

To describe the action of the decision circuit, let L^+ and L^- both be positive, the output phase point being in region I of Figure 4.1. The output of the L^- differential relay is then fifty volts positive, while the L^+ differential relay has a zero output. The positive fifty volts causes the output of the flip-flop formed with the high-gain A-box and the C-box to be a positive twenty volts.

This positive twenty volts is connected to the upper terminal of the third differential relay. This differential relay, however, has a zero output, for its input from the previous summer amplifier is a negative twenty volts, which is more positive than the negative thirty volts on the other input terminal. As the output phase point moves into region V of Figure 4.1, the L^+ differential relay output becomes a negative fifty volts. The flip-flop does not reverse, as this negative voltage to its input is cancelled by the positive voltage to its input from the L^- channel. The output of the summer feeding the third differential relay changes to a negative forty volts causing the relay output to be connected to the upper terminal. Thus, the decision for positive forcing is made.

The succeeding amplifier changes the positive twenty volts to a negative forty volts which is fed to the V-box of the sweep circuit. As previously described, the sweep circuit then sends a large negative voltage to the summer before the third relay. The differential relay output then returns to zero during the reset period. The deactivating signal is removed as the next sweep starts. A negative decision is describable in similar fashion.

The decision pulse from the last amplifier of Figure 4.12 is fed to the input of the flip-flop of Figure 4.13 which maintains the same forcing value until a pulse of the opposite sign causes it to reverse. The four amplifier circuit following the flip-flop is a standard REAC limiter circuit. The output of the final pot is fed to an output circuit as shown in Figure 4.6.

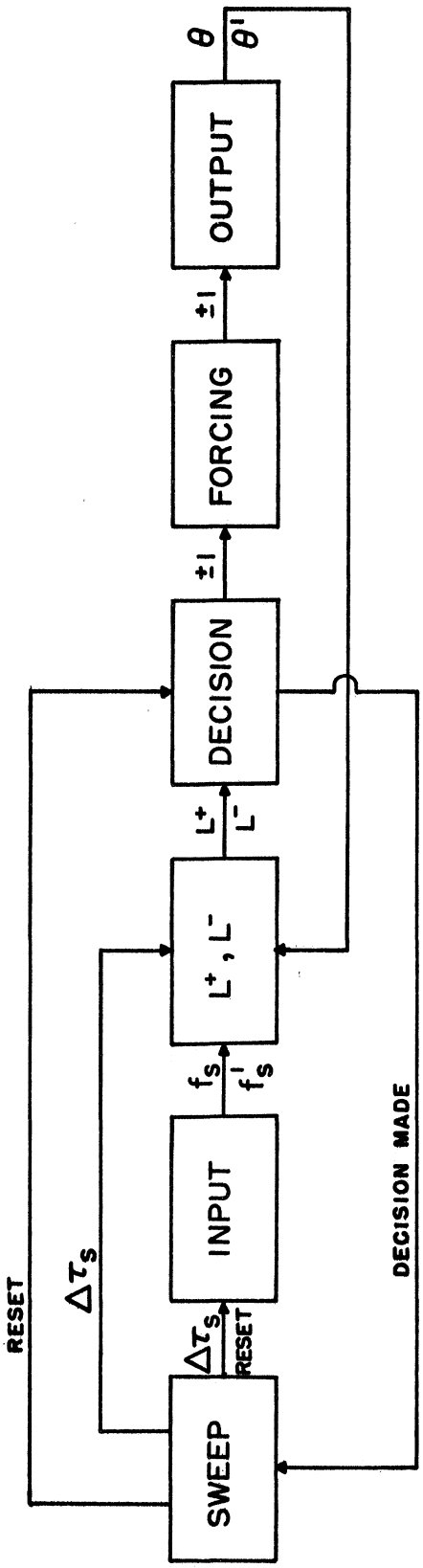

Figure 4.5 Block Diagram of Computer Circuit.

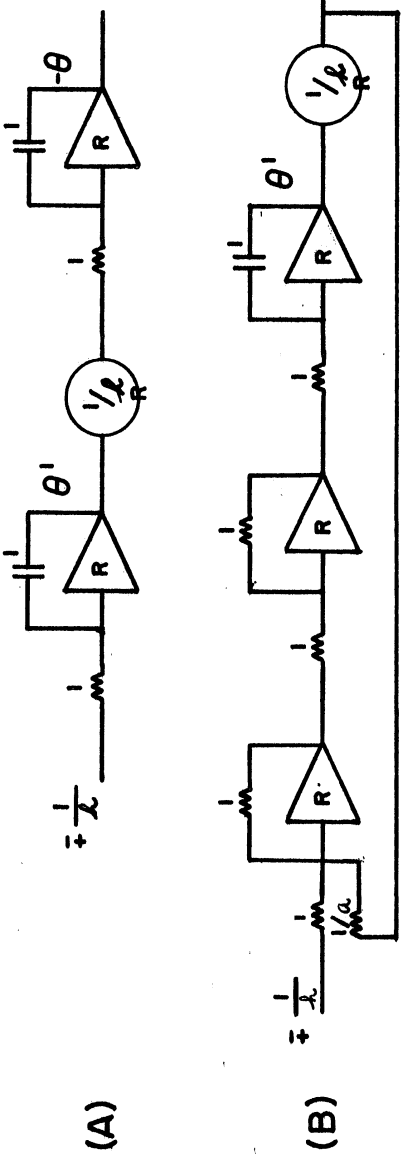

Figure 4.6 Output Circuits, Contactor Servos with (A) Inertia Only and (B) Inertia and Viscous Damping.

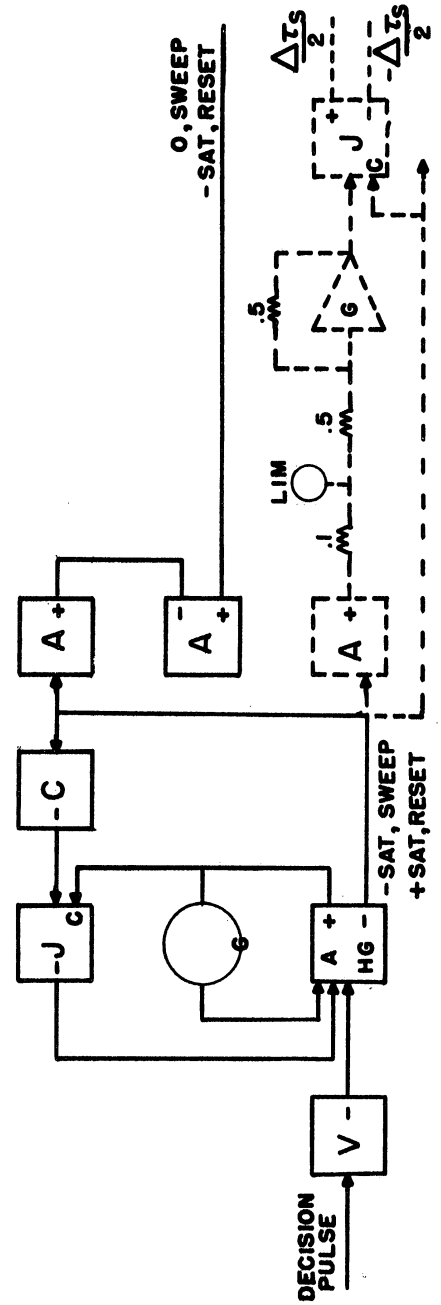

Figure 4.7 Sweep Circuits.

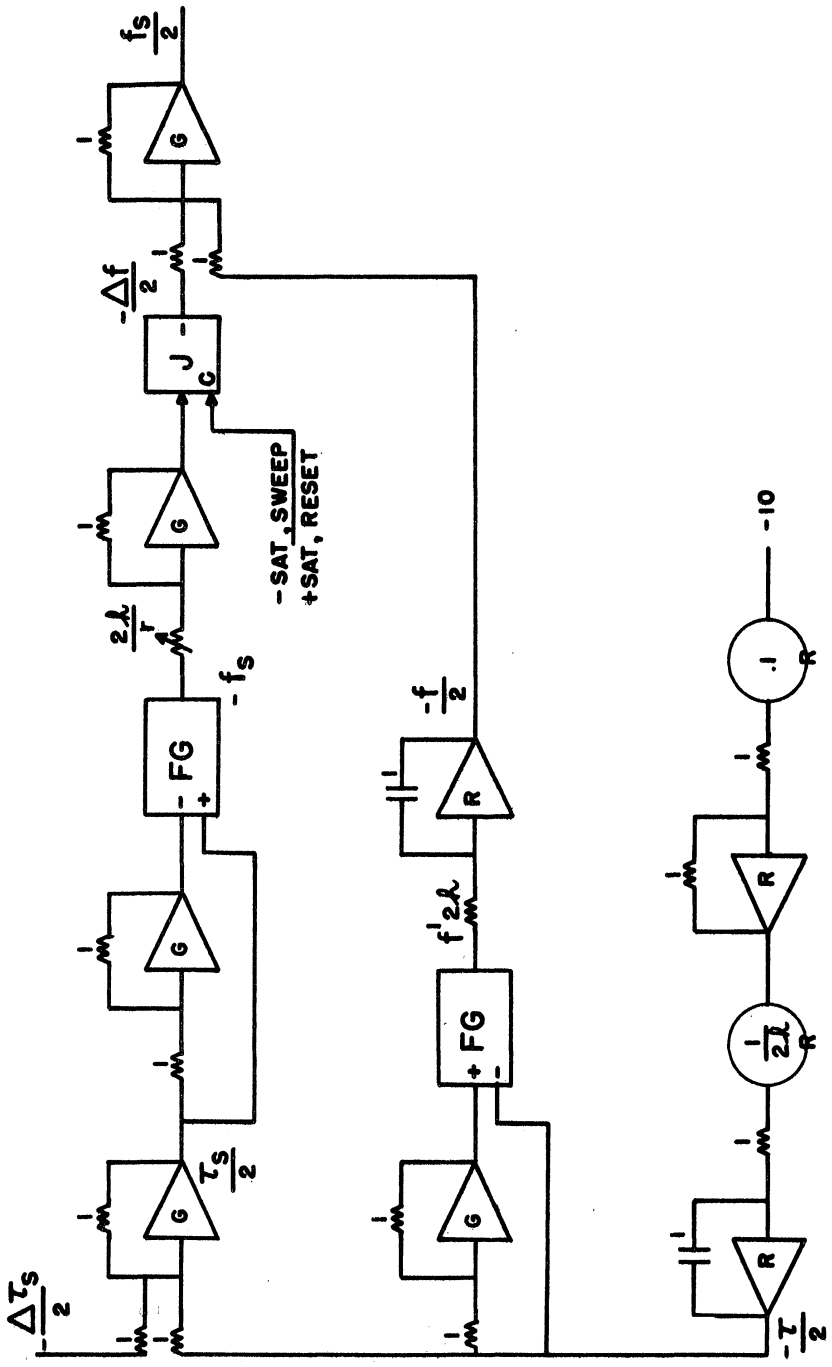

Figure 4.8 Input Circuit.

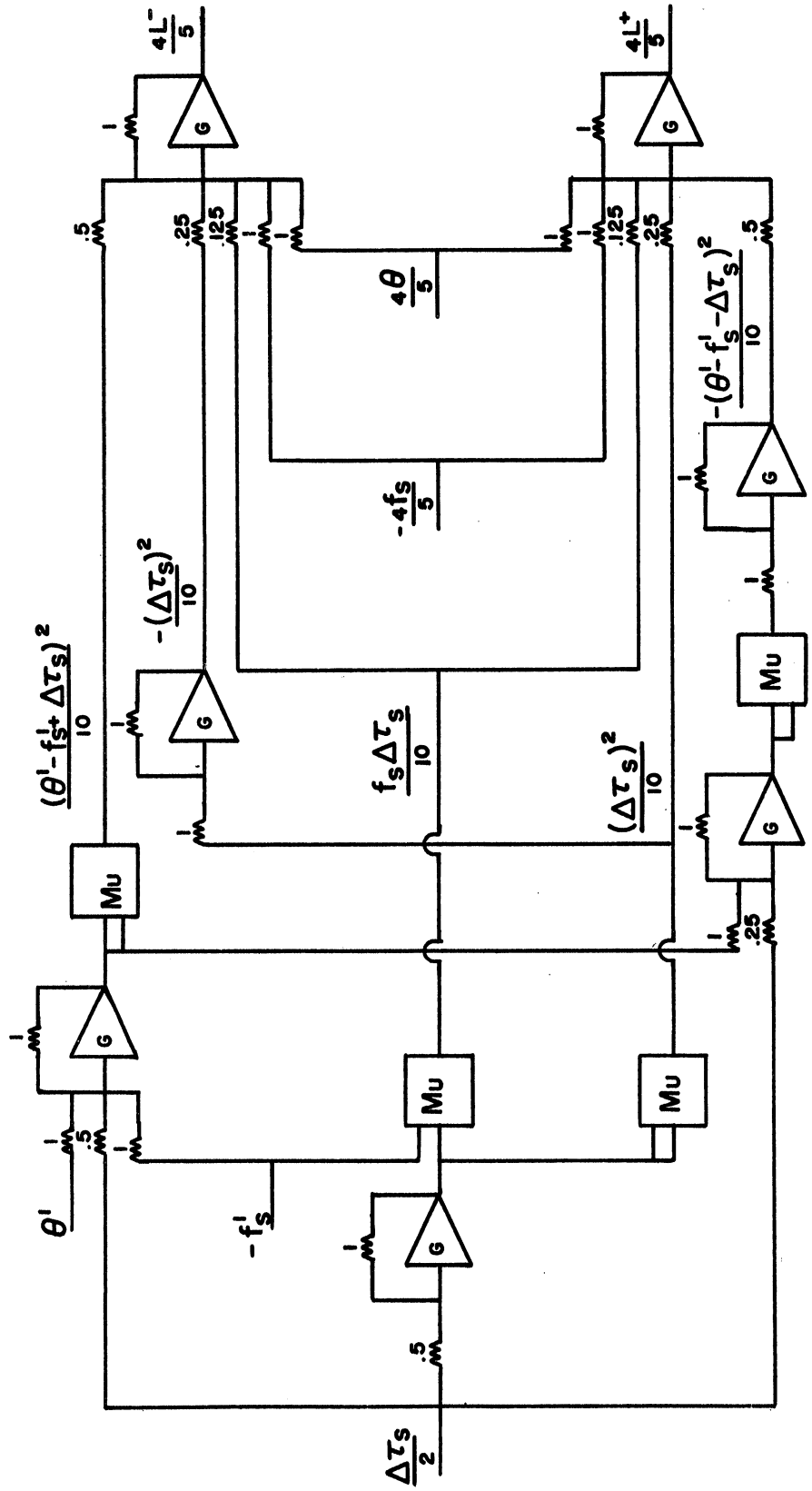

Figure 4.9 L ± Circuit, Contactor Servo with Inertia Only and with Known Input.

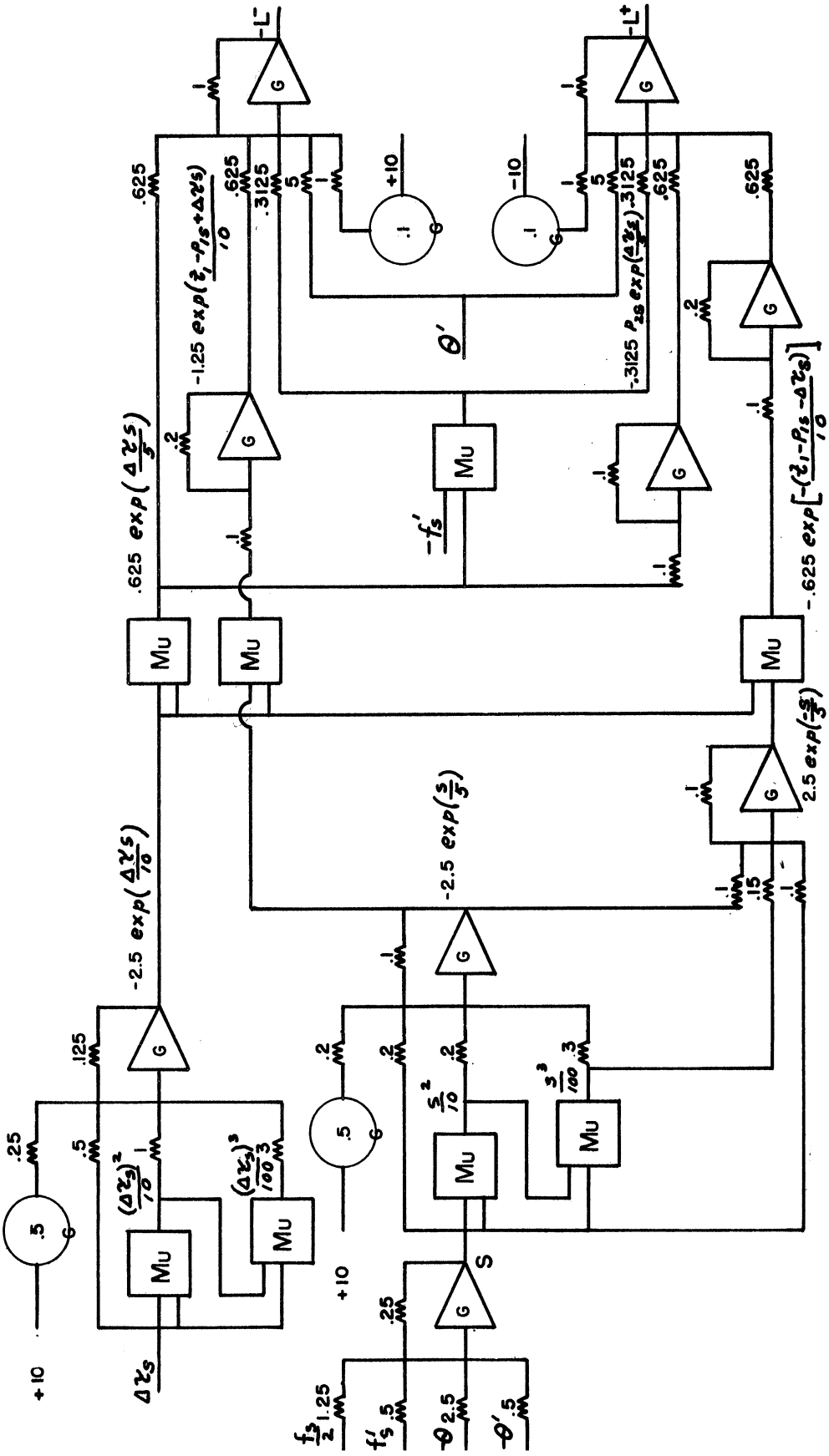

Figure 4.10 L ± Circuit, Contactor Servo with Inertia and Viscous Damping; Known Input.

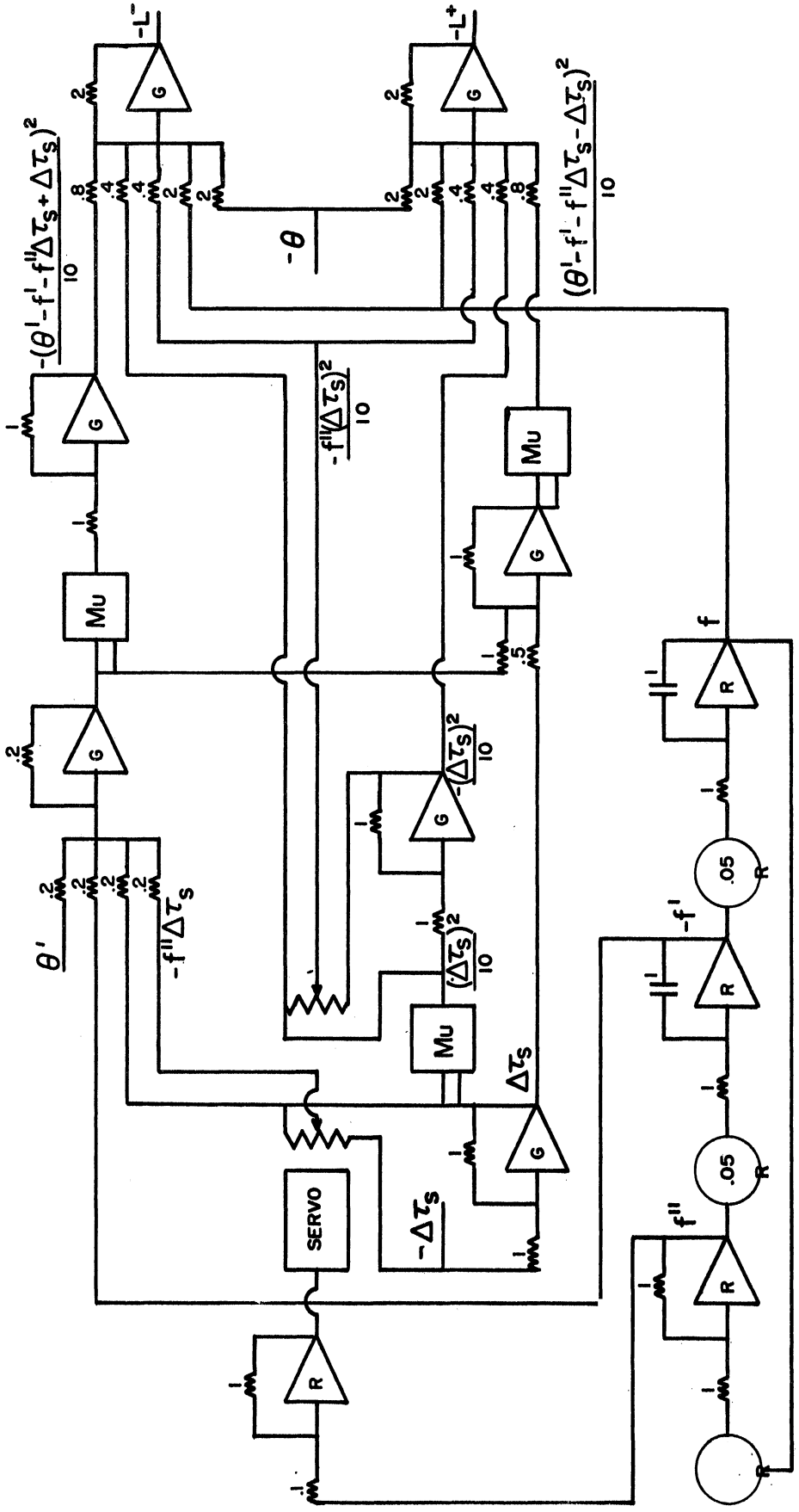

Figure 4.11 L ± Circuit, Contactor Servo with Inertia Only; Predicted Sinusoidal Input.

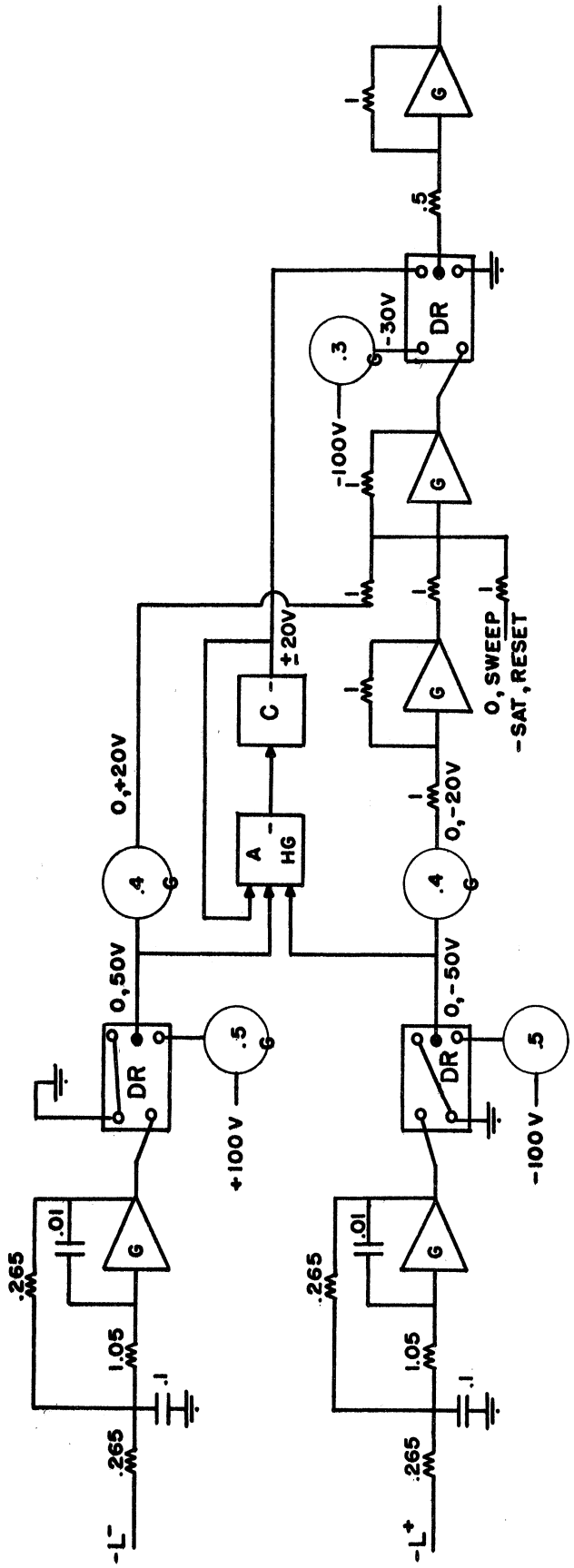

Figure 4.12 Decision Circuit.

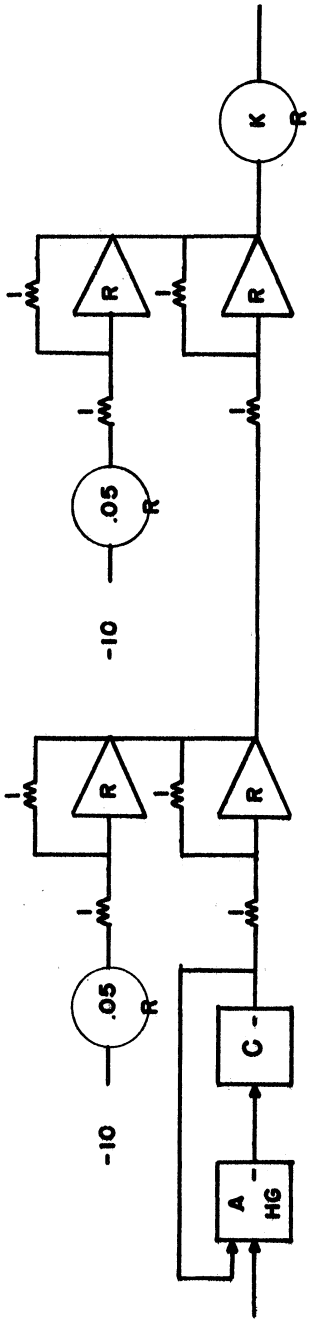

Figure 4.13 Forcing Circuit.

To complete the discussion of the computer circuits, mention should be made of two operating adjustments found useful. Normal balancing procedures were also used, of course. The circuit for the case of the servo with inertia only was adjusted on the basis of its response to a zero input signal. The θ and θ' values were adjusted manually to arbitrarily move the output phase point about in the phase plane. This was done until it was at a location in the plane where the decision mechanism would give forcing decisions of either sign. Several such points were located which then fixed the computer switching curve in the phase plane. It was found the computer switching curve was quite close to the theoretical one for the zero input. A less than one percent variation of one of the .5 megohm input resistors of the output amplifiers of Figure 4.9 virtually removed the difference. Varying these resistors varies the rate at which the parabolas containing the loci open up. Thus, the intersection points of the two parabolas which describe the switching curve are also varied.

The circuit for the servo with inertia and viscous damping was also checked against a zero input response. In this case, actual operation of the circuit resulted in a limit cycle action about the origin of the phase plane as expected. The size of the limit cycle was decreased to an acceptable value by about a one-fifth of one percent adjustment to the potentiometer shown feeding the .2 megohm input resistor at the left of Figure 4.10.

Known Input Study

Using the computer circuits described above, the transient behavior of the two contactor servos with swept-locus switching was

checked. Relatively simple input signals were used. Computer runs were begun with initial separation of the input and output phase points, and recordings were made of system behavior until approximate interception was obtained. A linear mode for small error,error-rate conditions was not used. The recordings consisted of two phase plane plots and a displacement, time plot. The three plots were made simultaneously for each run. Phase plane plots were made on two Model 205-G Variplotters made by Electronic Associates Incorporated, and the time plots were made on a Model 1 Autograf recorder made by F. L. Moseley Company.

For the contactor servo with inertia only, error,error-rate and output displacement-velocity phase plane plots were made. An Υ of two hundred was used. Recordings are shown in Figures 4.14 through 4.24 for this servo. The response to a constant input is shown in Figures 4.14 through 4.16, and comparison with Figure 2.2 indicates satisfactory results were achieved. Worthwhile noting are the larger displacement overshoots for the runs in which switching occurred at higher velocities. For these runs, the time for each sweep was longer near the switching boundary than for those runs which switched closer to the origin. This longer time between decisions and the higher output velocity, naturally, combined to give greater overshoots of the switch boundary. The same effect is seen in the ramp input plots.

Figure 4.21, the error, error-rate plot for the parabolic input, shows trajectories corresponding to sums and differences of the input and output accelerations as prescribed by Equations(2.3).

Figure 4.23 is the displacement,time plot of an input signal composed of parabolic arcs. The input velocity function was put on

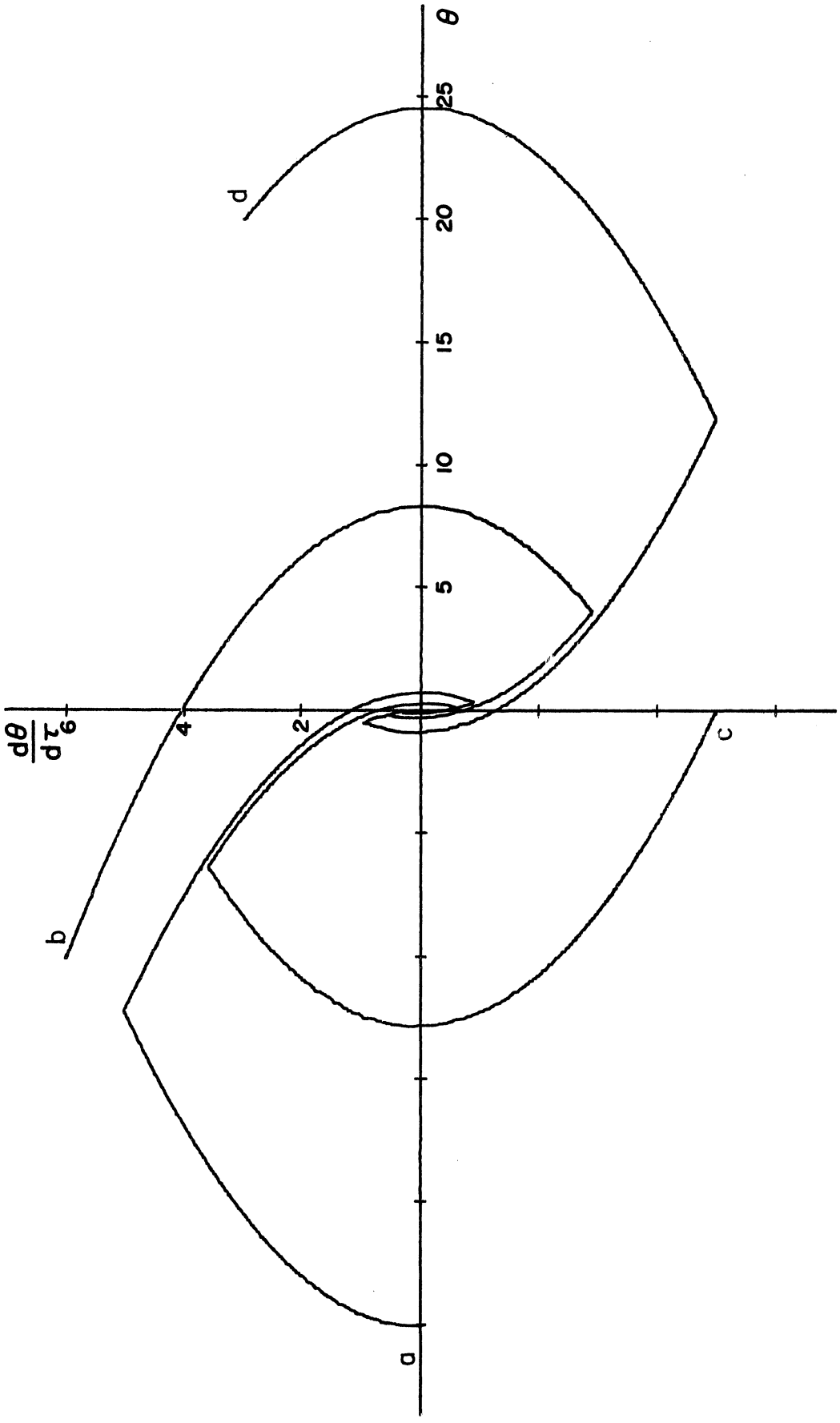

Figure 4.14 Response to Constant Input in Output Phase Plane, Contactor Servo with Inertia Only.

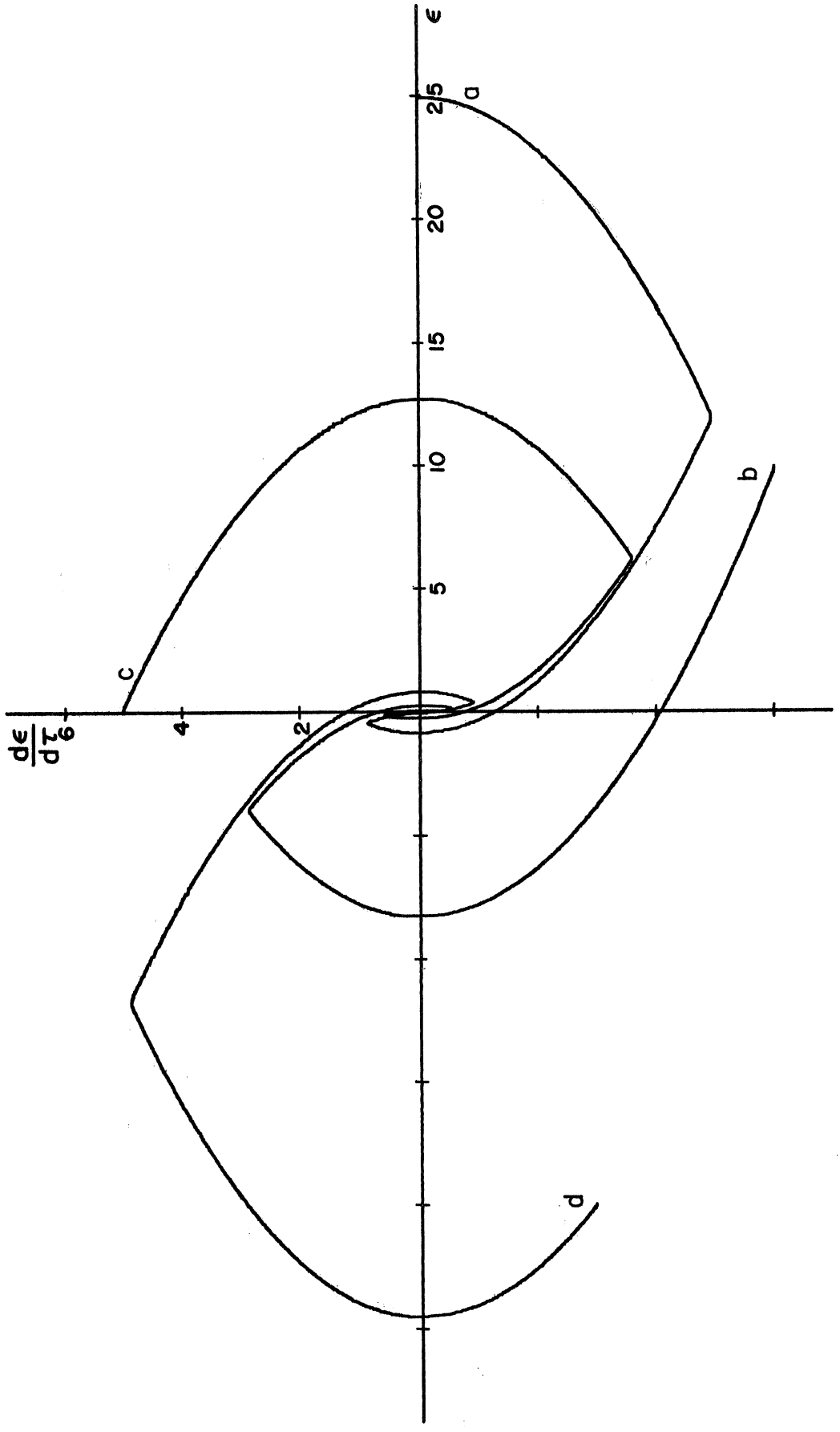

Figure 4.15 Response to Constant Input in Error Phase Plane, Contactor Servo with Inertia Only.

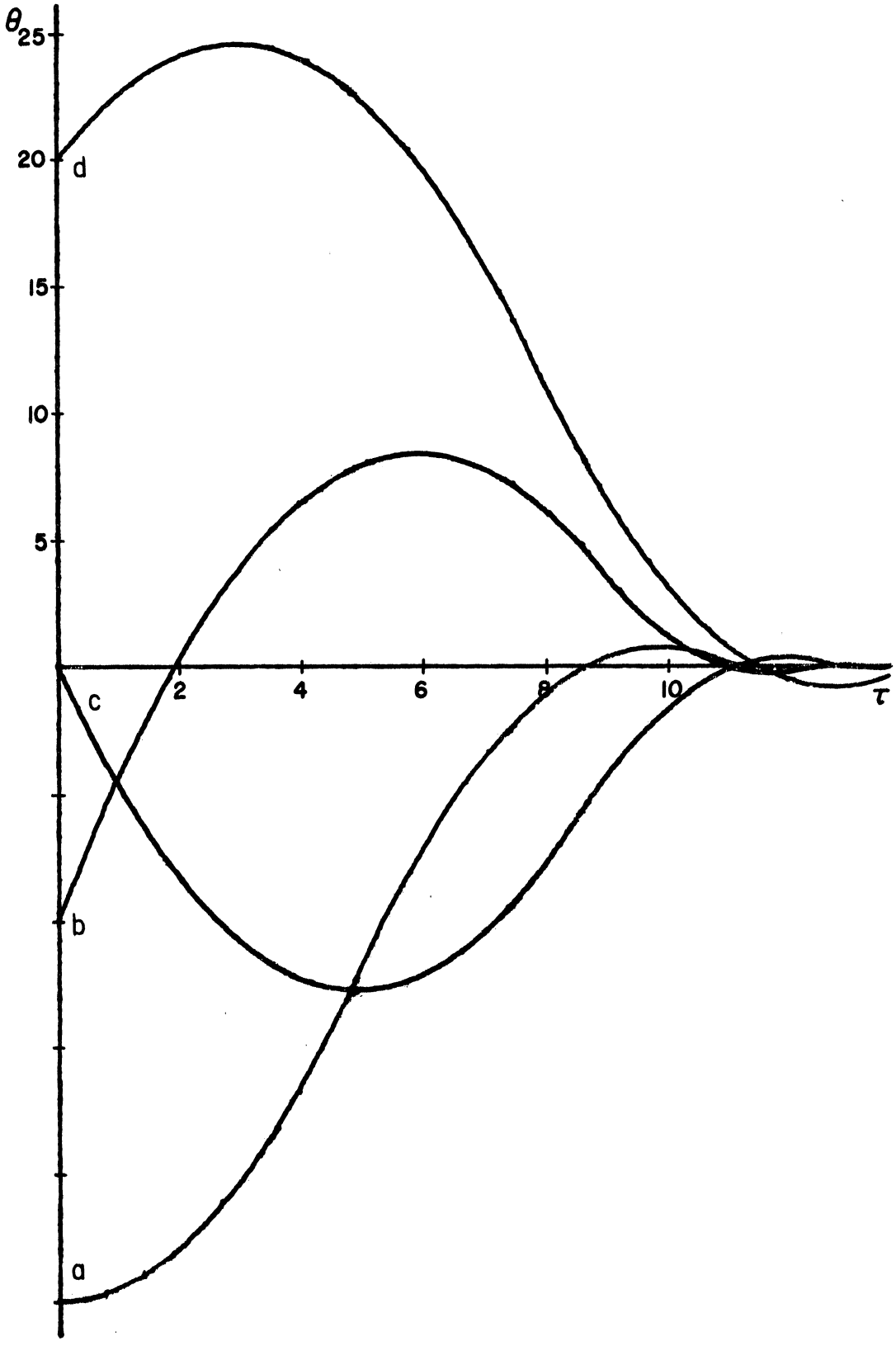

Figure 4.16 Time Plot of Response to Constant Input, Contactor Servo with Inertia Only.

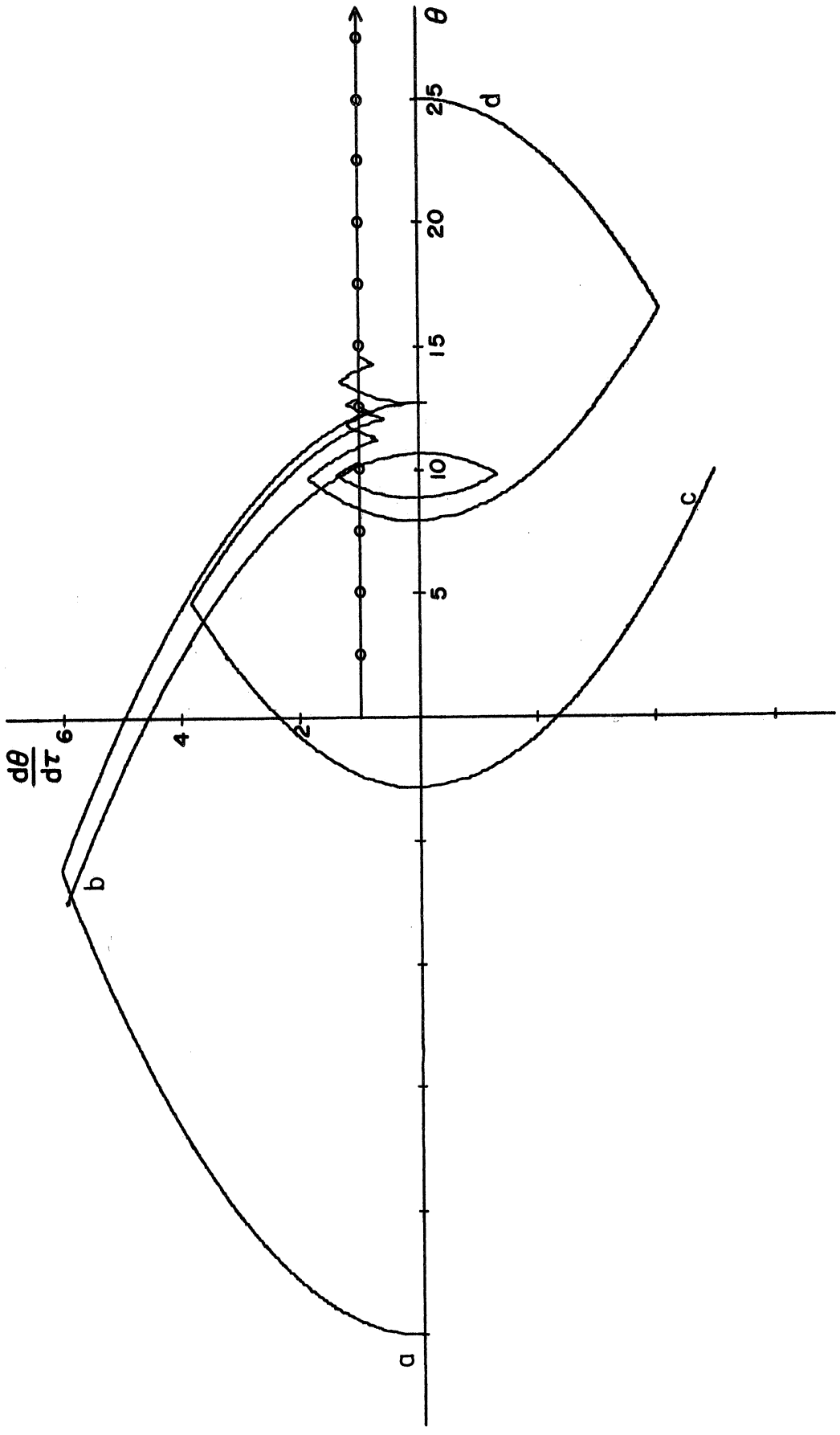

Figure 4.17 Response to Constant Velocity Input in Output Phase Plane, Contactor Servo with Inertia Only.

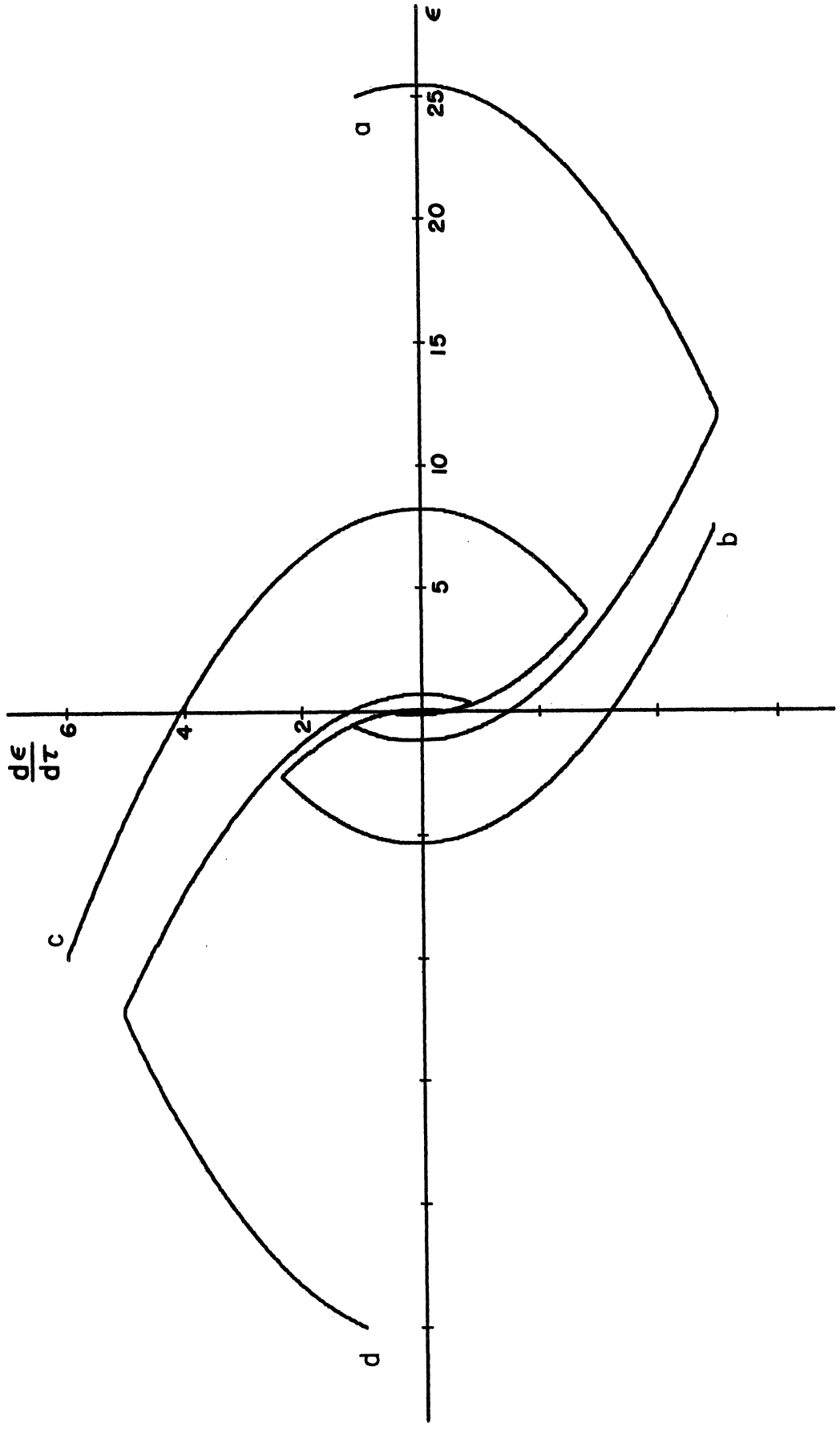

Figure 4.18 Response to Constant Velocity Input in Error Phase Plane Contactor Servo with Inertia Only.

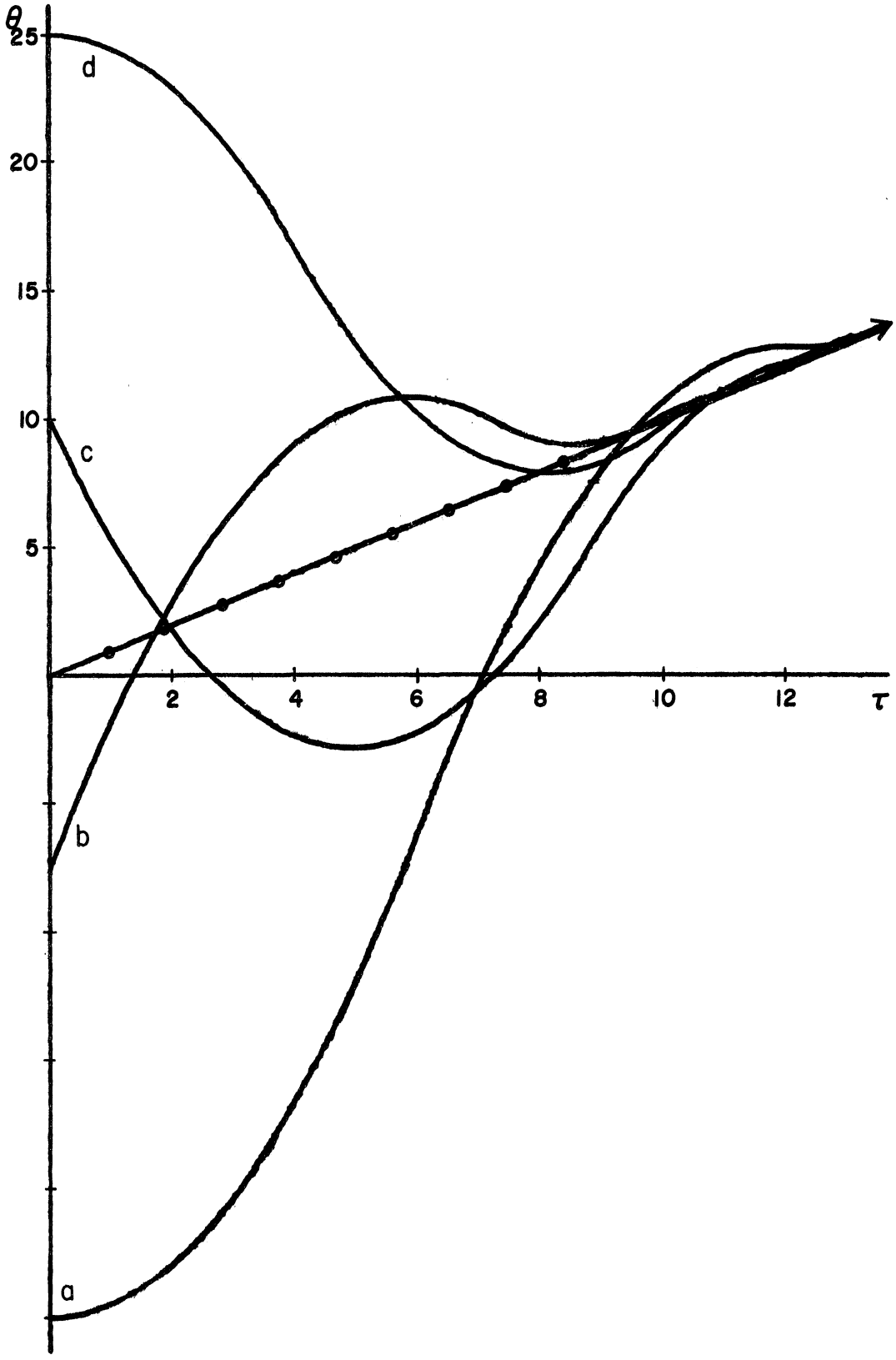

Figure 4.19 Time Plot of Response to Constant Velocity Input, Contactor Servo with Inertia Only.

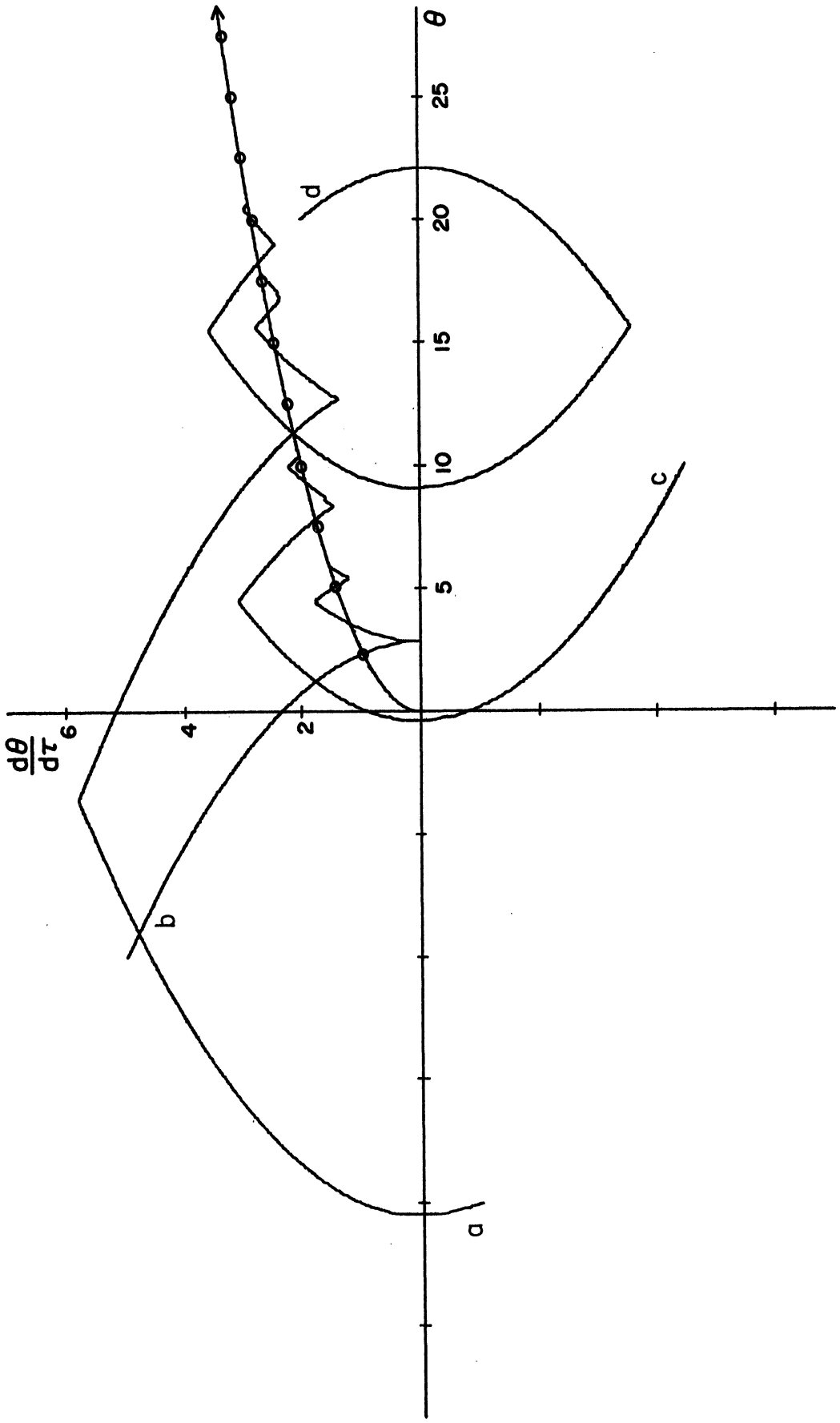

Figure 4.20 Response to Parabolic Input in Output Phase Plane, Contactor Servo with Inertia Only.

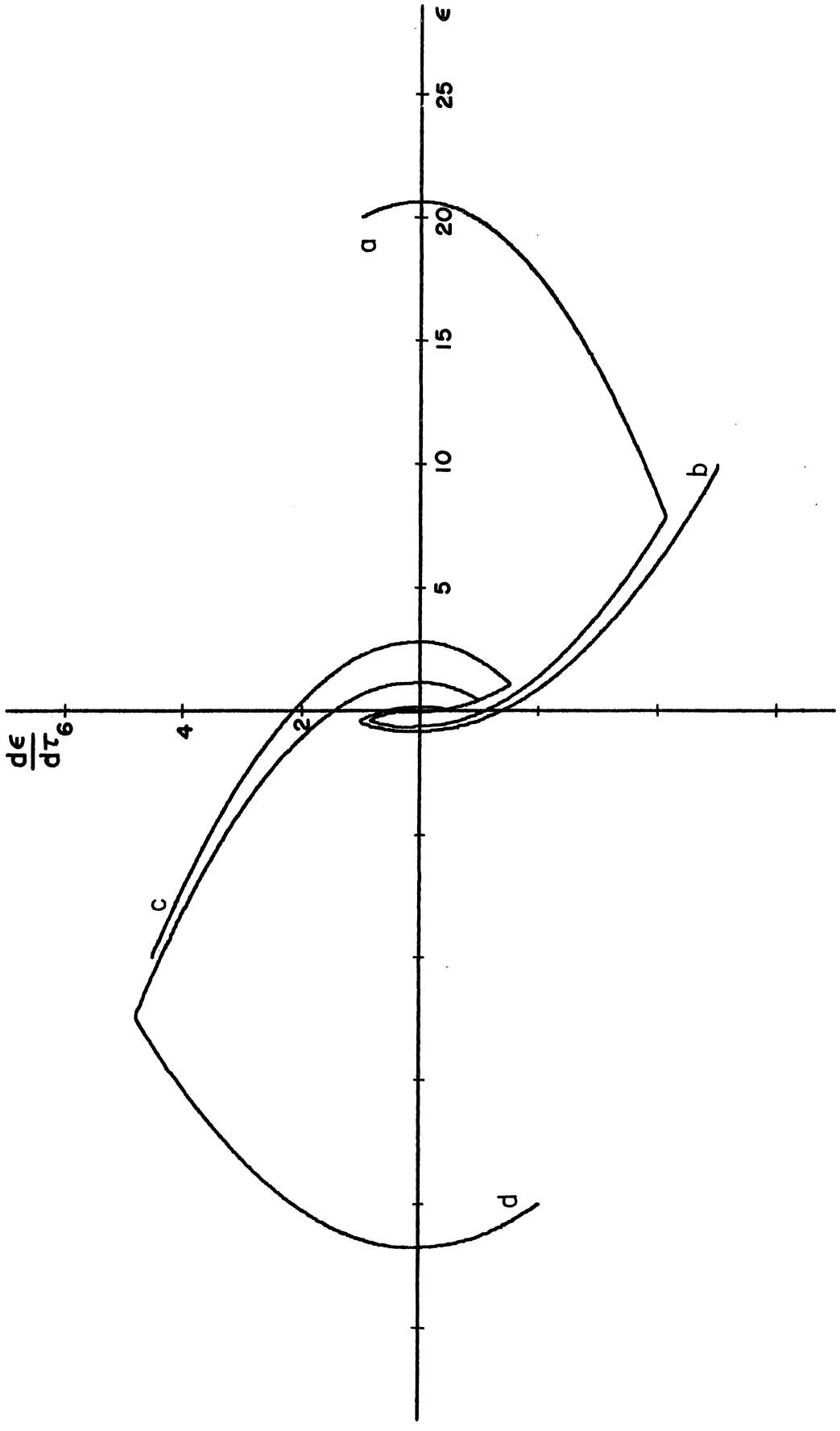

Figure 4.21 Response to Parabolic Input in Error Phase Plane, Contactor Servo with Inertia Only.

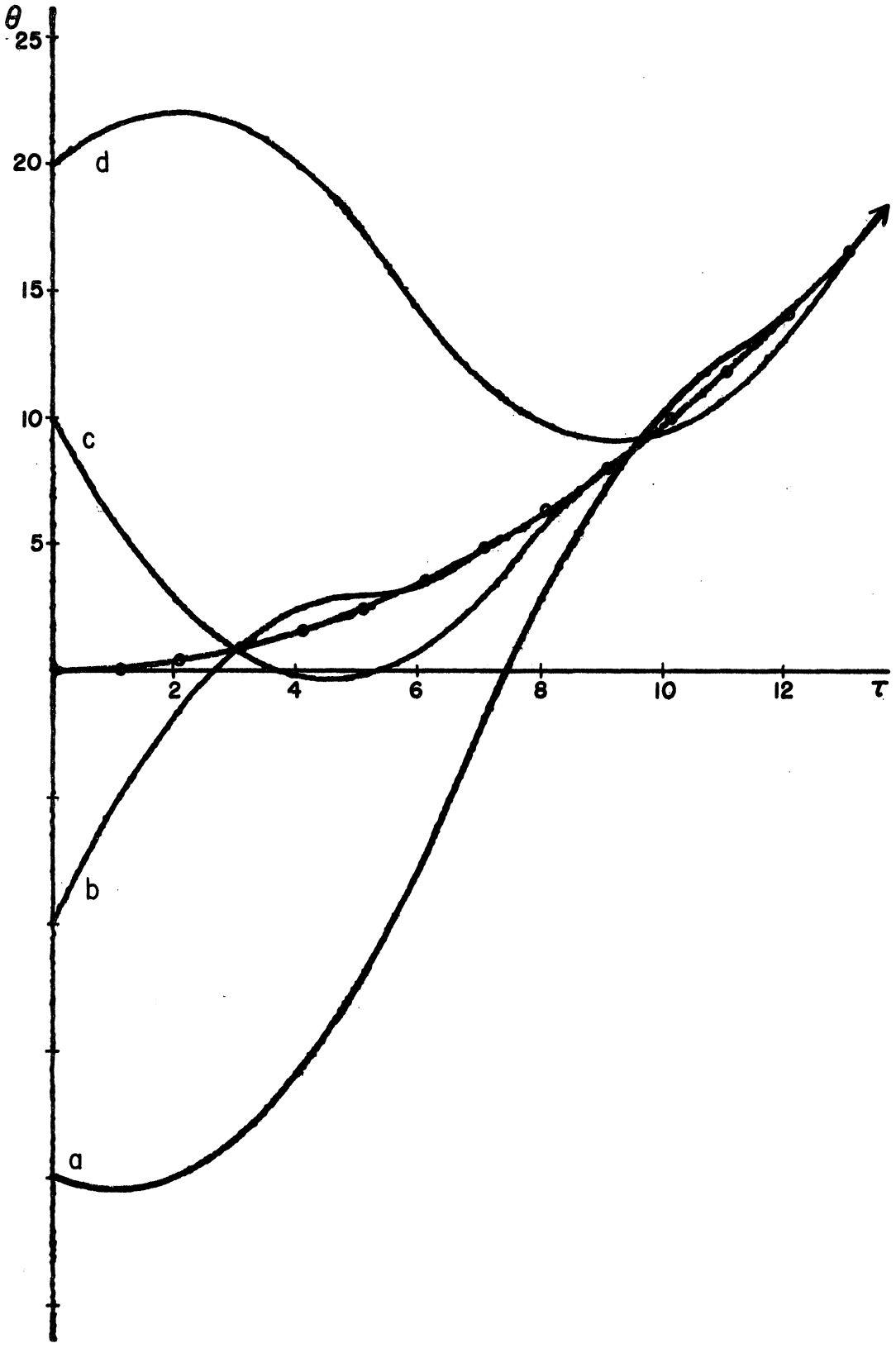

Figure 4.22 Time Plot of Response to Parabolic Input, Contactor Servo with Inertia Only.

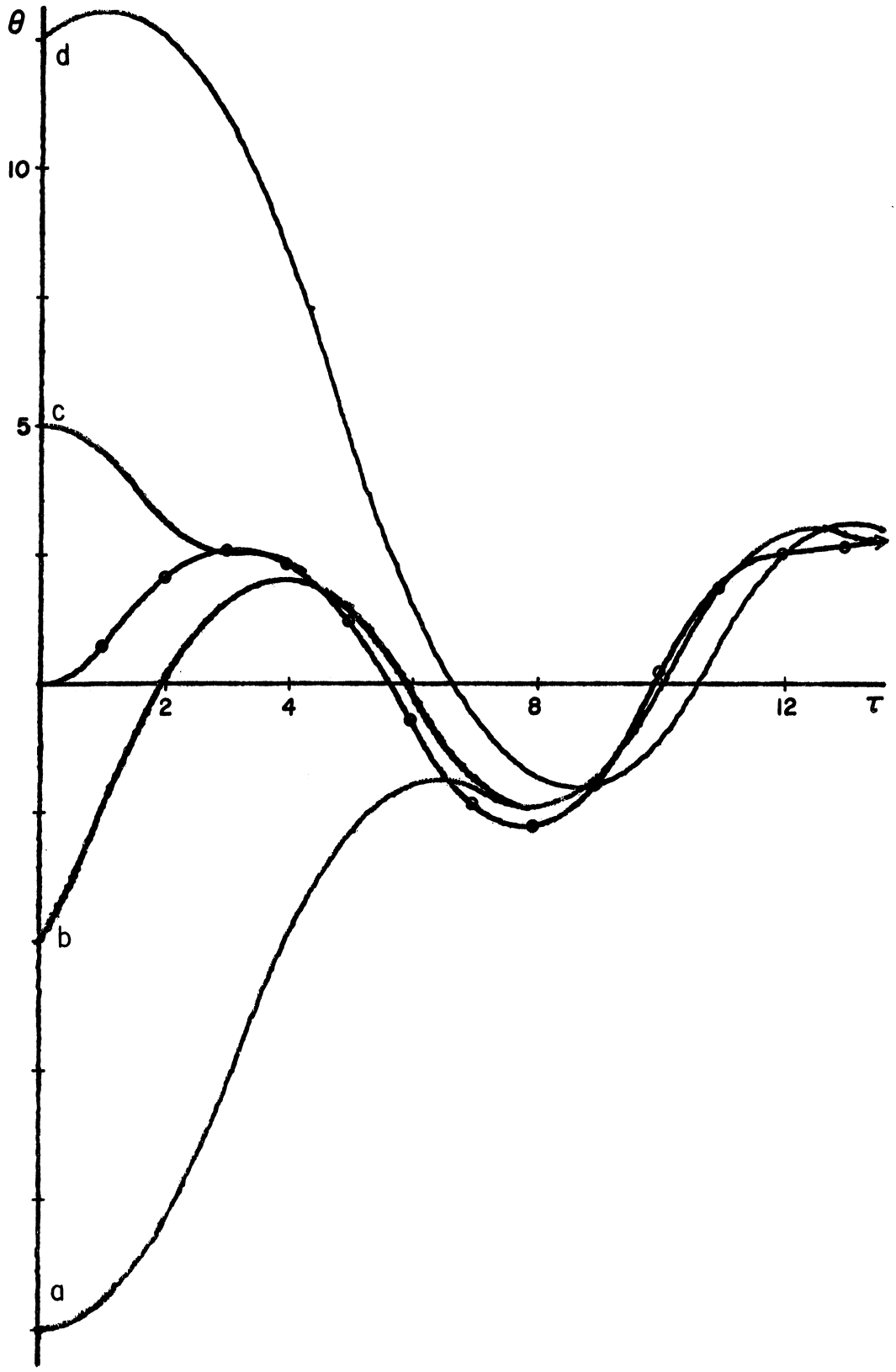

Figure 4.23 Time Plot of Response to Varied Input, Contactor Servo with Inertia Only.

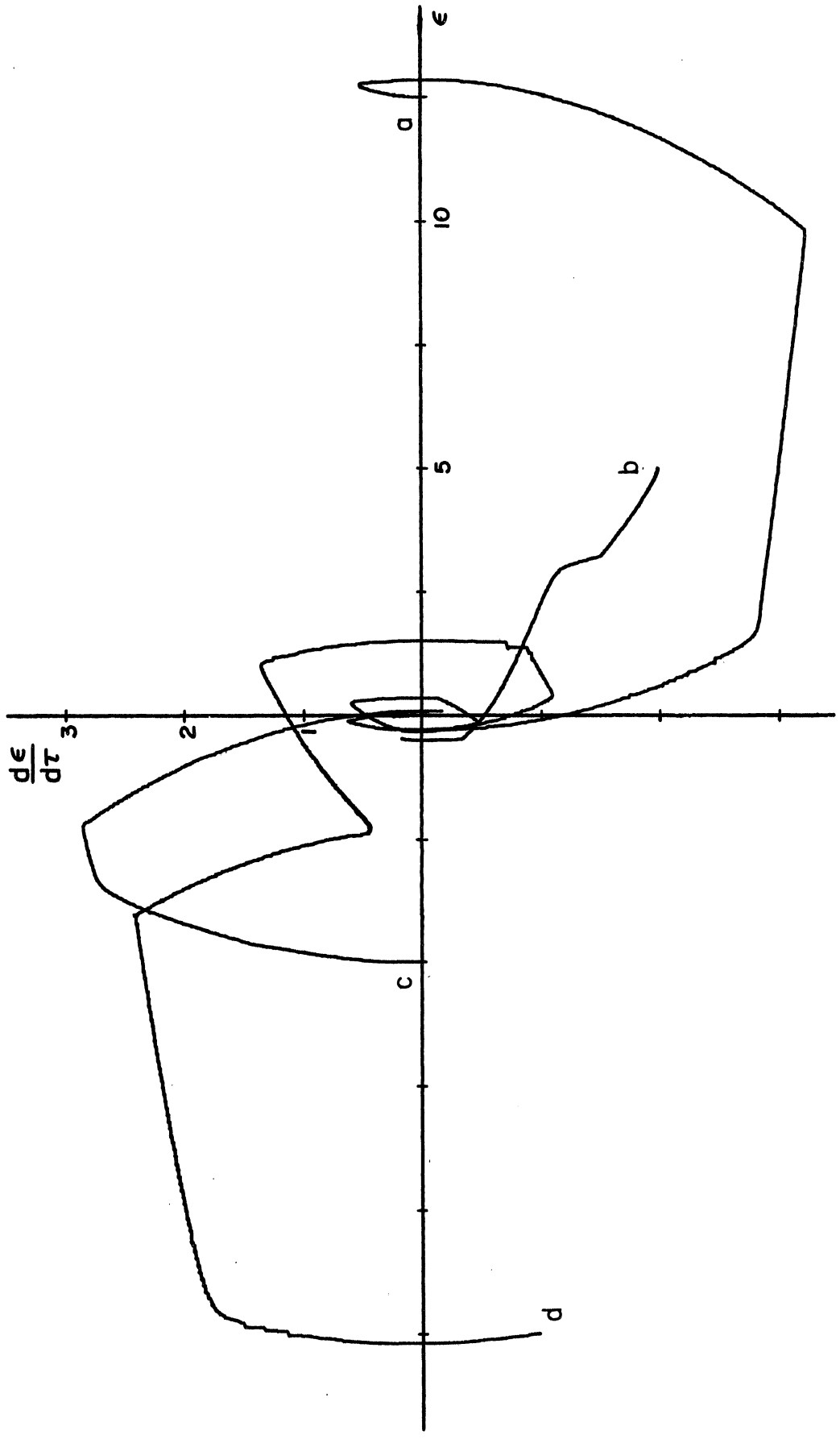

Figure 4.24 Error Phase Plane Plot of Response to Varied Input, Contactor Servo with Inertia Only.

the two GEDA function generators. Close agreement between the two was obtained by setting the function up on both generators, plotting their outputs versus their inputs on a Variplotter, and then causing the plot of one output to coincide with the plot of the other by systematically adjusting the first function generator's setting knobs. The error, error-rate plot, Figure 4.24, points up the deficiencies a switching system based on a fixed error, error-rate plane switch boundary would have for such an input.

For the servo with inertia and viscous damping, phase plane plots were made of the output variables in the displacement-velocity plane and in the principal coordinate plane. Input signal velocity was kept well within the servo velocity limits to hold down the transient time. An Υ of one hundred was used. Plots for this servo are in Figures 4.25 through 4.32. In general, the plots validate the theory. The overshoot for the more arbitrary input signal of Figures 4.31 and 4.32 is larger than desired. Much of this trouble is believed due to the fact that the function generator used for f_s' did not maintain a steady setting, so that the swept loci were in error. The approximations for the exponentials contributed to the error also. It appears that this effect diminished with diminishing sweep time, for the output came into the input curve in good fashion after the overshoot. The reason for the malfunction of the generator was not found before the author's computer time ran out.

Simple Input Prediction

As a first look at applying the swept locus switching scheme to the case of an arbitrarily varying input signal, a very simple

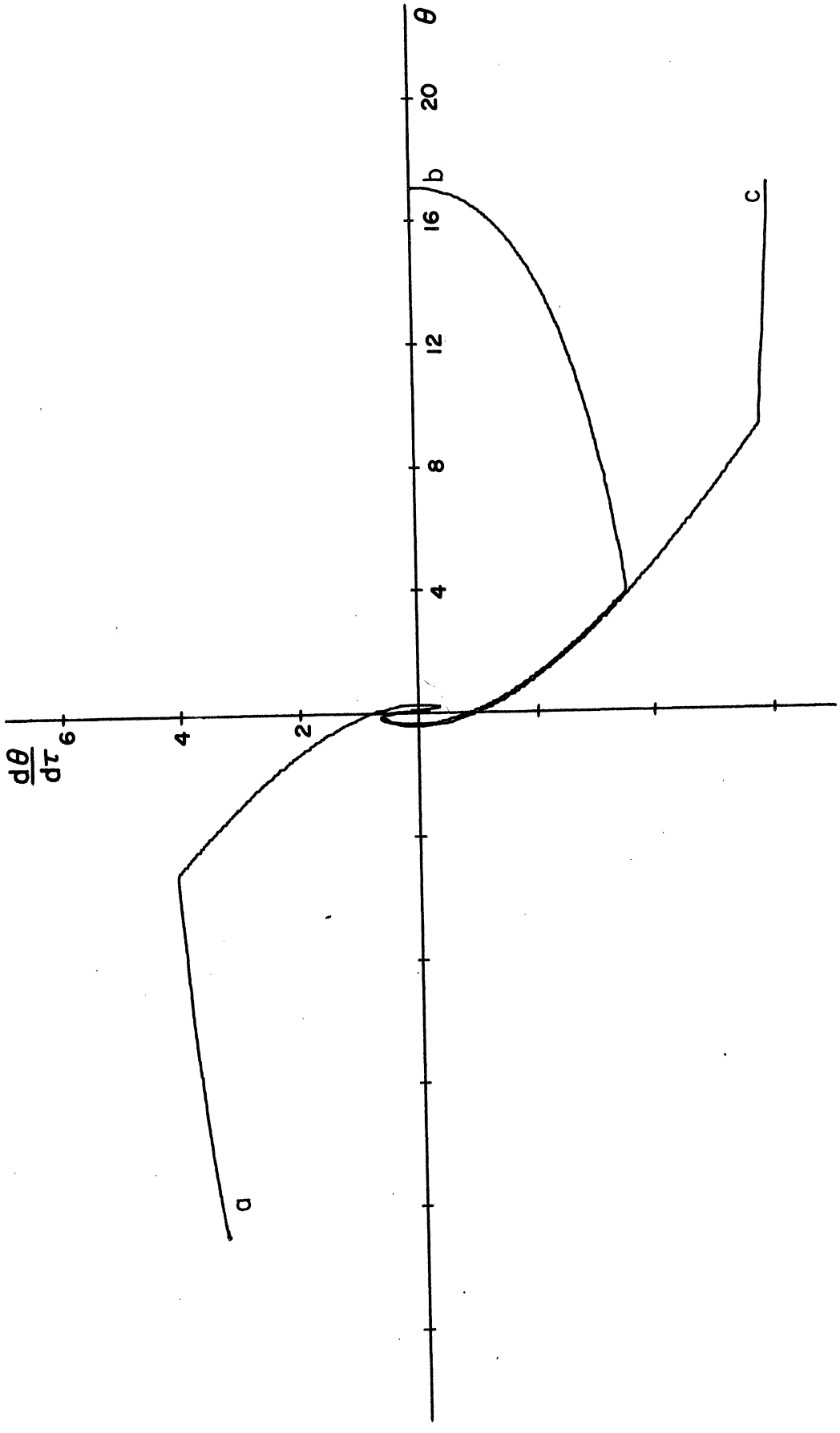

Figure 4.25 Response to Constant Input in Output Phase Plane, Contactor Servo with Inertia and Viscous Damping.

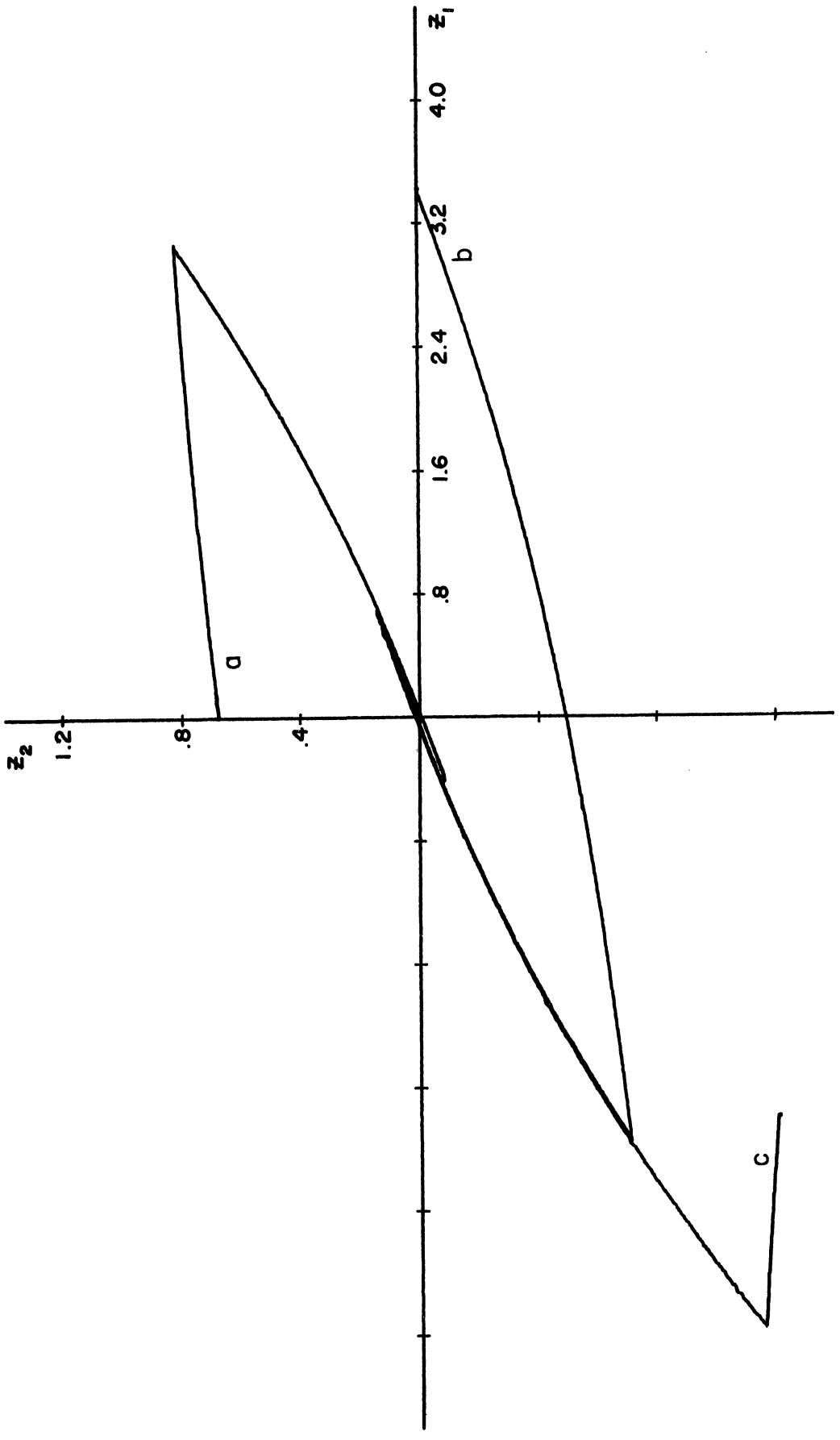

Figure 4.26 Response to Constant Input in Principal Coordinate Phase Plane, Contactor Servo with Inertia and Viscous Damping.

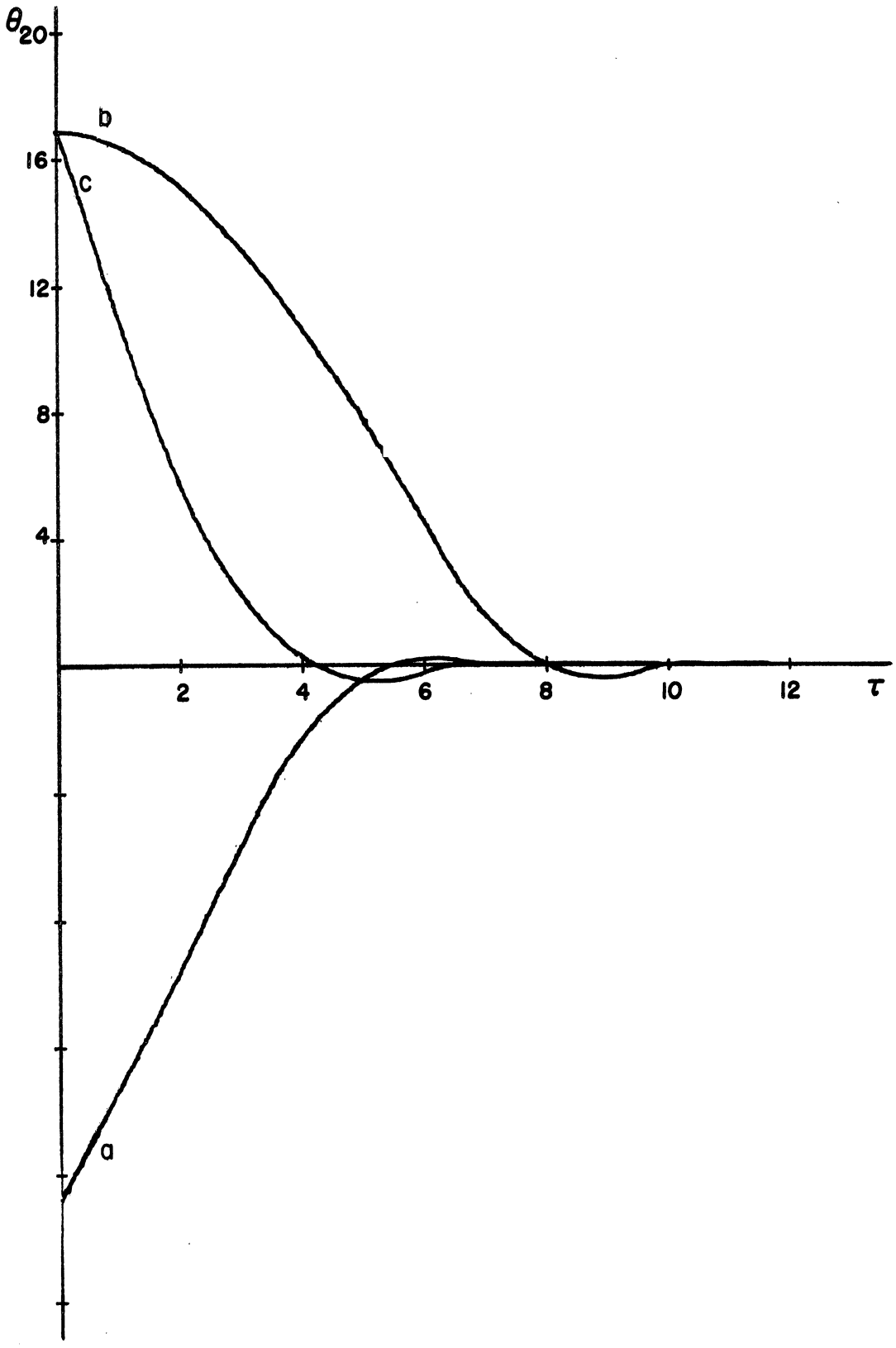

Figure 4.27 Time Plot of Response to Constant Input, Contactor Servo with Inertia and Viscous Damping.

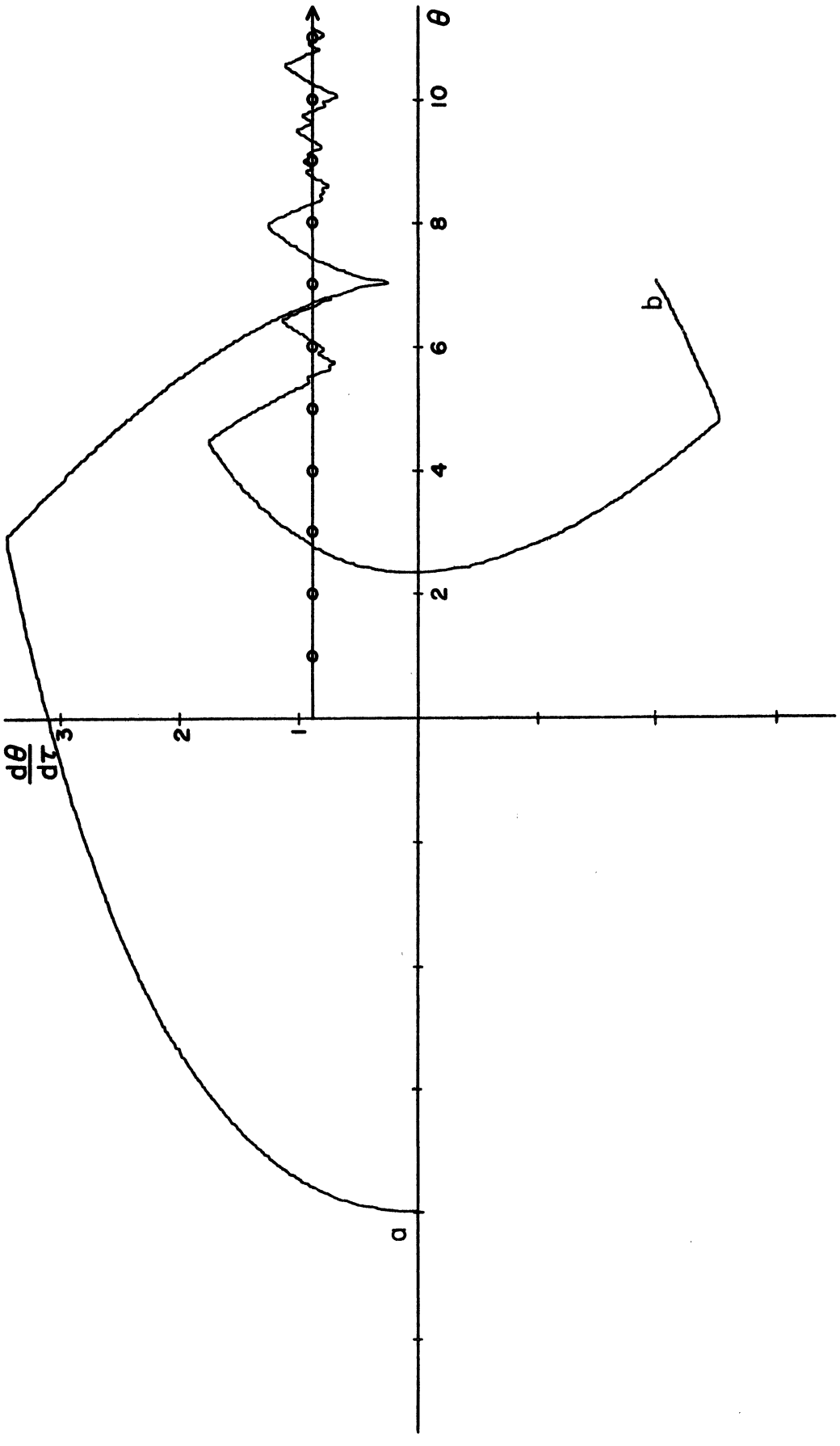

Figure 4.28 Response to Constant Velocity Input in Output Phase Plane, Contactor Servo with Inertia and Viscous Damping.

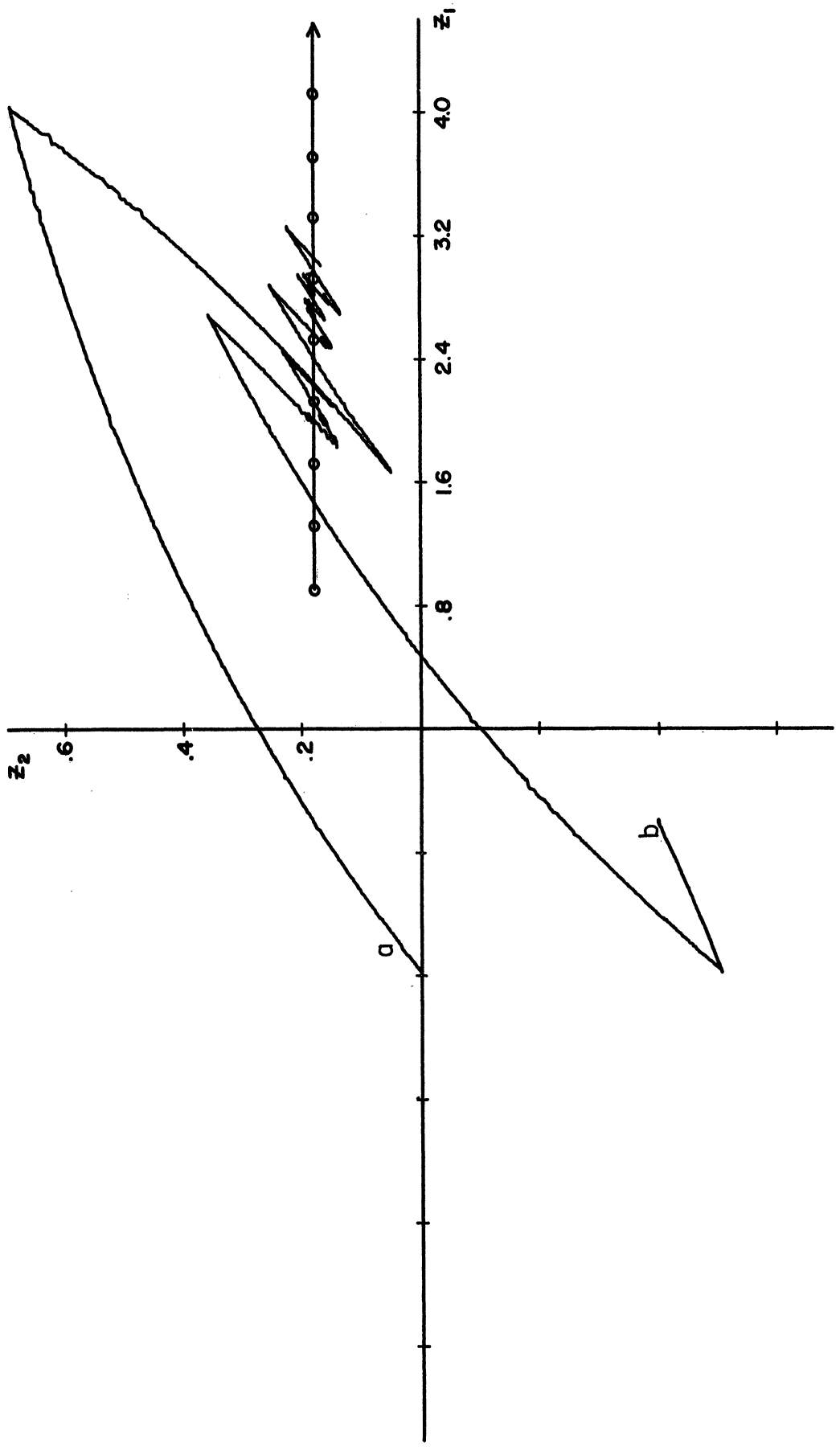

Figure 4.29 Response to Constant Velocity Input in Principal Coordinate Phase Plane, Contactor Servo with Inertia and Viscous Damping.

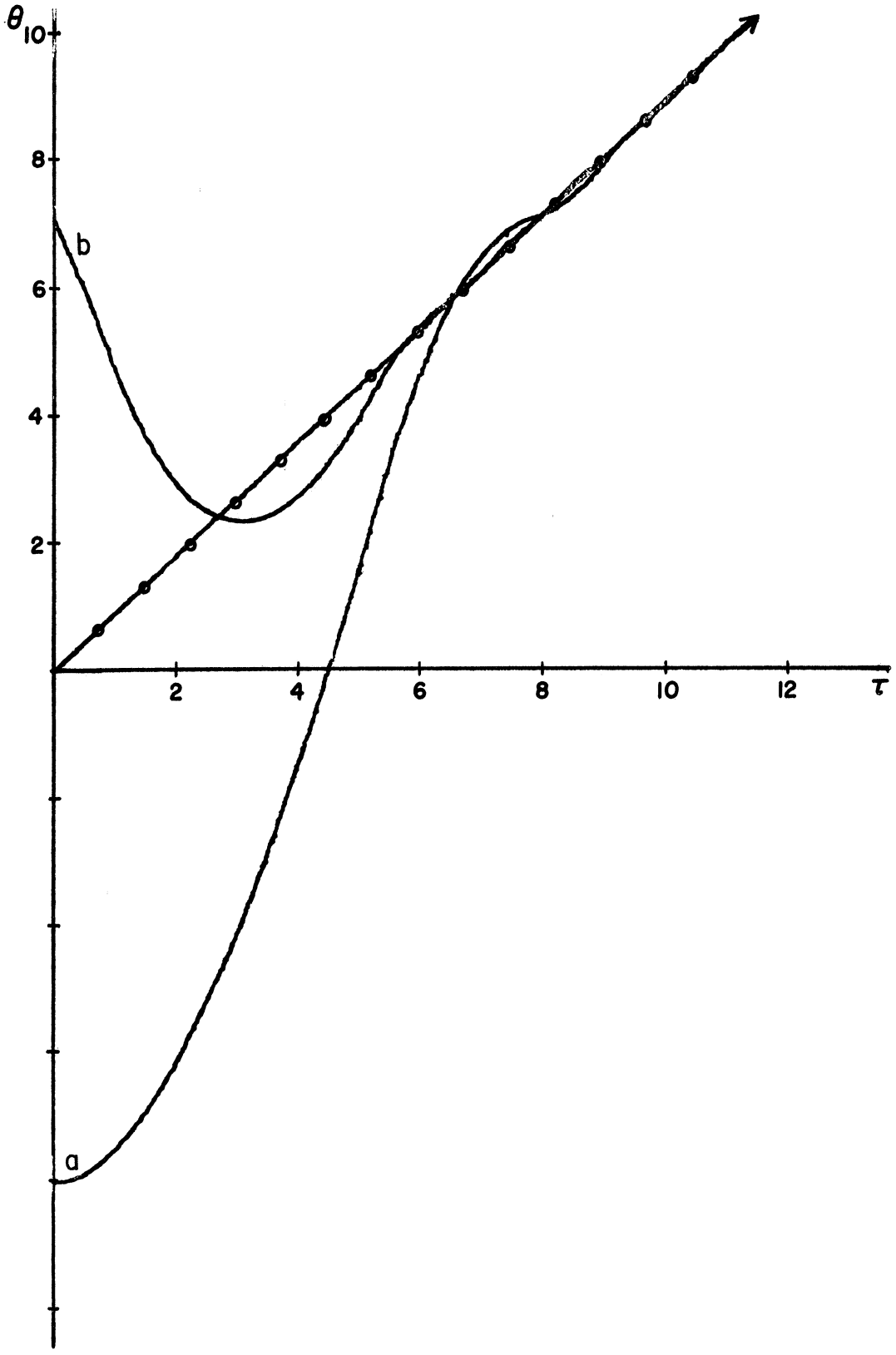

Figure 4.30 Time Plot of Response to Constant Velocity Input, Contactor Servo with Inertia and Viscous Damping.

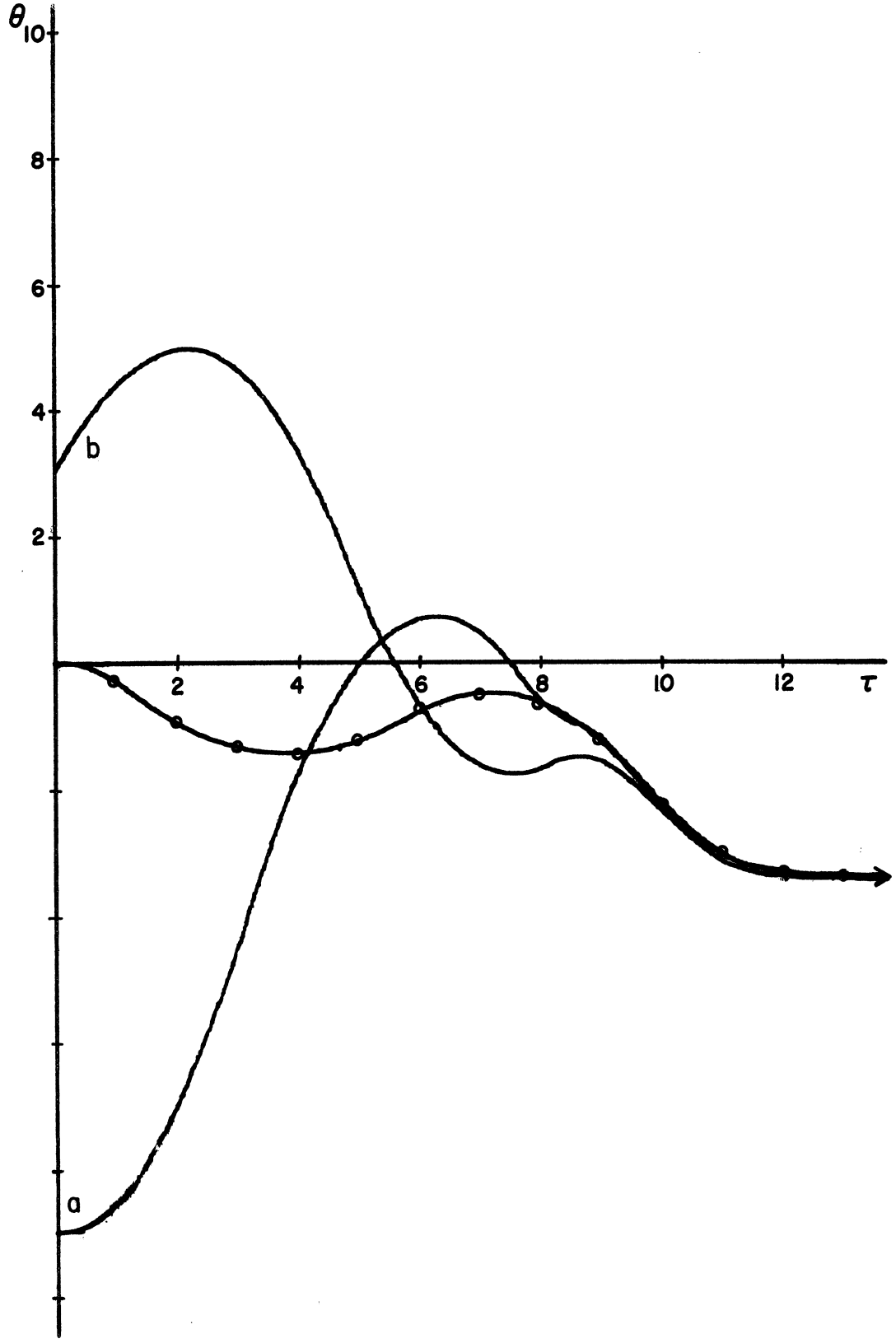

Figure 4.31 Time Plot of Response to Varied Input, Contactor Servo with Inertia and Viscous Damping.

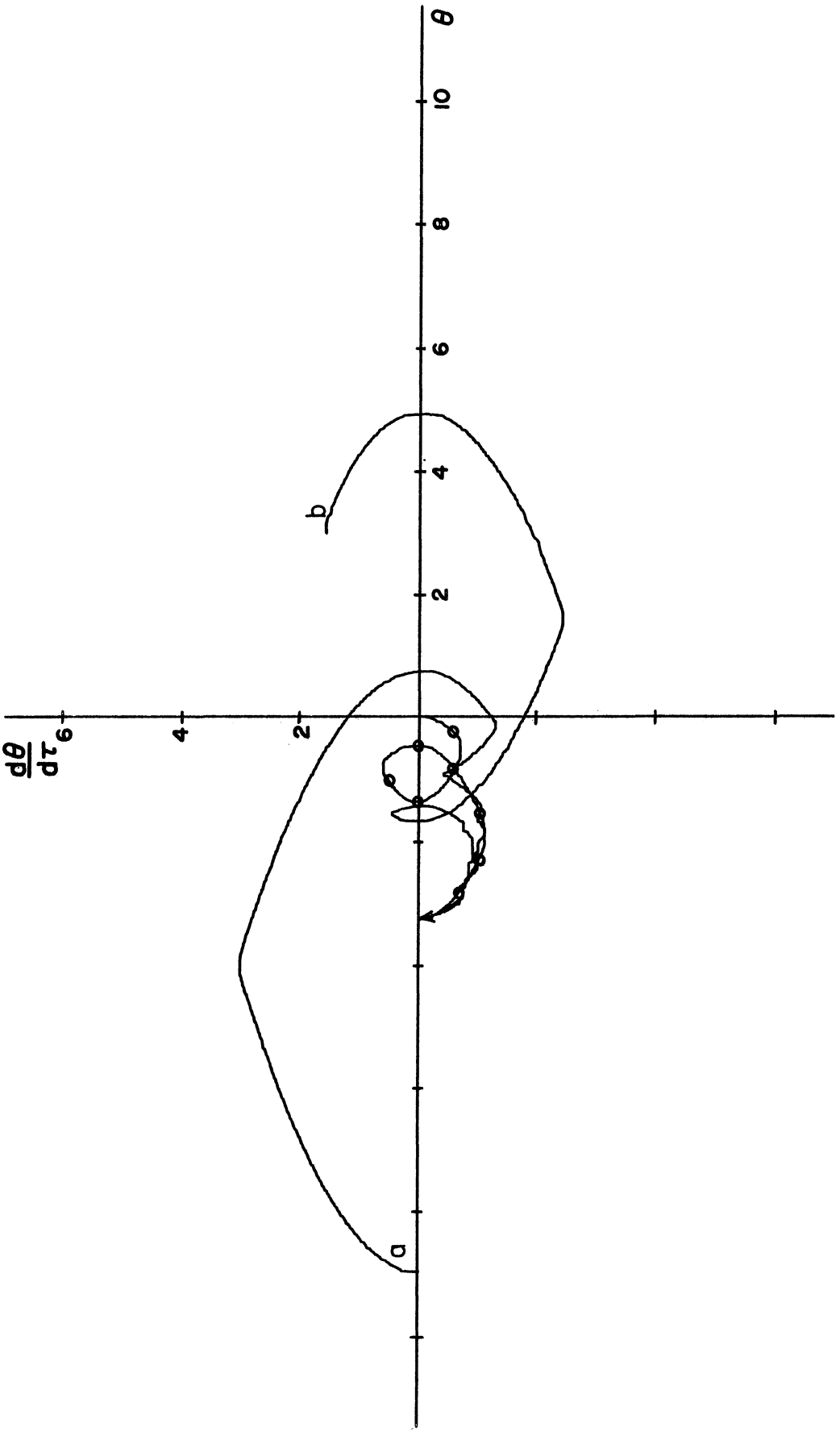

Figure 4.32 Output Phase Plane Plot of Response to Varied Input, Contactor Servo with Inertia and Viscous Damping.

prediction scheme was combined with the swept-locus circuitry to check system responses to sine wave inputs. The prediction used was to extrapolate f_s as

$$f_s = f + \Delta\gamma_s f' + \frac{(\Delta\gamma_s)^2}{2} f'' \qquad (4.14)$$

and f_s' as

$$f_s' = f' + \Delta\gamma_s f'' \quad . \qquad (4.15)$$

Sine wave inputs were used because of the ready availability of f, f' and f'' from the usual computer sine wave generator. Thus, for the study, the practical noise difficulty due to differentiation was eliminated.

The circuit representing the combined input and $\sqsubset^{+}$, $\sqsubset^{-}$ blocks of Figure 4.5 for the servo with inertia only is shown in Figure 4.11. Prediction was done both with and without the f'' terms of Equations (4.14) and (4.15). Eliminating these terms was merely a matter of removing the servo multiplier from the circuit of Figure 4.11. A circuit combining features of Figure 4.11 and Figure 4.10 was used for the servo with inertia and viscous damping.

Displacement, time plots for the servo with inertia only are shown in Figures 4.33 through 4.35. Part (A) of each figure is for prediction without the f'' terms; part (B), with the f'' terms.

Figure 4.33 i.e., the case of maximum input acceleration equal to one-half system output acceleration, indicates that the more sophisticated prediction probably gives a better transient response in general.

Figure 4.33 for maximum input acceleration equal to eight-tenths output acceleration appears to give the same impression. Extended runs of the seemingly divergent output trace in part (A) showed that the amplitude of the output did not continue to diverge. The amplitude did not assume a steady state value, however. The corresponding trace of Figure 4.35 showed similar behavior for the equal acceleration case. In part (B) of Figure 4.35 can be seen effects due to sweep saturation. The maximum sweep time increment was sometimes not long enough to allow a forcing decision to be made near a peak of the input wave where input acceleration was highest. The forcing from the previous sweep was carried over although in error for the new sweep. For the study, the sweep circuit was turned on and off manually during the divergent periods. Eventually, as the input acceleration diminished, the sweep circuit was able to function properly. It seems reasonable that for input accelerations temporarily greater than output acceleration, the condition would be aggravated. For general inputs, a more sophisticated prediction method would probably be in order.

For the servo with inertia and viscous damping the additional factor of output velocity limitation was naturally introduced. The sinusoidal inputs used were chosen with maximum velocities equal to the limiting output velocity levels. Two values of maximum acceleration were then selected. Figure 4.36 shows the case for maximum input acceleration equal to one-half maximum output acceleration. Prediction using the f'' terms appears to decrease transient error better initially. As the solutions were run faster for this servo, forcing decisions were relatively farther apart. It is believed this accounted for the "bumpiness" in the output curves.

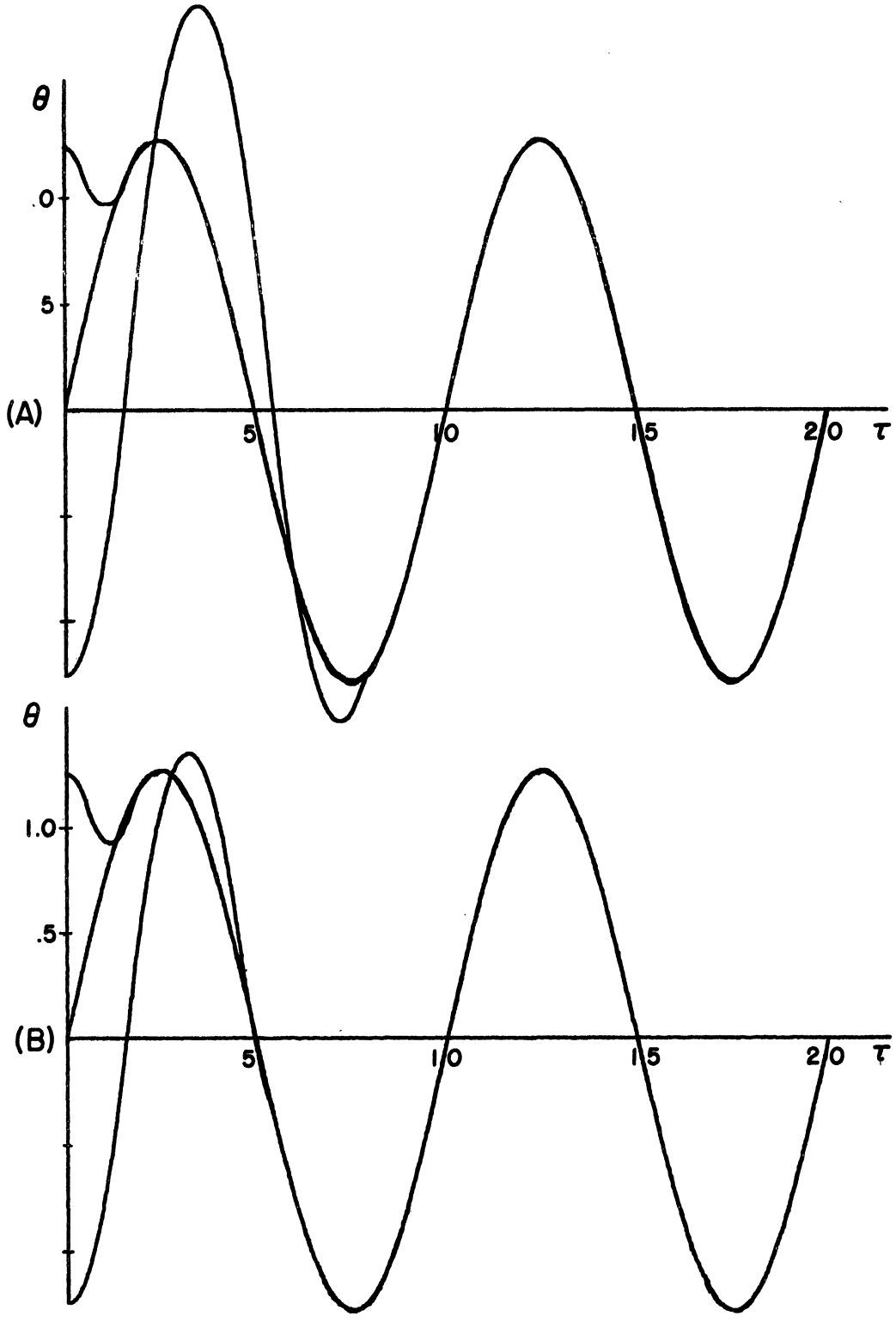

Figure 4.33 Responses with Prediction and Maximum f" = .5,
(A) Ramp Extrapolation, (B) Parabolic Extrapolation.

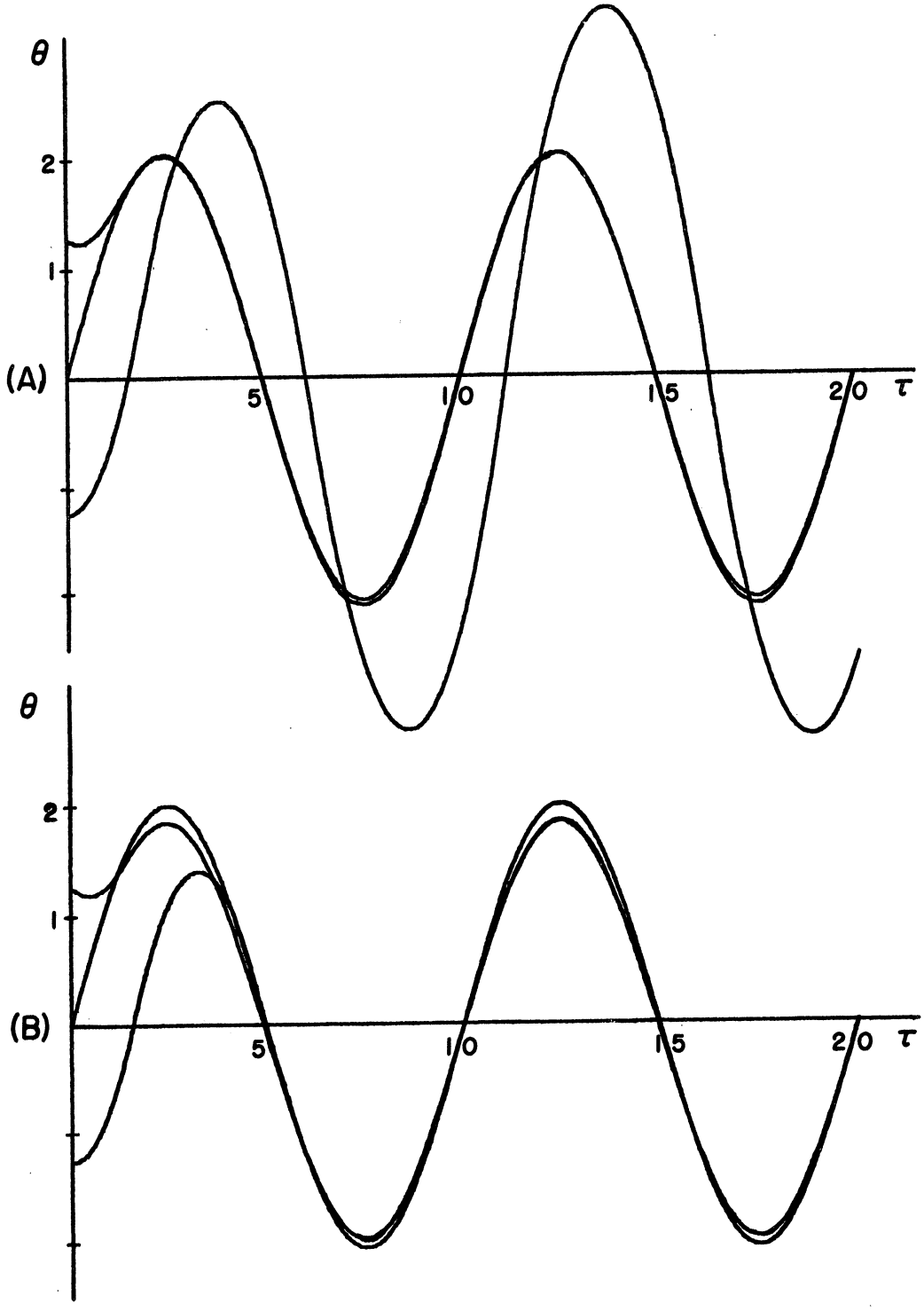

Figure 4.34 Responses with Prediction and Maximum f" = .8,
(A) Ramp Extrapolation, (B) Parabolic Extrapolation.

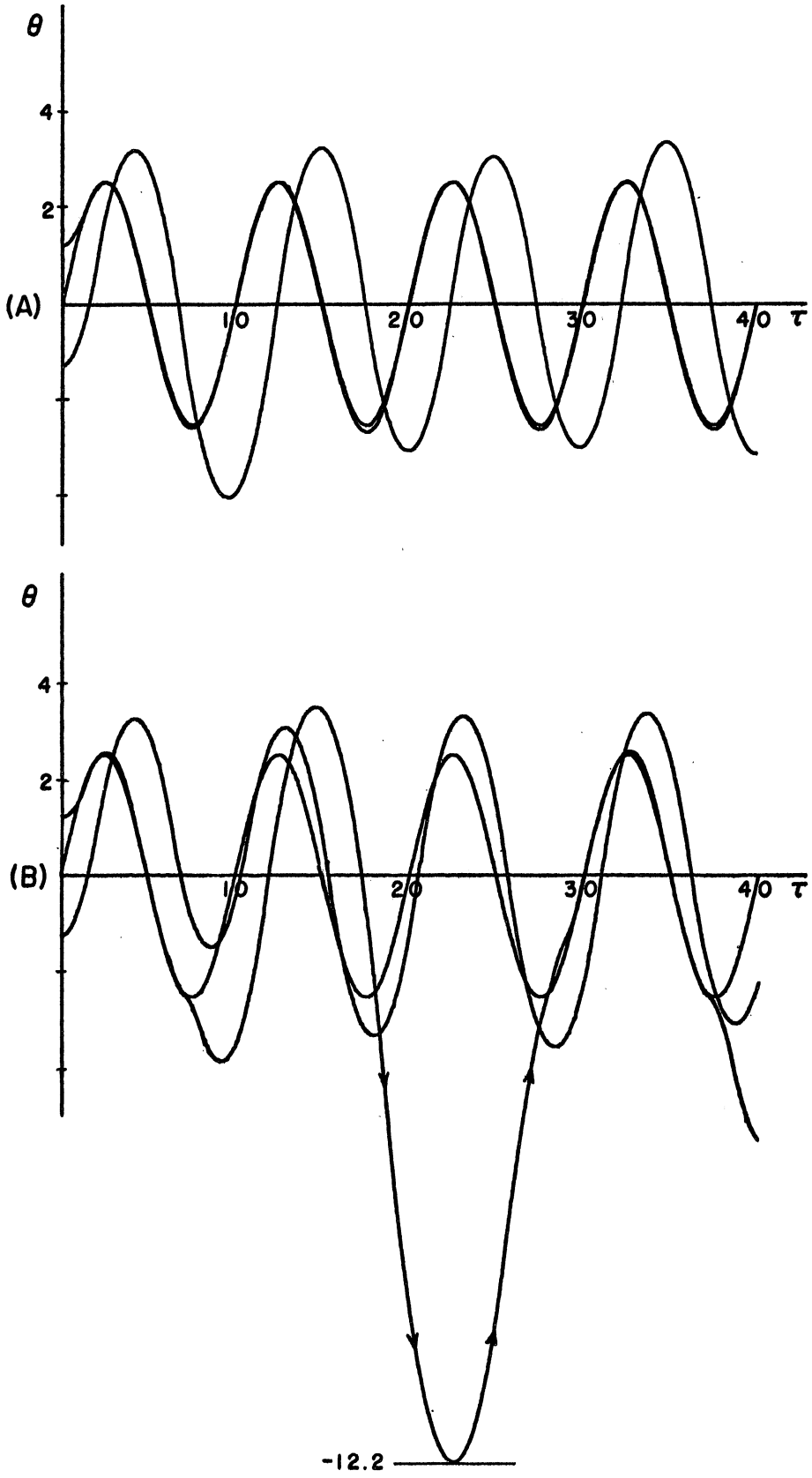

Figure 4.35 Responses with Prediction and Maximum f" = 1.
(A) Ramp Extrapolation, (B) Parabolic Extrapolation.

Figure 4.37 for maximum input acceleration equal to seven-tenths maximum output acceleration shows extreme sweep saturation for the parabolic extrapolation of the input.

One other item concerning the prediction study is worthy of note. As mentioned previously, $\Delta\gamma_s$ was not swept from zero each sweep by the prediction sweep circuit. Instead it was decreased at a constant rate during the reset period to a value greater than zero, so that the early and useless portion of the sweep was neglected. This would allow less time between decisions. It was found that a difficulty could be encountered here if the swept $\Delta\gamma_s$ did not decrease enough during the reset period to be below the $\Delta\gamma_s$ corresponding to the decision on the next sweep.

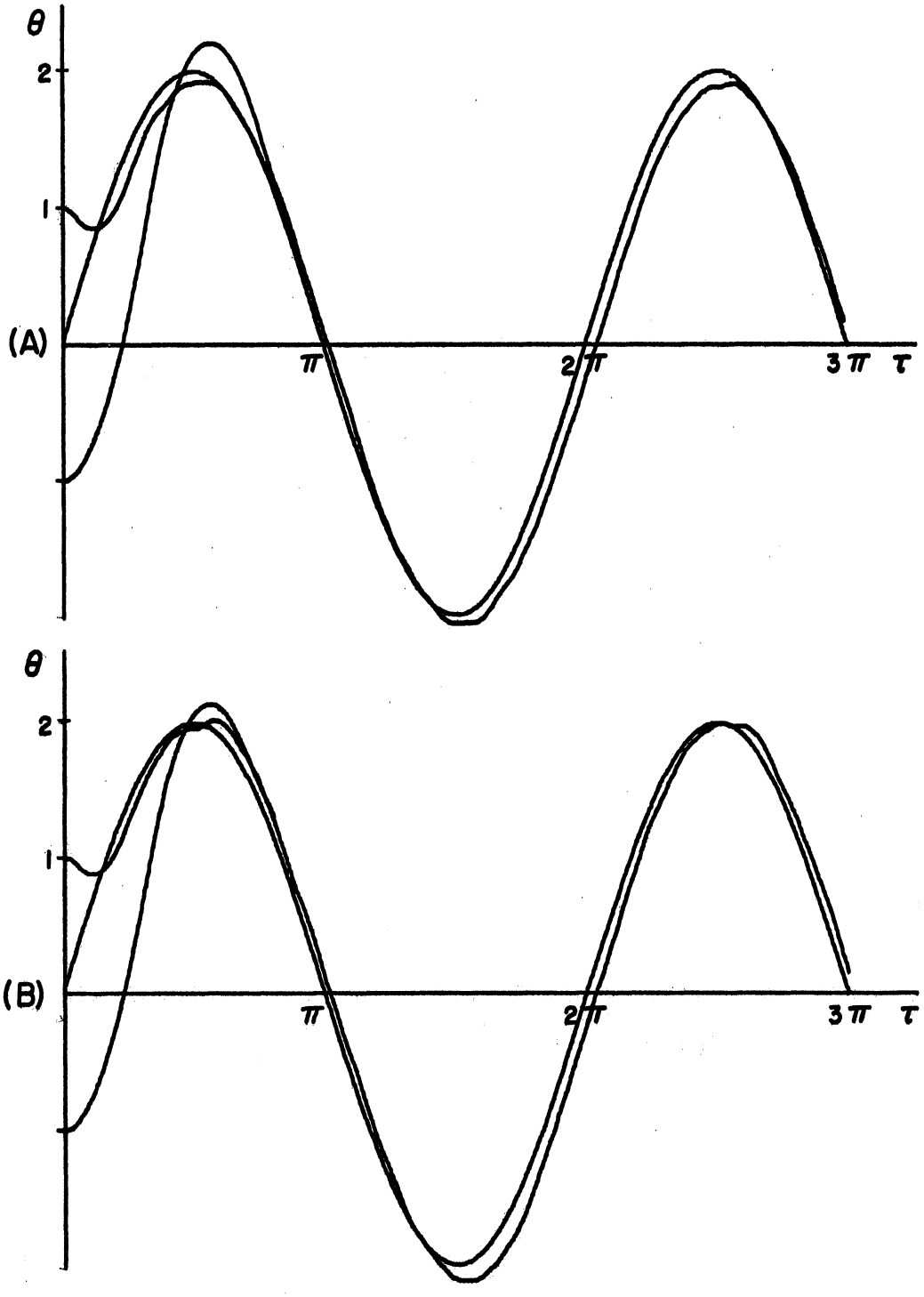

Figure 4.36 Responses with Prediction. Maximum f' = Maximum Θ' and Maximum f" = .5. (A) Ramp Extrapolation. (B) Parabolic Extrapolation.

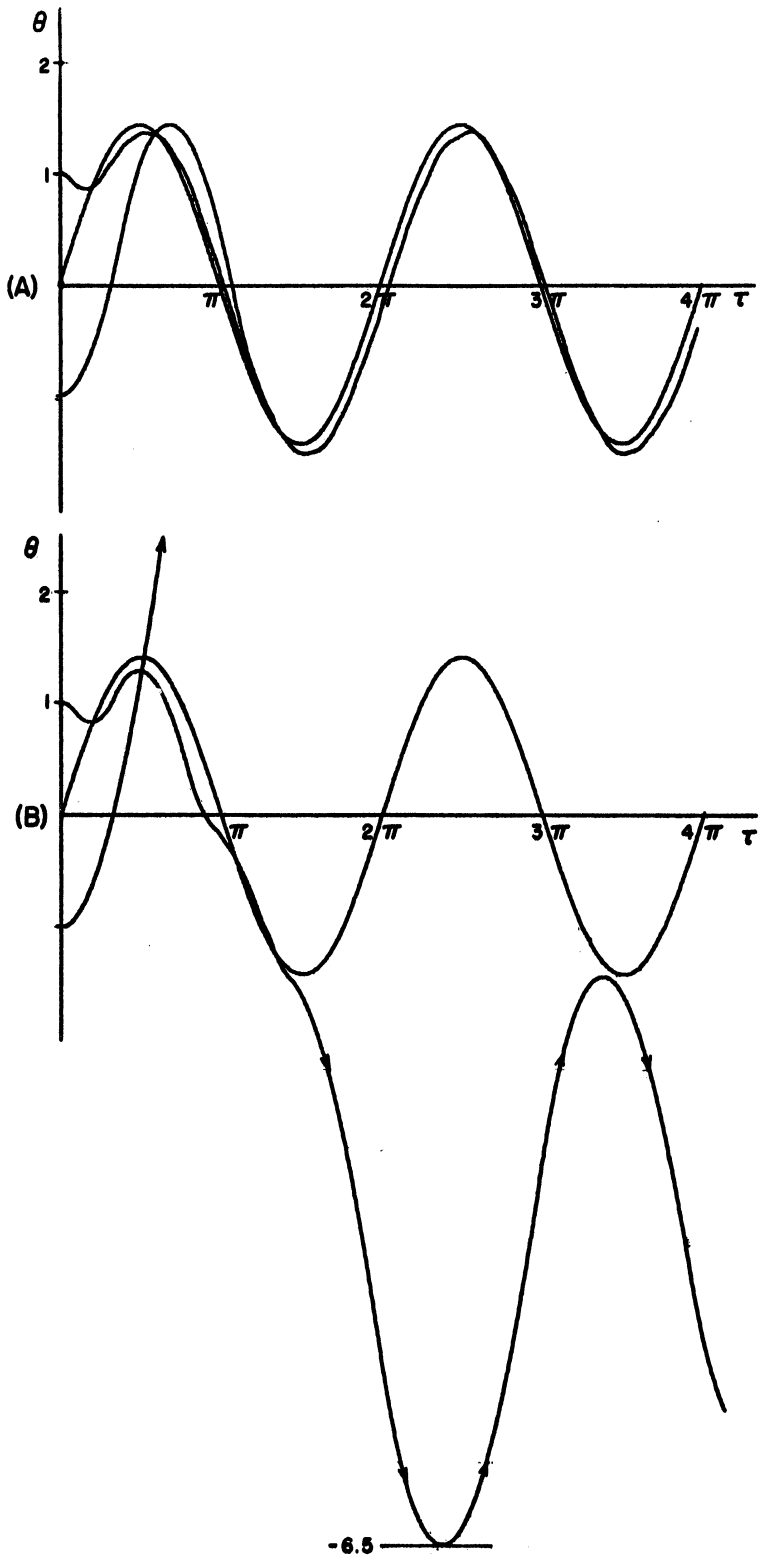

Figure 4.37 Responses with Prediction. Maximum f' = Maximum θ' and Maximum f" = .7. (A) Ramp Extrapolation. (B) Parabolic Extrapolation.

V. CONCLUSIONS

In this study, a new approach to the problem of determining switching criteria for optimum performance of contactor servos has been introduced. This swept locus switching concept is applicable to more general inputs than are the switching boundary schemes in the literature. The switching boundaries developed have been limited to those for step or ramp inputs, whereas swept locus switching has been shown to be applicable to any input functions of time of class C^{n-1} for the servos analyzed, n being the order of the differential equations of servo action.

The swept locus method was developed for inputs known as functions of time. The method takes advantage of the available future input information, in effect allowing the servo to "see" more than a constant position or constant velocity extrapolation into the future from present values. It is suggested that the general input signal, known only in the past and present, may be handled by a swept locus system using predicted input values.

The swept locus scheme is admittedly complex, but so is the optimum switching problem. The scheme is simplified by realizing that the switching of an actual servo may be treated by repetitively solving for the initial forcing of an (n-1)-switch program. High repetition rate, accurate locus computers, and a sensitive decision device would give a good approximation to optimum switching. Consideration of the initial forcing only would simplify the switch boundary analyses also. However, the author has not seen this idea stated or used elsewhere.

The servos analyzed have differential equations

$$D^2\theta = \pm 1 \tag{5.1}$$

and

$$D(D+K_2)(D+K_3)\cdots(D+K_n) = \pm 1 \tag{5.2}$$

where the K's are distinct positive real constants. For these servos, the loci for switch programs of (n-1) or less switches have been shown to be (n-1) - dimensional hypersurfaces topologically equivalent to hyperspheres in the space of output position and derivatives used for the analyses. It has been shown that the loci are on surfaces of invariant functional form in the phase spaces. These surfaces merely translate in the space as the input signal varies. This invariance of the functional form of the surfaces simplifies computer construction.

The computer study of the two second order systems showed that near optimum switching programs were obtained using the swept locus scheme, thus validating the theory. Possible practical problems of computer saturation were noted when imperfect input prediction was used. An automatic sweep reset device would help remove the trouble.

It is believed that it would be advantageous if switching for other types of contactor servos were analyzed on a locus basis. For the real root cases, this should not be difficult. The complex root cases are probably more difficult. The author has graphically analyzed a second order servo with differential equations

$$(D^2+1)\theta = \pm 1 \tag{5.3}$$

and found the locus approach applicable. Programs of more than one switch were found to be necessary, however.

Possible simplifying approximations for the loci might make this approach easier to mechanize for a practical servo system. Special computing components would help also.

For arbitrarily varying inputs, the prediction problem, only hinted at in this study, would need a great deal of study.

BIBLIOGRAPHY

1. Hazen, H. L., "Theory of Servomechanisms", J. Franklin Inst., Vol. 218, pp. 279-331; September, 1934.

2. MacCall, L. A., Fundamental Theory of Servomechanisms, D. Van Nostrand Company, New York; 1945.

3. Minorsky, N., Nonlinear Mechanics, J. W. Edwards, Ann Arbor, Michigan; 1947.

4. Andronow, A. A. and Chaikin, C. E., Theory of Oscillations, Princeton University Press, Princeton, New Jersey; 1949.

5. Kahn, D. A., "An Analysis of Relay Servomechamisms," Trans. A.I.E.E. Vol. 68, pp. 1079-1087; 1949.

6. Weiss, H. K., "Analysis of Relay Servomechanisms", J. Aero. Sciences, Vol. 13, pp. 364-376; July, 1946.

7. McDonald, D., "Nonlinear Techniques for Improving Servo Performance," Proc. National Electronics Conf., Vol. 6, pp. 400-421; 1950.

8. Hopkin, A. M., "A Phase Plane Approach to the Compensation of Saturating Servomechanisms," Trans. A.I.E.E. Vol. 70, pp. 631-639; 1951.

9. McDonald, D., "Multiple Mode Operation of Servomechanisms", Rev. of Sci. Inst., Vol. 23, pp. 22-30; January, 1952.

10. Bushaw, D. W., Differential Equations with a Discontinuous Forcing Term, Report No. 469, Experimental Towing Tank, Stevens Inst. of Tech.; January, 1953.

11. LaSalle, J. P., Study of the Basic Principle Underlying the "Bang-Bang" Servo, Goodyear Aircraft Company Report GER-5518; July, 1953.

12. Kazda, L. F., "Errors in Relay Servo Systems," Trans. A.I.E.E., Vol. 72 pp. 323-328; 1953.

13. Rose, N. J., Theoretical Aspects of Limit Control, Report No. 459, Experimental Towing Tank, Stevens Inst. of Tech.; November, 1953.

14. Bogner, I and Kazda, L. F., "An Investigation of the Switching Criteria for Higher Order Contactor Servomechanisms," Trans. A.I.E.E., Vol. 73, pp. 118-127; 1954.

15. Kang, C. L. and Fett, G. H., "Metrization of Phase Space and Non-Linear Servo Systems," J. Appl. Phys., Vol. 24, pp. 38-41; 1953.

16. Bass, R. W., "Extension of Frequency Method of Analyzing Relay-Operated Servomechanisms, Section III, Final Report, Contract DA-36-034-ORD-1273RD, The Johns Hopkins University; June, 1955.

17. Silva, L. M., Nonlinear Optimization of Relay Servomechanisms, Series No. 60, Issue No. 106, Electronics Research Lab., University of California; April, 1954.

18. Hagin, E. J., An Investigation of Higher Order Servo Systems with Non-Linear Computers Using Phase Space Techniques, Ph.D. Thesis, University of Illinois; 1956.

19. Tajima, K., Waseda University. Unpublished Work Concerning Switching Criteria for Higher Order Systems.

20. Wild, L. D., Glossary of Physics, McGraw-Hill Company, New York; 1937.

21. Goldstein, H., Classical Mechanics, p. 247, Addison-Wesley Press, Cambridge, Massachusetts; 1950.

22. Agnew, R. P., Differential Equations, p. 95, McGraw-Hill Book Company, New York; 1942.

23. Hildebrand, F. B., Methods of Applied Mathmatics, Chapter I, Prentice-Hall, New York; 1952.

24. Rauch, L. L. and Howe, R. M, "A Servo with Linear Operation in a Region About the Optimum Discontinuous Switching Curve," Proceedings of the Symposium on Nonlinear Circuit Analysis; April, 1956.

25. Wiener, N., Extrapolation, Interpolation, and Smoothing of Stationary Time Series, John Wiley and Sons, New York; 1949.

26. Stumpers, F. L., "A Bibliography of Information Theory (Communication Theory-Cybernetics)," Trans. I.R.E., Vol. IT-2, pp. 12-18; November, 1953.

27. Stumpers, F. L., "Supplement to A Bibliography of Information Theory (Communication Theory-Cybernetics)," Part IV, Trans. I.R.E., Vol. IT-1 pp. 35-37; September, 1955.

28. Howe, R. M., "Representation of Nonlinear Functions by Means of Operational Amplifiers," Trans. I.R.E., Vol. EC-5, pp. 203-206; December, 1956

29. Nichols, M. H. and Rauch, L. L., Radio Telemetry, Section 9.4, John Wiley and Sons, New York; 1956.